Effect of air pollutants on renderings and moisture-transport phenomena in masonry

Hoffmann, D.; Niesel, K.:

Bundesanstalt für Materialforschung und -prüfung

Update 2008

Abstract

Determining a pore structure's mechanical and chemical data on lime rendering exposed outdoors and including masonry in the laboratory, with regard to their behaviour on moisture transport and weathering was the objective. In search of clues for a dose-response relation - i.e. upon a connection between the emission rate of SO_2 and NO_x on one hand and the degree of damage to mainly plaster having a lime component on the other - it has been of interest to what extent their structural characteristics including pore space are modified and so consequently also physico-technical properties and chemical composition. For determining corresponding criteria, a widely diversified spectrum of test methods such as to obtain data concerning porosity and moisture transport, mechanical behaviour, and chemistry as well is available. A description of the manufacture of plate-shaped rendering specimens with lime putty, industrially hydrated lime and dolomitic hydrate (the last two also having a cement admixture) and also hydraulic lime as binding agents is included. First deposition velocity and absorption rate for SO_2 were determined in laboratory tests on these materials in dry and moist states. After their exposure on outdoor racks at six locations in the Berlin region with differing SO_2 atmospheric contents over at least 5 years, the samples of course show time-dependent modifications of chemical and physical qualities which are especially reflected in the form of profiles of structure, strength and concentration, e.g. for sulphate. Local climatic differences, however, partly exert a greater influence on material than emissions. Similar investigations were performed on samples of comparable composition exposed 4 and 17 years. But the real surprise is furnished by the renderings' behaviour depending upon orientation and upon height at a building. Since weathering behaviour and moisture transport (absorption, storage, release) are directly interdependent, further criteria are necessary for a critical assessment of a plasters' pore structure. Starting from sands, plasters were characterized. The structural parameters were lastly influenced by the respective contents of sand, binder and mixing water. These results and those gained from bricks naturally find their expression in masonry sections manufactured there from, and above all in their capillary and evaporative behaviours, and also when applying different test liquids. Summary and cited literature is given at the end of this report.

Inhalt [1]

Effekt von Luftverunreinigungen auf Putzmörtel und Phänomene des Feuchtigkeitstransports in Mauerwerk

Das Aufstellen von Dosis/Wirkungs-Beziehungen beim Angriff von schwefel- und stickstoffoxidhaltiger Atmosphäre auf freigelagerte, aber regengeschützte Platten aus unterschiedlichen Putzmörteln, von deren Kalkkomponente man eine verhältnismäßig rasche Reaktion erwarten durfte, erwies sich als schwierig. Denn nach Programmbeginn wurde die Intensität der Emissionsquelle plötzlich abgeschwächt, weshalb sich zwangsläufig der Schwerpunkt der Untersuchung auf Proben vom Bauwerk verlagerte, in denen ja die Effekte längerer Expositionszeiten aufsummiert worden sind. Einflüsse von SO_2, NO_x und Cl finden ihren Niederschlag aber nicht nur im Konzentrationsgefälle mit der Eindringtiefe, sondern hängen besonders von lokalen Umständen, wie Himmelsrichtung, Entnahmehöhe am Bauwerk und Orientierung gegenüber der Emissionsquelle ab. Entsprechende Tiefenprofile zeigen neben Unterschieden in der Verteilung der Reaktionsprodukte als Ausdruck von Chemismus und Oberflächenrauheit des Materials auch damit korrelierbare Veränderungen des Porenraums und demzufolge der physikalisch-technischen Eigenschaften und Merkmale, mit welcher Zielsetzung übrigens auch die Auslagerungsversuche noch mehrere Jahre fortgesetzt werden sollen. Unterstützung findet diese Aufgabe in der experimentellen Erfassung der Depositionsgeschwindigkeit und Aufnahmerate von SO_2 bei verschiedenen Gaskonzentrationen. Da das Verwitterungsverhalten im wesentlichen vom Materialgefüge, also von dessen Transport- und Speichereigenschaften für Feuchtigkeit abhängt, ist durch Variation der Mörtelkomponenten in bezug auf Bindemittelgehalt, Korngrößenverteilung des Zuschlags und Wasserbedarf sowie der Rohdichte der Ziegel versucht worden, deren Einfluß auf Kapillarität und Wasserabgabe eines Mauerwerks zu ermitteln. Wenn man den Wasserverlust unter vergleichbaren Umgebungsbedingungen, d.h. auch der Probekörpergeometrie, verfolgt und dabei den ersten, überwiegend klimaabhängigen linearen Abschnitt der entsprechenden Kurve außer acht läßt, kann deren materialspezifischer Charakter anhand des Verdunstungsparameters einer aus solchen Umständen resultierenden, neuentwickelten Regressionsfunktion überzeugend zum Ausdruck gebracht werden. Obwohl in seiner physikalischen Bedeutung noch nicht geklärt, kann dieser dem Fachmann als vielversprechendes Werkzeug dienen, die Eigenschaften eines porösen Materials vom Gefüge her zu deuten.

---

[1] Es handelt sich um die erweiterte englische Fassung des 1995 erschienenen BAM (Bundesanstalt für Materialforschung und -prüfung) -Forschungsberichts No. 209, Berlin, wobei die dafür geleistete Arbeit vom Umweltbundesamt (UBA) gefördert worden ist.

Содержание[2]

Эффект загрязнения воздуха на штукатурку и феноменах транспорта жидкости в кирпичной кладке

Определение соотношения количества / действия влияния серо- и азотосодержящей атмосферы на свободнохранящиеся, но защищённые от дождя плиты из различных штукатурок, от известковых компонентов оказалось, вопреки ожидаемой сравительно быстрой реакции, сложным. Поскольку источник эмиссии после начала программы испытания на атмосферостойкость неожиданно ослабился, центр внимания переместился на испытание образцов из зданий, в которых суммировались эффекты долгого времени экспозиции. Влияние SO_2, NO_x и Cl отражается не только на градиенте концентрации по глубине проникания, но особенно зависит от локальных обстоятельств, таких как направленность, высота снятия проб в здании и ориентация по отношению к источнику эмиссии. Соответствующие глубинные профили показывают помимо различий в распределении продуктов реакции химический состав и шероховатости поверхности материала, а также коррелующие изменения пространства пор и, следовательно, его физико-технических свойств и качеств, что являеться причиной необходимости проведения испытаний по хранению в следующие годы. Эти исследования находят поддержку в экспериментальном определении скорости осаждения и внедрения SO_2 при расличных концентрациях. Поскольку выветриваемость главным образом зависит от структуры материалов, т. е. от её свойств при транспорте и аккумуляции влаги, принимались попытки посредством варияцией компонентов штукатурки относительно содержания связывающих средств, распределения величины зёрен заполнителя и необходимого колличества воды, а также сырой плотности кирпичей определить их влияние на капиллярность и отдачу воды кирпичной кладки. Если исследуется потеря воды под одинаковыми условиями окружающей среды, такими как геометрия образцов и, если принебрегать линеарным отрезком соответсвующей кривой, зависящей от климата, тогда можно наглядно выявить материалоспецифичный характер результирующей кривой на основе параметра испарения новоразвиваемой регрессивной функции. Несмотря на в настоящее время физически не определенный характер этого параметра испарения, он может служить специалисту многообщающим инструментом для объяснения свойств пористого материала на основе его структуры.

[2] На основе расширенного на английском языке выпуска научно- исследовательского отчёта No.209 от 1995 г. Федерального Ведомства по Исследованию и Испытанию Материалов(BAM),Берлин. Научная работа для этой цели была проведена при участии и поддержке Федеральным Ведомством по Окружающей Среды(UBA).

Contenido[3]

El efecto de la contaminación atmosférica en los morteros de revoques, incluyendo los fenómenos de transporte de la humedad en fábricas de ladrillos

Establecer una relación entre dosis y efecto del ataque por óxidos de azufre y de nitrógeno contenidos en la atmósfera, en placas de diferentes revoques, expuestas al aire libre, pero protejidas de la lluvia, no resultó facil, a pesar de preverse una reacción relativamente rápida del componente calcáreo. Ésto se debió a la repentina atenuación de la intensidad de la fuente emisora contaminante al poco tiempo del comienzo del proyecto, por lo cuál la investigación necesariamente tuvo que concentrarse en muestras tomadas de un edificio, en el cuál se fueron sumando los efectos de una exposición prolongada de varios años. La influencia de SO_2, NO_x y Cl, no depende exclusivamente del gradiente de concentración según la profundidad de intrusión, sino que está afectada especialmente por las condiciones locales como son: la orientación y la altura en el edificio de la cuál fueron obtenidas las muestras y su orientación respecto a la fuente contaminante. Los perfiles correspondientes de alteración con la profundidad, indican además de las diferencias en la distribución de los productos reactivos como expresión de la composición química y de la rugosidad de la superficie del material, una correlación con las modificaciones del espacio de poros y también en las propiedades y características físico-mecánicas. Con ésta intención las pruebas continuarán durante varios años expuestas al medio ambiente. Ésta tarea encuentra apoyo en la determinación experimental de la velocidad de deposición y en la cuota de absorción de SO_2 utilizando distintas concentraciones de gas. Como la alteración depende esencialmente de la estructura del material, es decir de sus características de transporte y acumulación de humedad, se ha probado a determinar la influencia de la capilaridad y la capacidad de evaporación de la fábrica por medio de variación de los componentes del mortero es decir; el contenido de aglomerante, la distribución granulométrica del árido y la demanda de agua y la densidad aparente de los ladrillos. Si se observa la pérdida de agua bajo condiciones comparables, incluída la geometría de la muestra, y despreciando el primer tramo de la curva correspondiente, la parte lineal que depende predominantemente del clima, la propriedad específica del material se puede expresar adecuademente por medio del parámetro de evaporación de una función de regresión nueva, que resulta de las condiciones anteriormente citadas. A pesar que su significado físico no está suficientemente claro, éste parámetro puede servir al experto como herramienta muy prometedora para interpretar las propiedades de la estructura de materiales porosos.

[3] Se trata de una versión más amplia del informe de investigación BAM (Instituto Federal de Investigación y de Ensayos de Materiales) no 209, publicado en el año 1995 en Berlin; el trabajo correspondiente fué promovido por el Instituto Federal del Medio Ambiente (UBA), Berlín.

Sommaire[4]

L'effet des polluants atmosphériques sur des enduits et les phénomènes du transfert d'humidité dans la maçonnerie

Il s'est avéré difficile d'établir des relations dose-effet lors de l'attaque d'une atmosphère contenant des oxydes de soufre et de nitrogène qui ont lieu sur des plaques à enduits de types différents exposées à l'air libre, mais à l'abri de la pluie. Ainsi, au commencement du programme, l'intensité de la source émettrice diminua soudain, et, de la sorte, le point capital de l'étude se transféra sur des échantillons au bâtiment même, où sont accumulés les effets dus à des temps prolongés d'exposition. Les influences du SO_2, du NO_x et du Cl trouvent non seulement leur expression dans le gradient de concentration relatif au degré de pénétration, mais dépendent spécialement aussi de circonstances locales telles que le point cardinal, la hauteur de prélèvement au bâtiment et l'orientation vers la source émettrice. Des profils de profondeur correspondants présentent, outre des différences dans la répartition des produits de réaction, en tant que marque du chimisme et de la rugosité de surface du matériau, aussi et surtout des changements de l'espace poreux pouvant être mis en corrélation avec celles-là et, pour cette même raison, des modifications des caractéristiques. C'est avec cet objectif qu'on envisage d'ailleurs de poursuivre les essais d'exposition encore plusieurs années. Ce projet s'appuie sur la détermination expérimentale de la vélocité de déposition et le taux de SO_2 absorbé à des concentrations différentes de gaz. Comme le comportement à l'altération dépend prédomina ment de la structure du matériau, donc de ses qualités de stockage et de transfert d'humidité, on a essayé de déterminer leur influence sur la capillarité et le dégagement d'eau d'une maçonnerie en modifiant les composants d'enduit relatifs à la teneur en liant, à la répartition des grains d'agrégat et au besoin d'eau, ainsi que la densité apparente des briques. Lorsqu'on contrôle la perte en eau dans des conditions ambiantes comparables, c.-à-d. également celles de la géométrie de l'éprouvette, mais en négligeant cependant la première partie linéaire de la courbe qui dépend principalement du climat, son caractère spécifique au matériau peut être exprimé d'une manière plus convaincante au moyen du paramètre d'évaporation d'une fonction de régression en résultant et nouvellement développée. Bien que sa signification physique ne soit pas encore établie cela pourrait constituer un moyen efficace pour l'expert d'interpréter les propriétés d'un matériau poreux par sa structure.

[4] Il s'agit de la version anglaise augmentée du rapport de recherches BAM (Institut Fédéral de Recherche et d'Essais de Matériaux) no. 209, Berlin, paru en 1995, ce travail ayant fait l'objet d'une promotion par l'Office Fédéral de l'Environnement (UBA).

1 Introduction

The main objective of this research programme is to determine whether there exists a connection between immission rate of air pollutants and the degree of damage to a building material, and so to establish so-called dose-response relations. It is also of interest to know to what extent a rendering's physico-technical properties and structural characteristics will be subjected to a change as a consequence of differing pollutant concentrations, and if one could determine quantitatively corresponding influences, e.g. by SO_2 and NO_X. Test conditions were obtained by use of outdoor-exposure racks erected at various locations having different climates. At nearby measuring stations, one has continuously determined among other parameters immission, temperature and relative ambient humidity. Rendering was the principal test material the surface of which was roughened (scraped finish) to prevent local formation of thin sealing films of the hardened paste. A sandy limestone (Baumberger "sandstone") was included in the test programme.

Tab. 1. Characteristics for assessing behaviour of porous building materials

Concept	Characteristic values	Methods
Simulating weathering	scale factor p_1 of the mass loss curve, described by the W e i b u l l relation as a function of cycle number	sodium sulphate crystallization test (in variants)
Filling degree of pores	saturation coefficient S, "relative degree of impregnation" S_t critical saturation degree S_{cr}	water absorption at normal atmospheric pressure and at 15 MPa, capillary liquid rise, relative dimensional change while frosting
Pore-size distribution	specific pore volume, discrete values (e.g. microporosity, d_{10m} value, interval according to R a v a g l i o l i ; field capacity), specific surface area Σ_m	mercury porosimeter test, relationship matric suction / water content, physiosorption
Moisture content	water capacity Ψ_k, open porosity ε_o	capillary liquid rise, water absorption, underwater weighing
Moisture transport	water absorption coefficient w_o, length-related water penetration coefficient b	capillary liquid rise
Permeable porosity	specific gas permeability D_s, water vapour diffusion resistance index μ	fluid transport at defined pressure and concentration gradients
Evaporation	mass loss as a function of time	evaporation development, monitored by weighing
Mechanical characteristics	compressive and bending strength at "dry" and "wet" states, modulus of elasticity, surface hardness ("macrohardness"), surface abrasion, thermal expansion coefficient compression test, bending test, vibratory behaviour, ball indentation, grinding abrasion,	compression test, bending test, vibratory behaviour, ball indentation, grinding abrasion, relative length change

Methods provided for a measuring characterization of starting material were successfully proved and expanded. In this case one has attached importance to recognizing as many particularities of a material as possible, analogous to a work on natural stone [83], in order not to overlook any eventually promising correlation (see Tab. 1). This is extremely important

when considering additional difficulties arising from a material having a relatively small thickness and being quite friable. In addition there are inhomogeneities specific to production runs but by no means only originating from plastering.
Since some measures have been promoted to reduce air pollution by a factor of two, main interest in choosing exposure sites was directed to regions of considerable immission with SO_2 and NO_X sources in the vicinity. Exposure racks were erected close to several stations of the Berlin air quality measuring network. These sites are indicated on a schematic map of the city (Fig. 1) also marked with SO_2 concentration isolines

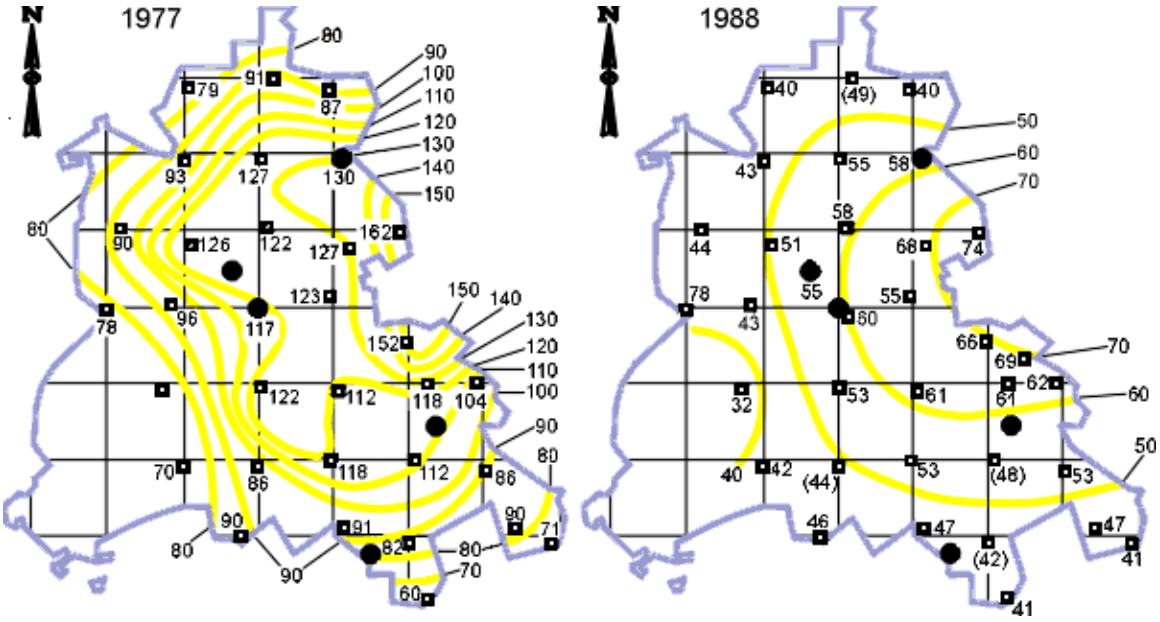

Fig. 1. Air quality monitoring network of Berlin (West): Comparison of yearly average of the SO_2 concentration in µg/m^3 for 1977 and 1988 as well as (black) points of exposure locations

The reason for concentrating on older façades is the closure of several industrial works in central Germany, i.e. the former GDR, where strongly emitting flue gas sources were situated, which furnished principally SO_2 to Berlin even at the programme's start. In recent years one has seen increasing improvement in air quality due to sulphur dioxide emissions in this region. The yearly average was reported to have decreased by 50% from 1977 to 1988 [32]. Thus differences found between exposure locations established near monitoring stations were also remarkably reduced. This tendency has continued over the last few years (compare Fig. 2 and Fig. 3). The same is true for the NOx emitters and suspended dust (Tab. 2).

Tab. 2. Annual means for SO2, NOx and suspended dust in the time span between 1989 and 1996 (till 1990 only for the western part, from 1991 for Berlin as a whole)

Year	SO_2 *)	NO_X *)	Suspended dust *)
1989	63	72	87
1990	48	57	70
1991	45	64	71
1992	32	61	61
1993 exposure time	26	56	59
1994	20	55	51
1995	18	51	49
1996	17	49	57

*) Concentrations presented each as an annual mean in µg/m^3 air

Of course this positive improvement of air quality reduces the chances to find distinct modification of exposed materials within a reasonable time period. These changes caused a shift from freshly prepared samples to

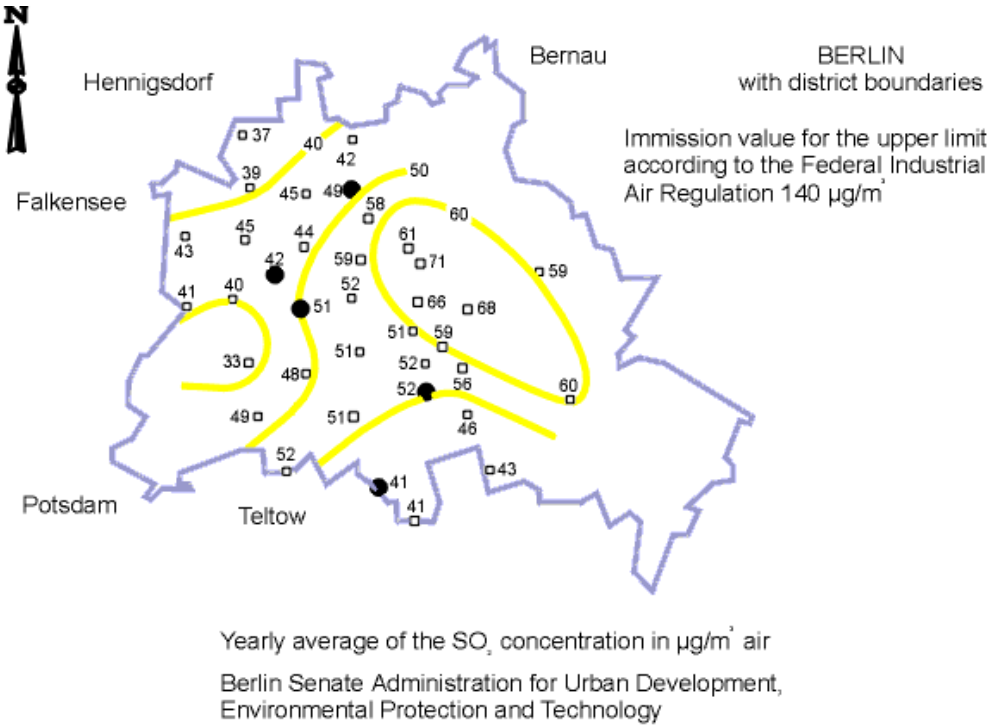

Fig. 2. Air quality monitoring network of Berlin 1990: Yearly average of the SO_2 concentration

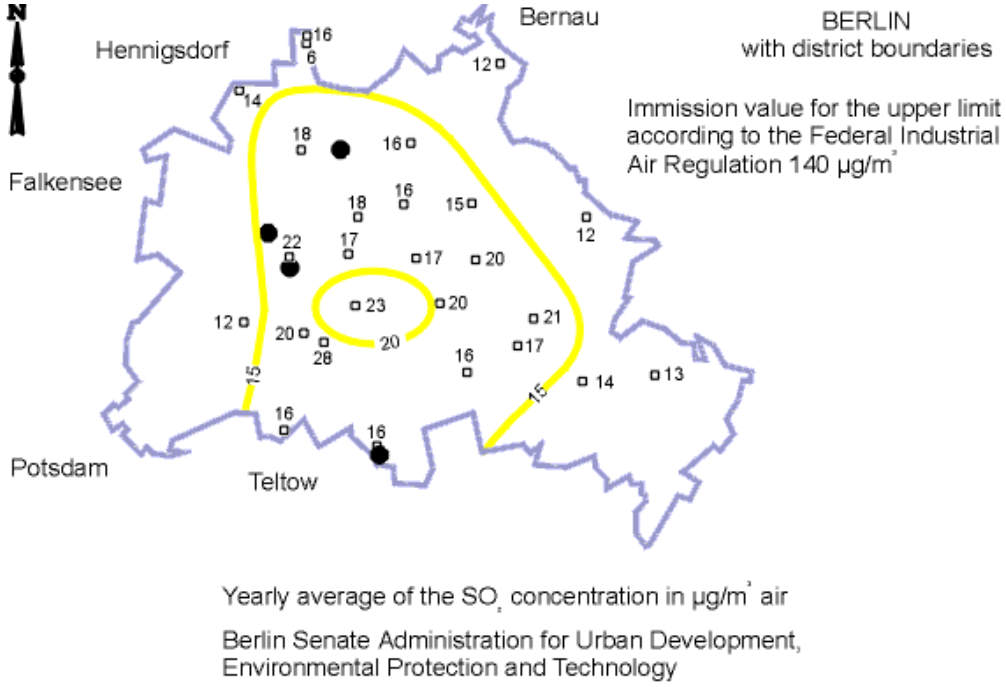

Fig. 3. Air quality monitoring network of Berlin 1996: Yearly average of the SO_2 concentration

research directed rather to in-situ findings on older buildings. This research effort was directed towards analyzing rendering samples from façades erected many years ago, which over time have formed a weathering profile. These results are complemented by a

determination of SO_2 uptake under defined conditions by various rendering types each having a planned composition as well as their field behaviour over 4.5 years.
Since concentrations were reduced by half, relative variations between monitoring stations were also smoothed. At Lerschpfad, an area very close to the city highway (Stadtautobahn) and normally representing a region of medium emission, the highest SO_2 concentrations of 57 µg/m^3 air occur as shown in Fig. 4.

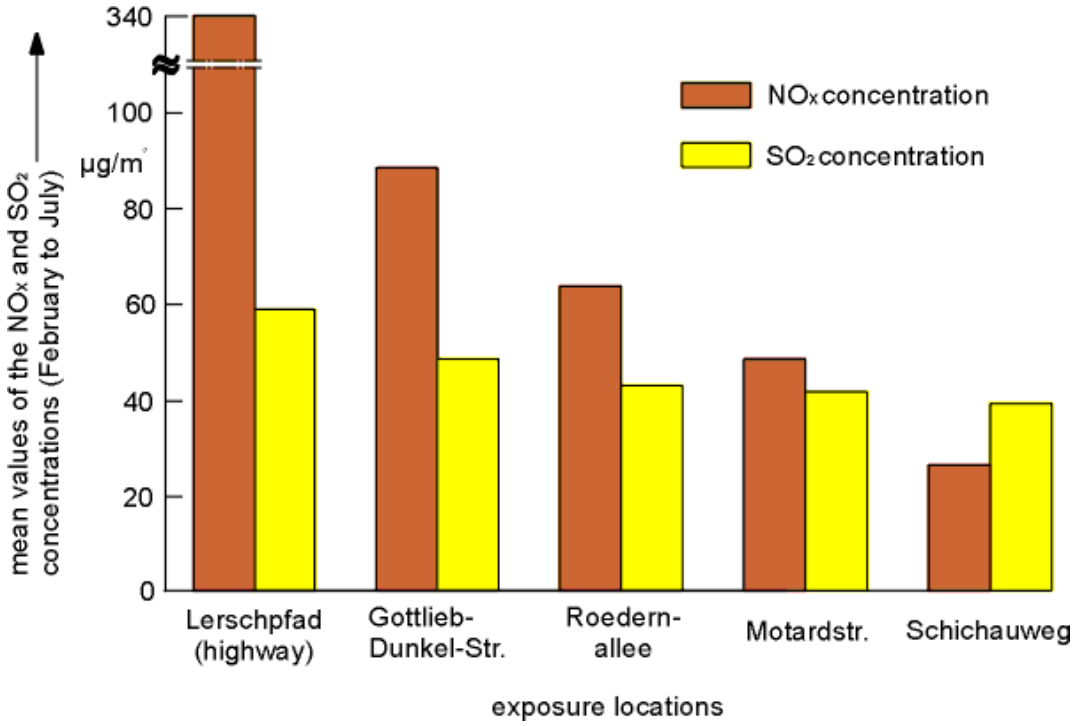

Fig. 4. Comparison of NO_X and SO_2 concentrations in µg/m^3 air as an average monitored at different exposure locations in Berlin from February to July 1991

In contrast, for Schichauweg at the southern boundary, the lowest value of 36 µg/m^3 was found. It decreased in the corresponding period of 1992 to 47 µg/m^3 and 28 µg/m^3 respectively (see Tab. 3).

Tab. 3. Annual means for SO_2 in the time span between 1989 and 1995 at the sites with the lowest (Schichauweg) and highest emission (Lerschpfad); exposure time: 1991 – 1995

Year	SO_2 in µg/m^3 air	
	Schichauweg	Lerschpfad
1989	56	79
1990	41	60
1991	36	57
1992	28	47
1993	21	40
1994	16	35
1995	14	27

It seems doubtful that one can clearly state the influences on renderings, distinguishing from one to the other exposure location, and whether there exists a corresponding factor not exceeding 2.0 in 1995. This situation is much better for NO_X concentrations and their possible

influence on material behaviour (cf. also Fig. 4). Corresponding values show a maximum at Lerschpfad with 340 µg/m^3 air and at Schichauweg a minimum with 25 µg/m^3 in 1991. Besides these data, it would be of interest to know how often and how long wetting by dew occurred. However such quantitative monitoring was not conducted. Therefore immission of pollutants measured by stations of the Berlin Air-Quality Monitoring Network over time might give a rough indication for classifying 5 exposure locations as was shown in Fig. 2. Since probably NO_X uptake, so far as biological origin, does not predominate and that of SO_2 anyway occurs via a liquid phase, i.e. via pore solutions or rain water, a significant absorption of the latter below the freezing point is doubtful.

2 Specimen preparation

2.1 Experimental

In contrast to a free standing column, materials exposed outdoors representing the contours of a building are not uniformly affected by atmospheric influences in all directions. Weathering such as that by SO_2 attack taking place mainly in rain-wash can be excluded using an exposure rack, as shown in Fig. 5. This approach was tested in a former programme [96]. The rack was faced south in order to avoid the effect of the principal rain and wind directions. Although such a design cannot be considered

Fig. 5. Rack facing south for exposing rendering specimens to ambient atmosphere (Air monitoring station shown at left in background)

as more than a compromise, because it does not present a closed surface of large extent as there is at a building, it may nevertheless be considered as a basis for comparing results.
As shown in detail in Fig. 6, clamping devices emplaced on such a rack consist of different metal parts where the fastening can be seen in an exploded view of the single base plates. In addition, the function of a splatterdashcoat, which makes it possible for the rendering system to adhere to the fibre cement plate, is fulfilled by coarse sand spread over the surface after having been first coated with an epoxy film. Afterwards a fresh mix was laid on, whereby the format of plates was created with the aid of appropriate stencils. One day after laying, the fresh surfaces were scratched in order to avoid the effects of a thin layer containing fines which could block the penetration of polluting gases.

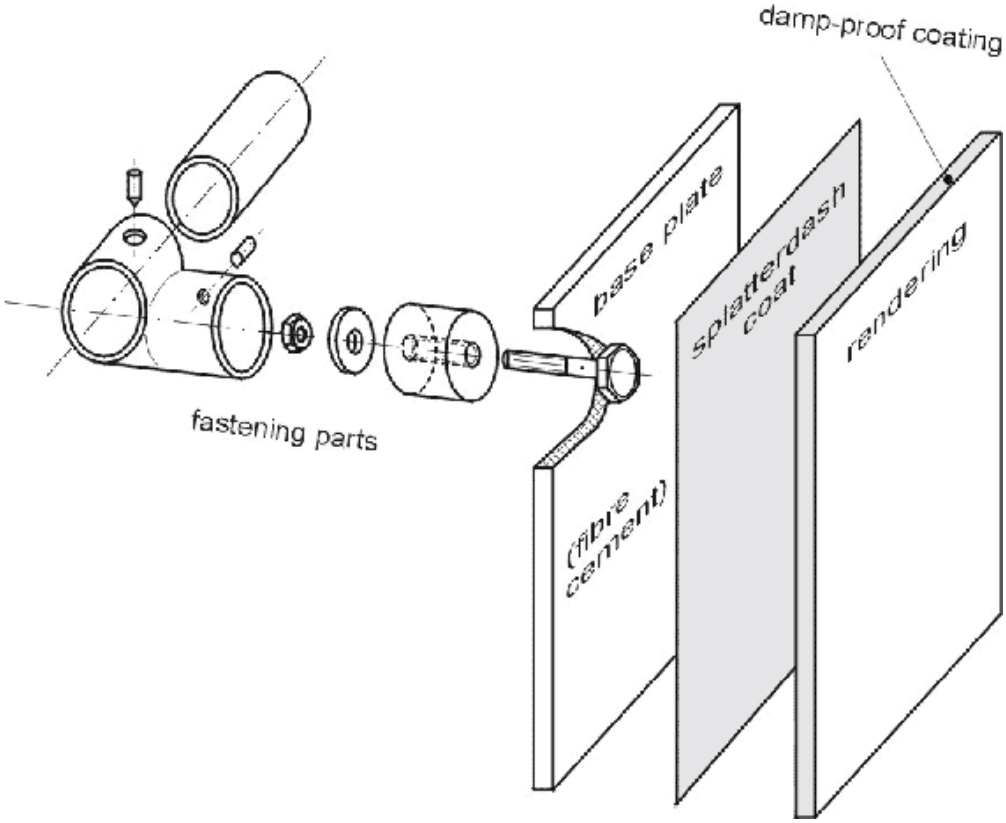

Fig. 6. Clamping device to mount rendering plates on an outdoor rack for atmospheric exposure (SO_2), shown in an exploded view (see also Fig. 5)

Then storage began in a climatic chamber having a constant relative humidity of 90 %. This procedure served to promote carbonation prior to exposure in an atmosphere containing SO_2. With an aim to support this process, every now and then the specimen surface was moistened by spraying water, so that the material underwent the most favourable conditions spatially and temporally for carbonating reaction several times. Afterwards, lateral margins of specimens, now hardened and in position to be transported elsewhere, were sealed to make them water-tight by applying a bituminous emulsion. This is how one common starting condition for specimen plates was achieved before they were mounted on racks. After the pre-treatment, the zonal succession of the concentration profile markings increased in quality the longer the test lasts.

2.2 Starting material

2.2.1 Binding agent

In order to simulate the historical composition of renderings which consist mostly of smaller quantities of hydraulic components than do modern renderings, and in order to avoid the local formation of thin films of hardened paste, lime hydrate or relatively pure dolomitic hydrate was chosen first of all for plastering. Thus, starting conditions could be simplified but also modified. Concerning the comparability of different rendering types against the attack of gaseous effusion, the basis for calculating mix proportions was to guarantee that their surfaces offered the same volume content of calcium hydroxide when exposed to atmosphere. In that case one has to take into account three differing binding agents, i.e. a hydrated lime produced by industrial slaking of calcined limestone and a lime putty, the raw materials for both coming from the same geological stage, and an industrially (completely) calcined and hydrated dolomite as well where each cementing component should be matched to the others in order to get comparable $Ca(OH)_2$ portions per volume. Therefore, in the case of dolomitic hydrate it

was necessary to equate its MgO and $Mg(OH)_2$ to calcium hydroxide equivalent according to its stoichiometrical portions. For this $Mg(OH)_2$ was translated to MgO, and $CaCO_3$ into $Ca(OH)_2$ as well, prior to calculation. In this way and considering impurities of each product, weight proportions result that relate to the aggregate quantity as 1 to 3.1 (or 1.0 for the dried equivalent) to 1.1 [industrially hydrated lime : lime putty : industrially hydrated dolomitic lime]. Material data as well as further characteristics, e.g. concerning the origin of binding agents, can be obtained from Tab. 4

Tab. 4. Chemical analyses of material types concerned

Constituents	Percentage by mass		
	Industrially hydrated lime	lime putty (dried state)	Industrially hydrated dolomitic lime
Portions insoluble in hydrochloric acid	0.60	0.31	3.57
Soluble silica SiO_2	1.66	0.70	1.88
Total oxides [1)]	0.74	0.64	1.64
Calcium oxide CaO	96.12	97.43	54.41
Magnesium oxide MgO	0.58	0.71	38.27
Potassium oxide K_2O	0.04	0.01	0.09
Sodium oxide Na_2O	0.05	0.05	0.11
Sulphate SO_3	0.08	0.05	0.03
expressed as $CaSO_4 \cdot 2H_2O$	0.17	0.11	0.06
Total sulphur S expressed as SO_3	0.08	0.05	0.03
Total	99.87	99.90	100.00
Chloride Cl^-	< 0.01	< 0.01	0.07
Nitrate NO_3^-	n.d.	n.d.	n.d.
Nitrite NO_2^-	n.d.	n.d.	n.d.
Residue (calculated)	0.12	0.09	---

Aluminium oxide, Al_2O_3; iron(II)oxide, Fe_2O_3; and titanium oxide, TiO_2
(n.d. = non detectable)

In addition to this, one can obtain details on chemical analyses in Tab. 5 and on mineral composition of these non-hydraulic binders calculated therefrom, as shown in the histogram presentation of Fig. 7

Tab. 5. Chemical analyses of material types concerned (continuation)

Constituents	Hydraulic lime ("Billerbeck lime") percentage by mass	Baumberger "sandstone" percentage by mass
Portions insoluble in hydrochloric acid	20.72	53.26
Soluble silica, SiO_2	13.59	2.11
Total oxides, R_2O_3	3.35	1.83
thereof:		
aluminium oxide, Al_2O_3		1.39
iron(III)oxide, Fe_2O_3		0.33
titanium oxide, TiO_2		0.11
Calcium oxide, CaO	59.49	42.27
Magnesium oxide, MgO	1.07	0.37
Potassium oxide, K_2O	0.12	
Sodium oxide, Na_2O	0.07	
Sulphate, SO_3	1.44	0.10
expressed as $CaSO_4 \cdot 2H_2O$	3.10	0.22
Total sulphur S		
expressed as SO_3	1.42	0.08
Total	99.85	99.94
Sulphite, SO_3^{2-}	n.d.	n.d.
Sulphide, S^{2-}	n.d.	n.d.
Chloride, Cl^-		
Nitrate, NO_3^-	n.d.	n.d.
Nitrite, NO_2^-	n.d.	n.d.
Residue (calculated)		

(n.d. = non detectable)

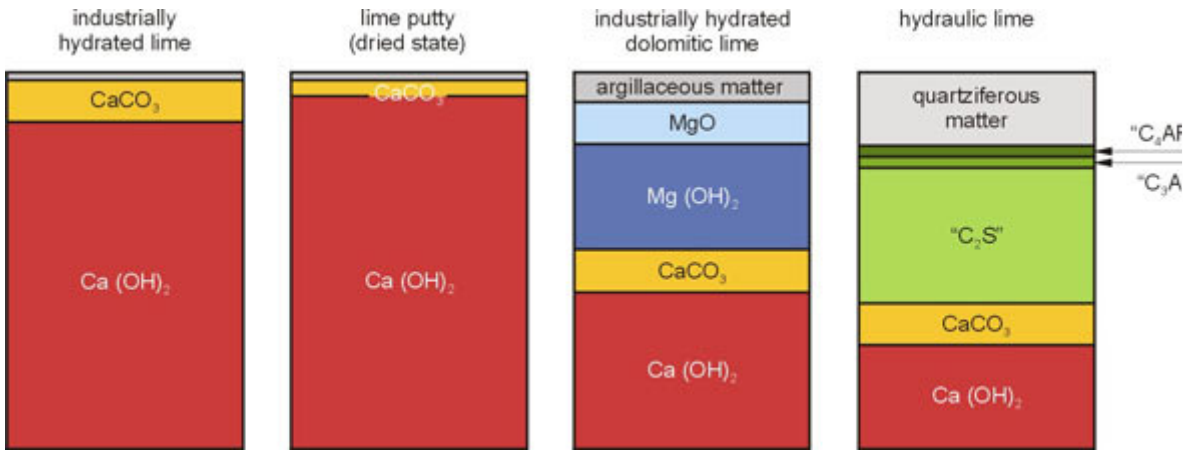

Fig. 7. Mineral composition calculated for plaster types; C_2S, C_3A, and C_4AF represent dicalcium silicate (belite), tricalcium aluminate, and tetracalcium aluminoferrite, respectively

2.2.2 Rendering

Rendering data as well as additional data concerning, e.g. the origin of binding agents, are shown in Tab. 6. In addition to materials cited, a lime plaster with cement admixture and a corresponding mix with hydrated dolomitic lime were used. Mix proportion [lime : portland cement : aggregate by mass] amounted to 1 : 0.6 : 16.3 or 1 : 0.6 : 18.3 while having a spread value of 18 cm and showing water-retention values of 86.3 or 88.3%. After having placed the fresh rendering on base plates, the hardening process began at once. In an early stage, drying is the decisive factor, which leads to shrinkage and consolidation of cryptocrystalline calcium hydroxide by mutual approach of lime-hydrate particles. Subsequently, or running parallel to it, proceeds the carbonate hardening. This is a rather complex process, since actual strength development takes place only by repeated dissolution and precipitation associated with recrystallization (cf. [49]. In the case of a rendering which predominantly contains lime, its hardening is based upon the chemically rather simple reaction of a transfer of lime hydrate into carbonate under water release, whereupon crystal coarsening [69] follows above all by contributing CO_2-loaded water to the dissolution process. The determining factors for the initial formation of binder/aggregate agglomeration and thus its geometric configuration, including the structure of the later significant pore system, are however contributed by the processes of transport and evaporation of the water portion, in which $Ca(OH)_2$ was originally found in suspension or solution.

Tab. 6. Characterization data of plaster types used in this project

Binding Agent	Raw Material						Rendering Mix			
	Type	Occurrence	Geological Origin	Mineral Phases [1]	Bulk Density ρ (in kg/dm³)	Specific Surface Σ_m (in m²/kg)	Proportion by Mass	Spread Value (in cm)	Water Retention Value in %
industrially hydrated lime	massive limestone	Painten near Kelheim, on Danube, Bavaria	Malm series, stage s - ζ	$Ca(OH)_2$, $CaCO_3$	0.42	16,230	1 : 16.3[3]	17.0[4]	84.1[5]
lime putty [stored more than two years with an excess of water (57 %)]	massive limestone	Altmann-stein near Kelheim, on Danube, Bavaria	Malm series, stage s - ζ	highly disperse $Ca(OH)_2$, $CaCO_3$	1.32	31,400[2]	1 : 7.2[3]	16.5[4]	89.3[5]
industrially (completely) calcined and hydrated dolomite	dolomite	Scharzfeld, Harz Mountain, Lower Saxony	middle Zechstein, main dolomite stage	$Ca(OH)_2$, MgO, $Mg(OH)_2$, $CaCO_3$, quartz	0.55	12,310	1 : 18.7[3]	17.2[4]	87.0[5]
hydraulic lime	lime	Billerbeck near Munster, Westphalia	upper Cretaceous	Ca_2SiO_4, $Ca(OH)_2$, $CaCO_3$, quartz	0.65	4,780	1 : 7.8[3]	18.2[4]	84.7[5]

1) after Calcining and Slaking

2) for the dried sample

3) standard sand according to DIN EN 196 part 1 [16]

4) according to DIN 18 555 [11]

5) according to ASTM C 91 [1], [94], however at a residual pressure of 8.16 Pa (= 60 mm Hg) instead of 50.8 mm Hg

From a chemical viewpoint, preparation should be carried out by following exactly a given mix proportion formula tested before fabrication. This, however, does not guarantee uniformity in local distribution of sand and binding agent, dispersion of lime, wetting of aggregate grains and subsequent compaction after laying, so that the reproducibility of a rendering is not warranted. Of course it is not possible to postulate a strict comparability in renderings because artefacts are caused by manufacturing and long-term effects such as carbonation also produce heterogeneous areas in this type of two-component system. Plaster hardening is a most complex process. Thus differences in the respective state of the binding agent give rise to distinguishing features in material cohesion which, however, have to be disregarded.

In 1934 G r a f [26] already described numerous possibilities for modifying lime mortar and rendering with regard to their properties or characteristics by applying different proportions of starting materials and the following treatment in the course of production and storage. He may be credited with having introduced tests on building lime to a standardized protocol. A lack of suitability concerning mix proportion and homogenization of the components, water addition, and pre-wetting of adjacent building stone including mistakes during application of rendering and its subsequent treatment during hardening find expression in the final product. Therefore it could be worth all the effort to trace this back by means of “finger prints” taken afterwards, provided that no admixtures for changing workability properties were introduced which unnecessarily complicated the picture. Many factors may influence test results, yet it is possible to deduce general trends. But this may be the largest handicap to a well-defined preparation having particular significance in a field where empirical experiences predominate. In any case, homogeneity provides the starting point required for exposure studies. Also some results recently obtained in characterizing salt distribution in porous brickwork after penetration by sulphate and chloride solutions, which lasted over months, may suffice to give an idea of problems met during preparation of samples for depth profiles [42].

One who is content with the customary mode of expression that a fresh mortar or rendering “clenches up” to its substrate should be made to clearly realize that the actual running processes may of course seldom fulfil this idealized conception, even though a plaster sludge saturated in calcium hydroxide can penetrate unhindered. How laborious it is in any case to microscopically detect interfaces with corresponding nonpoint contact becomes evident when one searches, e.g. in a polished section, for suitable regions at the boundary between plaster and brick [72], [81]. With the beginning of the industrial age, there also occurred a further development of plaster technology. So one could counteract against shortcomings as e.g. the presence of residues of burnt lime caused by incomplete slaking during a soaking process with the aid of an industrial slaking procedure. In this way results a more uniform usable mix, sometimes, however, leading to lower strength values of the final product.

More recent knowledge on the use of methods to characterize fresh and solid mixes (compare [90]) has given tools to a materials tester’s hand in order to advance, in quite another way, research which was being determined mainly by empiricism up to now, and this with the objective to systematically bring more light into the darkness of this subject that has been neglected for decades. So one encounters indications of uncertainty everywhere, even when dealing with the flow diagram shown in Fig. 8. How far one is still remote from the acquisition of defined characteristics relevant to plaster production is elucidated by a paper [78], which reviews the need for basic research in this field.

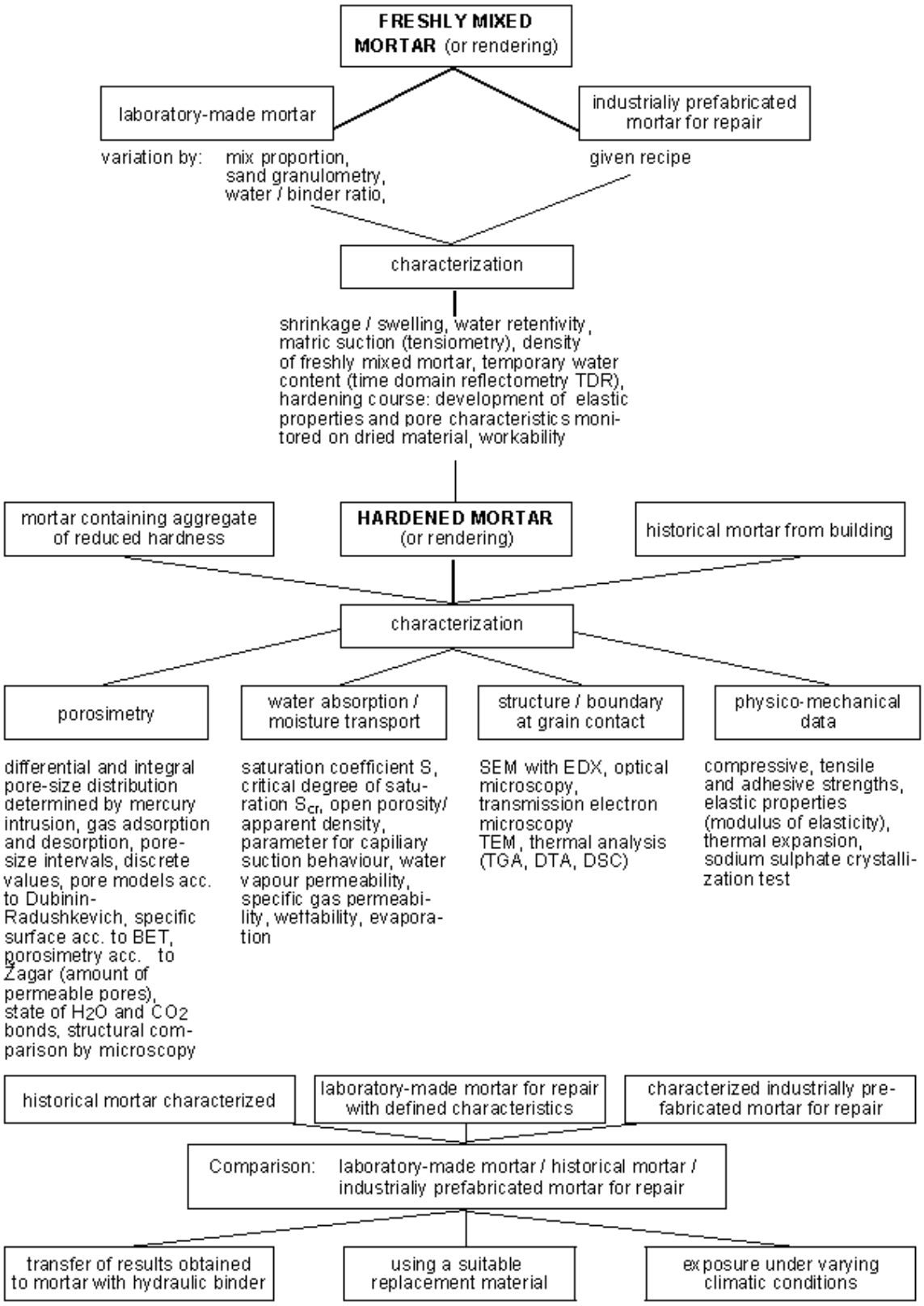

Fig. 8. Diagram of conceivable tests for characterising mortars and renderings

3 Rendering as a building material and the development of its structural features

A porous mineral material like a rendering or mortar can be characterized among other things by predominantly open and sometimes interconnected pore space being embedded in the matrix. In such a more or less homogeneous matter there play a role besides storage also diffusion, capillary rise and evaporation, provided that there exists a local gradient as a driving force. If anisotropies by formation or production, respectively, are not evoked the liquids therein can move uniformly in all directions. If it concerns a building's dampness, these dissolved salts and binding-agent constituents are transported along the pore space and are reprecipitated at given locations, whereby within rendering compacted zones enriched in binding agent as well as leached out and so mechanically weakened parts can originate in the long run. Such rearrangements however necessarily lead, by preference near interfaces to another medium, to formation of layers having different behaviour as they were described already by K i e s l i n g e r ([57], p.6) in the thirties during detection of the so-called sandy-mealy interlayer in weathering profiles of sedimentary stone. Here one can recognize a macroscopical appearance that under similar conditions at another place will be less distinct and rather corresponds to an intermediate state. Nevertheless, observations of this kind only gain access to relevant literature when the substance or aesthetics of a building have already become questionable (cf. [64]). This may be a reminder on the assumption of K ü n z e l [60], who describes a so-called resistance phase (duration of latent damage) occurring before the appearance of deterioration, which can possibly last decades.
Concerning sulphate distribution in porous building materials, the results of F é l i x [22] on a molasse stone of the Lausanne region can thus furnish some insights. On places sheltered from direct rainfall - caused by particularities of a building and occurring mainly at its northern side - the calcium sulphate shows considerable enrichment in the first millimetres of the profile, that finally leads to scaling off of parts formed in this way. In this case calcareous components of the actual crust interspersed with soot particles among other things, however, shall only be derived from original rock. On the other hand the material at a building's sides that is strongly stressed by rain or effluent water experiences only a relatively insignificant enrichment in the outer zone, but at a depth of 5 to 20 mm. For the cited type of weathering, the "normal content" is reached already, i.e. an elevated concentration with microscopically detectable cracks, which the author cautiously writes that they should not be interpreted with certainty as a consequence of damage. Equally clear evidence is missing on how far the frequently occurring precipitation loaded with CO_2 by migration within a pore system can also influence besides sulphate the distribution of a highly dispersive calcareous portion especially susceptible to SO_2 across the entire profile. In any case one cannot escape such a complex phenomenology, since here regularities were practically studied on one and the same rock type. So at least similarities may be assumed with the structure of renderings, for which reason factors determining the formation of such profiles could also be transferred accordingly to a large extent. But then size and ratio of surfaces of a plaster's body freely exposed to atmospheric contact in comparison to "sheltered" equivalents gain importance.
Mortar is the building material surrounding bricks and having a surface running parallel to their header or stretcher faces respectively, as long as cracks do not appear parallel to joints or peelings. Rendering contrarily represents a shell of a cyclically hardened mix of aggregate and binder and by preference vertically orient ed and exposed to one side. Depending upon roughness and cracks, it is subject anyway to a carbonation progress of more or less regular duration. Since a corresponding reaction face practically always goes along with capillary moisture transport, it is really effective in all directions. Under equal consideration as natural suppliers are dew water and rain, whereby all stages between complete saturation and the

isolated pore water film ought to play a role. Of crucial significance besides the local CO_2 offer is therefore each moisture content present, which incidentally also depends upon the mediatory role of adjacent building materials, i.e. with absorption, storage and release ability but also with its vicinity to flashings, as e.g. plinths. The distance from each free boundary face to its surroundings as well as frequency and duration of rhythmical moistening additionally determine the further course of conversion into carbonate. From an analytical standpoint, an investigation of overall volume-related CO_2 content would therefore not seem helpful, which is equally applicable to sulphate generated by reaction at a later moment. Therefore one should rather consider the kind and local enrichment of the salts for character izing the conditions. During pore space formation, of decisive importance with regard to packed assemblage of aggregate grains is the lime-hydrate portion and its degree of admixture as well as mixing water content, compaction and binding geometry. Solute partitioning, sedimentation and moisture transport in an early stage might hereto also furnish a contribution, particularly as early hardening is principally based upon an approach of the individual binder particles capable to be taken up one to the other. For this is the case of air-setting plaster drawing moisture from a raw mix, in order to bring about a compacted body together with the aggregate grains' framework [92]. Such a definition, nevertheless, may anticipate that one cannot so easily judge by means of relevant processes in contrast to the almost inert brick material, which this mix shall liaise to masonry or cover over as a rendering layer. It must not be especially mentioned that processes of manufacture in the course of putting on the multilayered plaster, as well as intensity of curing of rendered surfaces by smoothing or scraping, have influence on its texture and permeability. Formation of stratiform inhomogeneity ranges - how effective they may ever be - was discussed years ago [71]. In the same manner, this kind of layer formation can be contributed by the request expressed by certain construction firms and sometimes b monu ments' preservation people to treat rendering already present at a building with impregnants. Here it makes no principal difference concerning the actual existing state whether it thus deals with intermediate or final stages of an inhomogeneity caused naturally or even artificially by impregnating measures, although one can possibly detect which kind only indirectly by means of deformation properties, thermal, and hydrometric characteristics (compare also [61]).

Essential for estimation of the carbonation degree during sampling of rendering or mortar is its age being of utmost importance, of course. However, dating often cannot be carried out accurately enough. For to trust in statements made by house-owners and tenants or to find hints on it in building particulars and plans is still a matter of luck. By the way, comparable difficulties on the occasion of mapping natural stone components at buildings in the Munich city centre were reported by G r i m m and S c h w a r z [28], in whose program a similar judgement of exposure duration against atmospheric influences had been provided. A knowledge thereof however would be even more essential, since one has to consider that a substrate, especially if a mortar joint is present there, proves to be a reservoir medium for processes of material migration when affected by moisture. Almost gloomy in the case of rendering is the ignorance on its structure, above all regarding circumstances caused by a particular physical condition on a building. So practically no experiences are available on deviating development of an external ceiling plaster on a balcony during application and afterwards in contrast to its equivalent at an above-grade masonry. So probably under the influence of an intrinsic local load, perhaps scarcely perceptible differences are initiated with respect to hardened mortar properties which nevertheless can later on become meaningful for mechanical, thermal or hydrometric behaviour.

For a system mortar/building stone the following arguments may still finally be added complicatedly: One can hardly satisfactorily characterize most essential properties of fresh and hardened plasters in a quantitative manner. Also mutual relations within mortar/substrate combinations of any kind remain furthermore unclear so that the effect of a rendering base on

plaster can be reliably estimated just slightly. That means that this deals with imponderabilities not only deriving from the presence of both constituents of bond, but also from their mutual influence which make such a system complicated at a higher level. One could eventually clarify this dilemma by means of capillary moisture transport, where for binding conditions at the interface of both media, besides water retentivity and evaporation behaviour, pore volume and size distribution are responsible. How many uncertainties must still be cleared away in order to be able to understand and experimentally capture at least partial aspects of the processes! Up to now nothing is yet said about the kind of plastering, let alone on placing at quoins and flashings, which however would be interesting for questions on the effect of a mechanical abutment. For such fresh plasters with their intrinsic factors influence consolidation processes during setting and carbonation, and that occurs hand in hand with locally conditioned changes of moistening and drying, whereby developing calcite crystals coarsen at the same time (compare [69]). In the late stage of hardening, i.e. after dessication for the first time of the fresh rendering applied, moisture transport is not only controlled by diffusion but - corresponding to local placing at the building - also by capillary conduction of liquid water which when loaded with carbon dioxide sets the “lime cycle” going. This ought to be the main factor of that cyclic recrystallization of carbonate at the expense of small particles. In the wake of these stages - disregarding for the time being an unavoidable structural weakening - there is thus developed a binder matrix by a diminishing of its reactive surface, which in the long run is really more resistant since it is less subject to attack; this can finally be cited as an advantage of an old plaster. One should also not forget that the reaction with SO_2 starts at nearly the same time.

During discussions on lime mortar and rendering, it is often overlooked that it does not deal with a simple binary system of aggregate and binding agent. Rather next to it is present the pore space, which - intragranular or intergranular - just does not represent only an air-containing void, but causes among other things a kind of leaning effect and moreover serves as a reservoir space and above all a transport for moisture and solutions. But even this complex framework made of aggregate and a mix of binder, water and air being a configuration which aims in the direction of the ternary system aggregate framework/binder hardening over a long time. Pore space can only be imperfectly comprehended by quantifying scientific methods. This is not only true for differences given by a binder’s manufacture, but for geometric arrangement of individual constituents in the final product, which just according to its exposure is also subsequently subjected to atmospheric influences. In the case of historical material as a rule, it still deals additionally with a more or less developed hydraulic component, whether it comes from a binder’s raw material itself, from activation at a boundary face to the aggregate grain as a result of a common slaking process as it was exercised in former times, or it would be introduced deliberately by means of pozzolana-containing admixtures, as e.g. clay brick chippings or dust in order to finally improve mechanical properties of the plaster. In this circumstances are again becoming confused, so it hardly appears surprising if a local or chronological assignment, being also specific for composition and production, pushes to insurmountable limits.

Most problems may exist therein to overview and state compulsorily the respective significance within a spectrum opening necessarily of all possible characteristic values [54]. Equilibrating processes from pore to pore - also via vapour phase - and migration of highly soluble salts directed to gradients of concentration and moisture play a role. Locally different moisture contents can also partially lead to temporary losses in strength of the grain binder. This is above all important in connection with volume changes caused thermally and equally dependent on location. For a tiny modification of aggregate mix not only brings about a change in grain packing but also that of the water demand for plaster production, which after evaporation of residual water will finally be expressed in a different pore structure. Such complications however lend recognition that a partial replacement of any kind of the mix -

whether by a solid matter with given grain-size composition or a liquid admixture within a certain volume - modifies binding geometry of single components in such way that e.g. convenience of a comparison with a material "without admixture" becomes uncertain, because there a reference point simply leaves the field of vision. Furthermore a change of that framework is namely not only influenced by number of next neighbouring ones related to individual structural grain and the given contact points, but as well as by space filling through the grains' framework.
When remaining by an analogy of lime plaster and sandstone having calcite as a binder, one can find spectacular differences. Whereas in natural sediment over geological periods the grains' binding agent densified or consolidated because of alternating conditions of dissolution and reprecipitation, so diminishing its total volume in the course of diagenesis, plaster had less opportunity for that. The necessary consequences in the latter case were mostly a point contact only between binding agent and aggregate. It has proved even more difficult to make visible at all a full-surface contact between plaster and brick in a microscopic image of a thin section ([72] , compare also Fig. 9). Such a bonding full of gaps between the components did reduce the overall strength, but on the other hand supported the material's flexibility during volume changes.
Only after periodic moistening and drying as occurring in a rendering shell over a long duration can a comparable consolidation therefore take place.

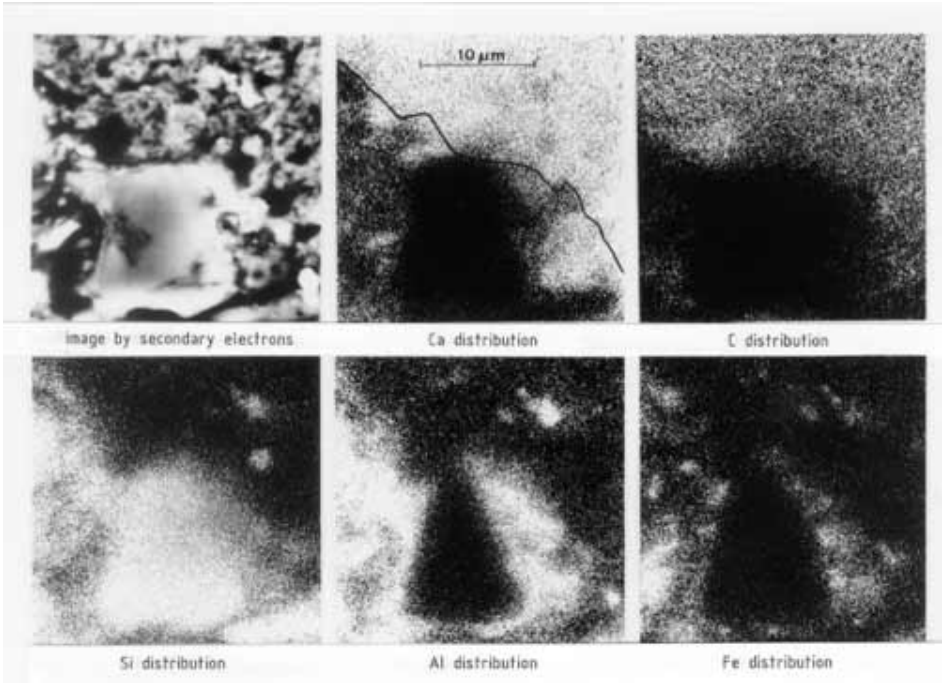

Fig. 9. Electron microprobe analysis: boundary layer between masonry brick and lime mortar

Former interpretations bringing weathering processes exclusively together with beginning or total dissolution of grain boundary basically apply to facts revealed. One rather has to take seriously for this the differing thermal expansion of individual rendering constituents, influencing thermal gradients and damage through volume increase by the combined effect of moisture and frost as well as hydrating or crystallizing salts. Also in this case a clear drawing of limits is scarcely possible, with which an obstacle is once again placed in the way to the need of a stringent definition for the term "weathering of mineral building materials". In all cases the impression appears as if the phenomenon "layer formation" would be always liaised to a shorting brought about by manufacture and/or a loss in homogeneity.
Concerning respective strength achievable and maintainable for a long time, only a few aspects at all are hitherto known. A plaster system limited and wedged in marginally by a

further rigid material is namely subjected with regard to formation and lifetime to several processes which overlap one another and are sometimes really counter current. So cohesion and therefore long-term behaviour - in order to cite a few of them - are not only influenced by calcite crystals' coarsening but also in early hardening through the leaning effect, which plays a role in mutual action with surrounded aggregate grains and primary pores in the case of those hydrate particles well-digested during lime soaking (cf. [80]). A comparable mechanism as is based upon the original ion-dispersed side-by-side of Ca and Mg portions in a dolomitic plaster [82] ought to be equally important for strength development. Further factors are leaching out of binding agent or becoming brittle in the course of cementation processes of single components, which causes differences in their hydrometrically and thermally conditioned expansion and so eventually leads to cracks that are mostly close to grain boundaries.

The presence of microorganisms contributes without doubt to the layer formation already cited. Nevertheless, its effect is not only based upon clogging of transport paths for moisture but above all on the hygroscopically active behaviour of a slimy biomass the kind and quantity of which depends quite essentially upon pH value and prevailing microclimate and thereby increases the material's moisture. Leaving aside the less frequent case of damage close to a surface, e.g. by working with a blunt tool, so can sedimentary rocks - apart from their stratification - be considered commonly as fairly homogeneous with respect to physico-technical properties, for which reason such a phenomenon only occurs after longer service exposure e.g. in the course of alternating moisture migration or SO_2 attack. This is not so with rendering which already during putting or throwing on and trowelling has developed a distinct texture parallel to the external surface so that there inevitably result uncertainties in conse quence of their juxtaposition for the results of hardening and weathering. In other words: One could hardly explain in what way a strength profile, e.g. determined through abrasion, is in fact causally connected to one or another possible formation process. The trigger for this is finally fronts of diverse effective mechanisms having differences in prolongation velocity and temporal sequence. Under these severely controllable starting conditions, it already will come to a reaction with an atmosphere containing sulphur dioxide and that after all during an early phase of setting and before carbonation starts. Thereby one should not give rise to any doubt that for lime components during exposure to be considered as a reaction partner, it is not only the important average concentration in air but rather the significant immission rate. The latter has to be defined according to L u c k a t [63] as "the quantity of noxious pollutant absorbed by a surface area unit in a time unit". Also herefrom it is revealed how diverse and so hardly surveyable the processes are, and what should be considered when planning test techniques.

Neither an enrichment nor a distribution of reaction products of any kind, which originate from isochemical or allochemical conversions, necessarily lead to weakening of material structure, because by means of crystal growth, e.g. of $CaSO_4 \cdot 2H_2O$, the pore system first of all is only narrowed but damages can indirectly occur in the wake of forming moisture traps (compare [69]). In what disposition - from crusts of parallelly running crystal aggregates to whisker-like single species - gypsum crystals attain precipitation and fill up pore space obviously depends thereby upon solution supply and local moisture conditions as tests with sodium nitrate carried out by Z e h n d e r and A r n o l d [108] also suggest. This local chemistry must not vary remarkably, whereas at the same time physico-technical properties underly a profound modification. Such findings can furnish no more than hints thereon what difficulties one has to take into account when judging quantitatively the before and after during the exposure event. These experiences finally also diminish the expressive force of depth profiles, as they are known from EDX analyses in scanning electron microscopy. In order to satisfactorily describe a temporal state, however, one should rather strive for a profile-like plotting of a parameter of mechanical strength [51] or that of a pore characteristic. Layer formation itself is not to be considered as a concomitant accordingly but as one of the

main causes of weathering. In the course of long-term exposure of building material in the open air, it is at the same time a motor and object of stresses, and finds its expression in the change of structure and chemistry. In such way new geometrical circumstances are originated little by little, within material or its open pore space, which eventually also cause a modified penetration and permeation of fluids.
One can observe again and again that during moisture transport, soluble salts precipitate close to an evaporation face near a material's surface or immediately beneath it. This is true in the case of plaster for chemical compounds originated by reaction between one component and atmospheric agents as well as those in which it contains a priori, like e. g. calcium hydroxide. As a weathering protection of a building this is exposed to attacks of chemical and physical kind as well. Aggressive media, i.e. above all those reacting with the binder phase, do not exert their effect so regularly on the entire material's volume. Local geometry of the rendering and also the possibility of dew formation or dispersivity and covering of crystal surfaces with reaction products which finally give rise to a gradient, namely considerably influences each behaviour. The basis for it besides gas permeability is also capillary rise connected directly to pore-size distribution. Hereby there can be equally generated a heterogeneity perpendicular to the surface which in addition overlaps textures as a consequence of manufacturing and carbonation. To reconstruct later these spatially and temporally different processes causing the state of depth profile is virtually hopeless. For regarding itself, each of them is a quasi starting point for the following one. In order to obtain here a general overview, an appropriate digestion method is needed as for instance a water extraction. With its aid one can analyze water-soluble compounds without favouring an undesired dissolution of less typical constituents. Because of large scattering in this type of tests, single findings are not of utmost importance, whereas tendencies merit closer consideration in any case. The central problem of deterioration, however, consists of kind and intensity of processes hereby effective.
Whilst a lime-containing sandstone with a less developed pore space will react in a specific manner to its structure by a differing depth position of the already mentioned "sandy-mealy interlayer", one can expect such formations in rendering profiles only when a tightening crust composed mainly of salts and soot depositions produces a condition for this. Since the pores are mostly too coarse, which then have to be clogged, it only seldomly succeeds. In such a case one has nevertheless to expect therewith that because of the rather small mechanical cohesion in a possibly originated weakening zone, webs of solid matter break and then a surface-parallel layer in the form of a shell is blistered off, so that this process shortly can begin anew. Since a corresponding behaviour is advanced above all by a high reactivity of binding agent, e. g. dolomitic hydrate and a strong soot immission, one can therefore hardly encounter it outside a combination of such factors.
Of course one has to visualize that most damage is based upon different causes which are important if selective information on deleterious main factors is desired. This may lead thereto that apparently secondary influences unexpectedly turn out to be primary ones. Although problems arising during analysis of such materials were already described before more than a decade ago (e. g. [70]), they are simply not borne in mind at many places. Equally often was encountered a lack of comprehension that temporal chemical and mineral composition each do produce a basis for SO_2 attack, but dispersivity of reactive phases and pore structure intrinsically represent sensitive points during the physical stress. To analyze these relationships was among others a task of the research program. Of course characterizing physical data on buildings including their changes and shift of elemental concentrations in depth profiles are in the forefront of these endeavours.

4 Characterizing the material and its modifications

Lime-plaster technology - supported by accompanying tests having a scientific standard - was a predominant thought in the last century up to the beginning of the First World War. Apart from exceptions, this theme only comes into the field of vision again during a reconstruction phase after the Second World War. Until finally in the way of increasing mechanization of plaster manufacture and the standardization connected therewith, a displacement took place in favour of more cement-containing binding agents. The range of experiments for characterizing fresh plasters and its final products before an exposure, however, with respect to structural characteristics is not particularly developed nowadays. Hereto may have contributed the fact that hydraulic portions underly a continuous change by neo-formation of calcium hydroxide and calcium silicate hydrates naturally backfeeding on the structure. Equally a small thickness of a mortar layer relative to its extension produces difficulties, especially because of a stratiform protrusion of carbonating reaction whereby one can only restrictively obtain a specimen of acceptable size and having characteristics remaining the same. One could remedy this circumstance by using e.g. a limestone having high porosity and reduced size of single crystals. This again, however, would show less inclination to reaction with sulphurous air pollutants, which would be disadvantageous in being contrary to rendering provided with a lime hydrate component of high dispersivity, but which needs more time for its hardening. Deviating from building practice conditions, one can nevertheless achieve a regular almost overall CO_2 reaction when storing plaster in the laboratory, especially at a high air humidity.

For profile-like characterizing, e.g. after different exposure time, the small number of procedures appropriate for such investigations proves to be an obstacle. For it is always lacking homogeneity perpendicular to a material's boundary with the atmosphere, which gives rise to considerable restrictions of tools due to experimental technique or allows only to obtain untypical mixed values for a characteristic. The least problem is a grasp of its chemistry. Besides the already mentioned thin stratification standing in the way of investigating a homogeneous material of given size, in the case of rendering its experimental handling is aggravated by friability combined with a reduced cohesion of single components. So this is easily subject to an impairment of the grain bond characterized mainly by punctiform contacts - whether by dissolution processes or mechanical stress as a result of different thermal expansion behaviour of aggregate and binder or in the presence of moisture.

In order to clear up weathering results on rendering concerned, one first has to find out material characteristics which behave so that detectable or even measurable changes can be obtained during this process. These can be of phenomenological or structural type and are as a rule being determined indirectly. With regard to a corresponding analytical instrumentation it is sometimes not yet possible to say whether one can expect a useful outcome or not, even if all possible precautions have been taken. Another difficulty arises not only due to the shortcomings of appropriate test procedures but also with the long experimentation time, after which one can assess their usefulness. Despite this, corresponding attempts to foresee whether appropriate results will ensue may not be possible. Therein, however, exists one of the principal problems. Namely one observes a change caused by chemical reaction, detectable microscopically but not in measuring parameters related to pore structure. For instance, if blocking of the pore system by crust formation due to SO_2 attack takes place, a corresponding effect cannot be detected when the pore channels' diameter before and after coating by expected reaction products show such a dimensional ratio that measuring makes no sense. According to this classical point of view, it seems useful for the time being to monitor enrichment or depletion of any chemical constituent by the distance from the material surface into its interior.

4.1 Properties and characteristics related to pore space

Much damage on buildings has to be associated with the effect of water. So impairment of mineral building materials frequently has as its cause the dissolving, transporting and reprecipitating of highly soluble often hydrating salts, and that occurs in pore space and at a material's surface. This entirety is favoured by moisture fluctuation or as a consequence of freezing, the excessive portion being in brickwork. The extent of moistening does depend upon absorption and filling degree of pores with water respectively, so that corresponding material data essentially contribute to characterizing of porous building materials. Pore space, especially its open portion suitable with regard to moisture transport, is therefore decisive for weathering behaviour.

A real crust formation on mortar and rendering cannot be excluded, which however is less likely in most cases. So the greatest part of external building layers produced in a comparable manner as mortar designation might hardly ever reach such a state. Required strength gradient in the direction to a building's external side already demands a rather "open" structure while producing this material. Nevertheless, some instances give evidence therefore that in single cases with increasing exposure, it really can come to a compaction near the surface. For this there are doubts whether one can always monitor by tests the influence of measurable permeability. With this reservation here there will be reproduced first of all methods describing the pore space indirectly, as far as they have been practically relevant for the present task.

4.1.1 Pore-size distribution (Mercury intrusion porosimetry)

Principle of method

The pore space, in which moisture and gases are able to migrate, shall be examined. Of crucial importance hereby is the distribution of pores besides their volume, which can be determined by means of a mercury porosimeter test. The apparatus applied operates according to a method presented by R i t t e r and D r a k e [91] and P u r c e l l [86] as well, by which mercury as a non-wetting liquid is pressed into pores of the evacuated material. The contact angle equals >90 so that it normally does not enter small pores. An injection pressure only has to overcome counteracting capillary pressure before the void will be filled therewith. Under the simplifying assumption that it deals with cylindrical pores, pressure p affects their cross section πr^2. Into counter current direction from surface tension results the force $-2\pi\delta\cdot\cos\vartheta$. In an equilibrium state both forces are equal. Hence it follows

$$\pi r^2 p = 2\pi\delta \cdot \cos\vartheta \qquad \text{eq. (1)}$$

In this equation:

p = injection pressure
δ = surface tension
ϑ = contact angle and
r = pore radius.

In this δ and ϑ remain almost unchanged. Surface tension fluctuates between $484.2\cdot10^{-3}$ N/m at 25°C and $472\cdot10^{-3}$ N/m at 50°C. Commonly a value of $480\cdot10^{-3}$ N/m is taken. The differences in the contact angle of mercury are between 135° and 142° according to its degree of purity. One has measured 141.3° for silicates.

When solving the formula towards r it is obtained:

$$r = \frac{2\delta \cdot \cos\vartheta}{p} \qquad \text{eq. (2)}$$

Therefrom it results that with growing pressure the narrower pores are filled up increasingly with mercury. Regarding its accuracy, the procedure is restricted by the following conditions:

1. Calculation starts from cylindrical pores whose ideal shape is by no means typical for a building material's structure.
2. During mercury injection into pore space, local structural damage may be expected.
3. As a main source of errors, a contribution of bottleneck pores to the measuring result is to be observed.
4. If material contains hydrate water compounds, cracks can be originated during dessication and vacuum treatment in such way to also falsify the result.

Application field

For determining pore-volume distribution, an apparatus produced in series and operating on this basis was used. With it one can generate pressures up to a maximum of 0.2 MPa for pore radii between ca. $75 \cdot 10^3$ nm and 3.75 nm. Radii distribution will be traced as a histogram or a cumulative curve. From their course one can gain data for judging the frost behaviour by associating with certain size intervals.
Dried samples of about 3 to 6 g having a grain size of 3 to 5 mm will be brought into a dilatometer vessel of 20 cm^3 volume. After evacuation down to a pressure of 0.2 mbar, one fills the receptacle with mercury and measures its height. Later on it will be aerated, whereby Hg penetrates pores dependent upon each air pressure. The corresponding volume can be calculated from the changing Hg meniscus, by which one obtains the portion of macropores. Then the test vessel will be transferred into the actual porosity meter and submitted to an automatically controlled pressure increase. The relation between recorded pore volume V and Hg injection pressure p is shown in Fig. 10.

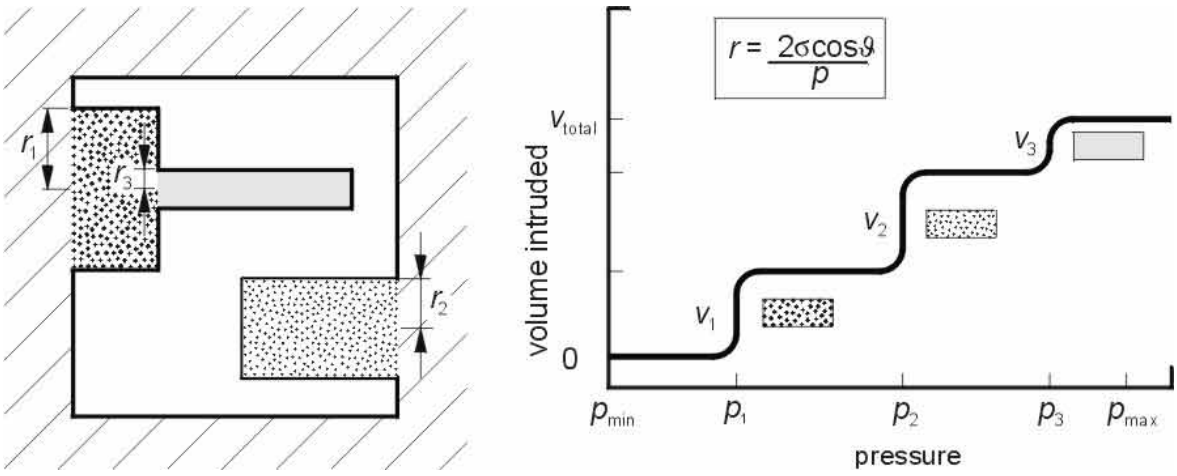

Fig. 10. Schematic diagram of mercury intrusion in pores of different size (by courtesy of K. R ü b n e r)

Presentation of results

By H i r s c h w a l d [35], who defined saturation coefficient, it was already recognized that a close connection exists between pore-size distribution and frost stress or damage by salt crystallization respectively. With this point of view, values obtained by means of measuring

pressure and volume are presented by the cumulative sums of pore volume in dependence on the logarithm of pore radius r. From such curves one can now select certain intervals. So H o n e y b o r n e and H a r r i s [53] defined a so-called microporosity, whereunder one has to comprehend the portion of open pores ≤ 5 µm diameter. This takes into account that smaller pores generally participate sooner in decay mechanisms than coarser ones. Material whose microporosity amounts to > 30% should be no more resistant according to the authors' opinion.
For ceramic products, D ' H a v é and M o t t e u [8] used the mean critical diameter d_{10m}. Hereby it deals with the pore diameter of the upper 10% fractile of an entire pore volume determined by means of the Hg porosity meter test. If the corresponding value exceeds 3 µm a material is said to be frost-resistant. But one commonly fixes it at 2 µm. The lower limit is defined whereby water does not penetrate into fine pores, whereas the upper limit is marked in such way that coarse pores show a tendency to be incompletely filled. For characterizing renderings of the type tested and in as far as being transferable from ceramics, however, it does not bring the expected benefit, because in the case of lime plaster it mostly exceeds the measuring range of the method. Also for porous ceramics R a v a g l i o l i and V e c c h i [87],[88] cite an interval between 0.25 and 1.4 µm in diameter. It is expressed as a portion of total pore volume and in the following is also designated as R interval. At pore sizes of ≤ 0.25 µm, no frost damage is said to occur and at such ones ≥ 1.4 µm only in severe climates. When the portion of pores within the interval amounts to more than 25%, a brick should be no longer resistant. Also the median corresponding to the 50% fraction of the frequency curve seems to be successful.
By test results with regard to alteration processes obtained for historic renderings M e u c c i and R o s s i - D o r i a [67] e. g. furnished already corresponding hints, while bringing an increasing tendency of conversion to sulphate into connection with rising porosity and pore size.

4.1.2 Specific surface area (Gas adsorption)

Principle of method

The entire surface area of a material is formed of external geometric contours of its constituents and the internal surface area as well. The latter is composed of the entirety of pore walls' surfaces and such of primary particles. These can only be determined if they are accessible for sorption of a gas. For this the low-temperature nitrogen adsorption according to B r u n a u e r, E m m e t t and T e l l e r (BET method [4]) is applied, which has been proved as a standard procedure. Analyzed is the dependence of adsorbed gas quantity on equilibrium gas pressure p at the temperature of liquid nitrogen. In a defined pressure range, one can represent adsorption isotherm as a straight line from whose slope and the axis section a monolayer capacity is calculated, whereunder the number of gram moles of gas is to be understood which is required to form a monomolecular layer on the surface area of 1 g of substance. Using Loschmidt's number and the area demand for a nitrogen molecule, one finally obtains specific surface area. Principles of the method are treated in DIN 66 131 [14].

Application field

Reaction behaviour of a material in contact with its surrounding is among other things determined by the size of its surface area as it becomes conspicuous in the case of adsorbants such as activated carbon or catalyzers. Also the binding characteristics of plaster of Paris, cement, lime, and also ceramic masses are influenced by specific surface area or particle size respectively. The method of low-temperature nitrogen adsorption has found widespread application also in the case of all porous building materials. It was discussed in relevant literature being cited in excerpts [21], [25], [27], [33], [56], [85].

Preparation of samples

The sample's mass for investigation complies with an expected specific surface area. However, one has to take into account that in case of a large mass of test portion, the volume constancy of a measuring vessel can be impaired. So it is advisable to dry material at test start to constant mass. With regard to hydrate-water containing samples, one has to consider that temperature is not chosen too high, since other wise the crystal structure as for gypsum $CaSO_4 \cdot 2H_2O$ can be destroyed which would result in an increase of specific surface area. The same is true for subsequent out gassing in a dry nitrogen stream. For sensitive material like clay or so, the sample should therefore only be evacuated. Afterwards the adsorption vessels are cooled to room temperature under flowing measuring gas, and evacuated vessels are filled with nitrogen. The closure of vessels with a stopper finishes the samples' preparation.

Mode of operation

A "one-point" method according to H a u l and D ü m b g e n (DIN 66132 [15]) serves for determination. Use was made hereto of a surface-measuring device "Areameter" constructed by the firm Ströhlein, where absorbed gas quantity is measured volumetrically. One adsorption vessel with the sample and the other of the same volume used for reference are both filled with nitrogen of identical pressure (atmospheric pressure) and cooled subsequently to the temperature of liquid nitrogen. Uptake of measuring gas by a sample causes a pressure difference between vessels for adsorption and for comparison which can be read on an oil differential manometer. From this and the filling pressure (atmospheric pressure), one can calculate nitrogen quantity adsorbed by a sample. Equilibrium pressure in the adsorption vessel adapts automatically in the BET range because of cooling. The surface area size is calculated according to BET theory on the basis of a "one-point" evaluation.

Presentation of results

The surface area obtained in m^2 is generally related to a sample's mass, and that to 1 g. A volume-related indication is often difficult, but nevertheless sometimes seems convenient. Since the pore structure of weathered samples was modified, in comparison to their unweathered equivalents, surface area values furnish interesting hints on chemical conversions. Interpretations of results, however, should always be left to an expert. The surface area registered with the available apparatus reaches from ca. 0.1 to 1000 m^2/g, whereby ca. 6 to 50 m^2/g are indicated in the case of a 1g mass of the test portion. The weighed sample has to be correspondingly varied for other ranges.

4.2 Moisture transport characteristics

4.2.1 Capillary water absorption

Principle of method

Capillary moisture rise is a characteristic of each fine pore material provided that for this a common connection between pore channels produces the prerequisite. Dynamics of liquid transport are mainly influenced by surface tension forces as well as pore-size distribution and are based upon the equation

$$y_s = a \cdot \left(1 - e^{-b \cdot t^{0,5}}\right) \qquad \text{[41], [42], [94]} \qquad \text{eq. (3)}$$

where y_s denotes mass of liquid absorbed at the time t and related to surface in kg/m^2 and a is the maximum liquid mass reached in kg/m^2 absorption area, where as b having the unit 1/h$^{0.5}$ is a factor involving length-related water penetration coefficient, absorption velocity and pore space filling. In this formula being also valid over long duration (cf.[101]), one finds the square root-time expression, being hitherto considered directly proportional in another place, namely on the exponent level of the function. One can define a water absorption coefficient w at the time t = 0 as being the product w_o= a·b. If a material's structure at contact with rising moisture is not remarkably modified, i.e. it behaves as inert, and w_o remains as a proper characteristic value. If then a is elevated, e.g. by increase of surface tension through an admixture of a salt, or lowered by means of a surfactant, b changes automatically in a reversed sense [102]. A testing effort for gaining these parameters remains within limits. More particular information hereto is given in previous work [48], [73] (the corresponding algorithm is part of a FORTRAN programme existing at the Federal Institute).
Since for a reliable determination of w_o, satisfactory stability of a as well as a b being prerequisites, the curve should be plotted near to maximum capillary absorption height s_{max}, so sometimes requiring an increased time. Best results are obtained if this so-called capillary head is situated within a specimen's dimensions, i.e., the material of which, as also influenced by accessible pore volume and portion of capillary-active pore size, really per se determines its absorption height or length, although such a statement may not amuse standards' writers at all. The product a · b, however, will be already only insignificantly modified at a former time. Basically parameter a should serve really alone as a unique scale for characterising capillary liquid rise. If specimen height is chosen so that it still just involves s_{max}, one could namely forgo b. Since due to a sample's dimensions, the required distance for complete rise is frequently unavailable, especially for highly porous material it must remain with application of w_o. Moreover, one should confront that misleading opinion that anisotropic behaviour caused by stratification, e.g. in sedimentary rock, plays a crucial role for the test result. Then the conception of a simple net capillary rise in a perpendicular direction, however, has to be finally qualified in such way that each region once moistened by test liquid operates as a starting point for a transport in every spatial direction. For only in the case of embedment of a strongly intensive retardation, as e.g. argillaceous layers or an accelerating effect as a rule already macroscopically recognisable, can one experimentally provide evidence upon the influence of w_o. Disregarding a material's hydrometrical inhomogeneity, there are other sources of inconveniences and misleading conclusions. Consequently the results obtained can be influenced, especially when not considering the intensified evaporative effect near a zone of maximum absorption height of a monolithic specimen having an elevated maximum liquid mass related to surface area a. Although a dense coating of its contours by impregnation can rather impede this process, such a measure is effective only in the case of a non-excessively

high water absorption coefficient. Otherwise one has to contend with air inclusions impairing each weighed mass. Thus corresponding steps should be taken into account in order not to obtain inaccurate values for w_o, that are again unstable after a longer duration as was originally present at a test's start, namely when the velocity of absorption is reduced to less than 5% of that prevailing initially (cf. [101]). So it seems sometimes advisable to predict the appropriate interval for weighings as a result of preliminary trials. At any rate all such aspects have to be considered when applying e.g. the annex of the standard EN 1925 on determination of water absorption coefficient by capillarity [20], i.e. determining one of the most significant characteristic values concerning weathering phenomena in our latitudes. Different respective test methods are thereby required in order to maintain a test liquid's level constant (Fig. 11) as well as for the type of plotting of weighing results (Fig. 12).

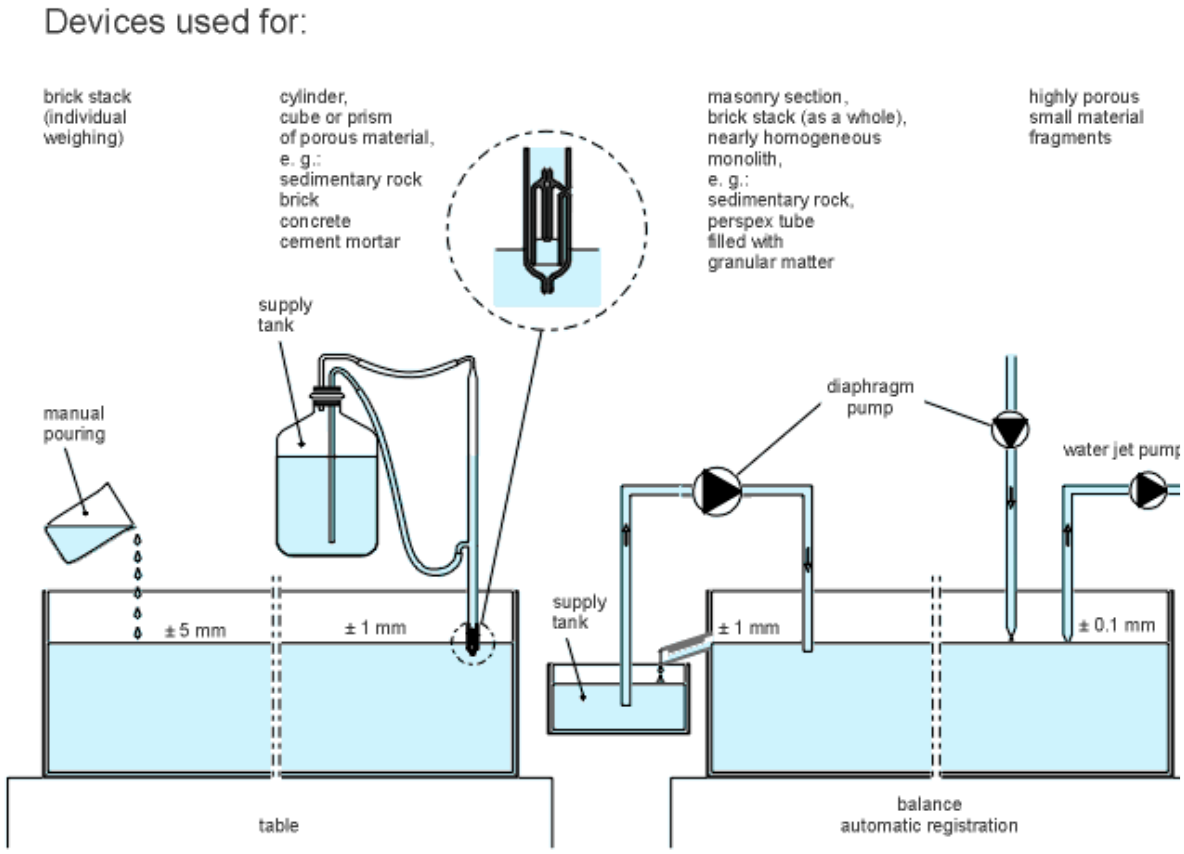

Fig. 11. Various possibilities of holding a test liquid's level constant (the corresponding device(cf. [52]) within the dashed circle can be separately enlarged. It is based upon the same principle as a simple automatic bird watering-place.)

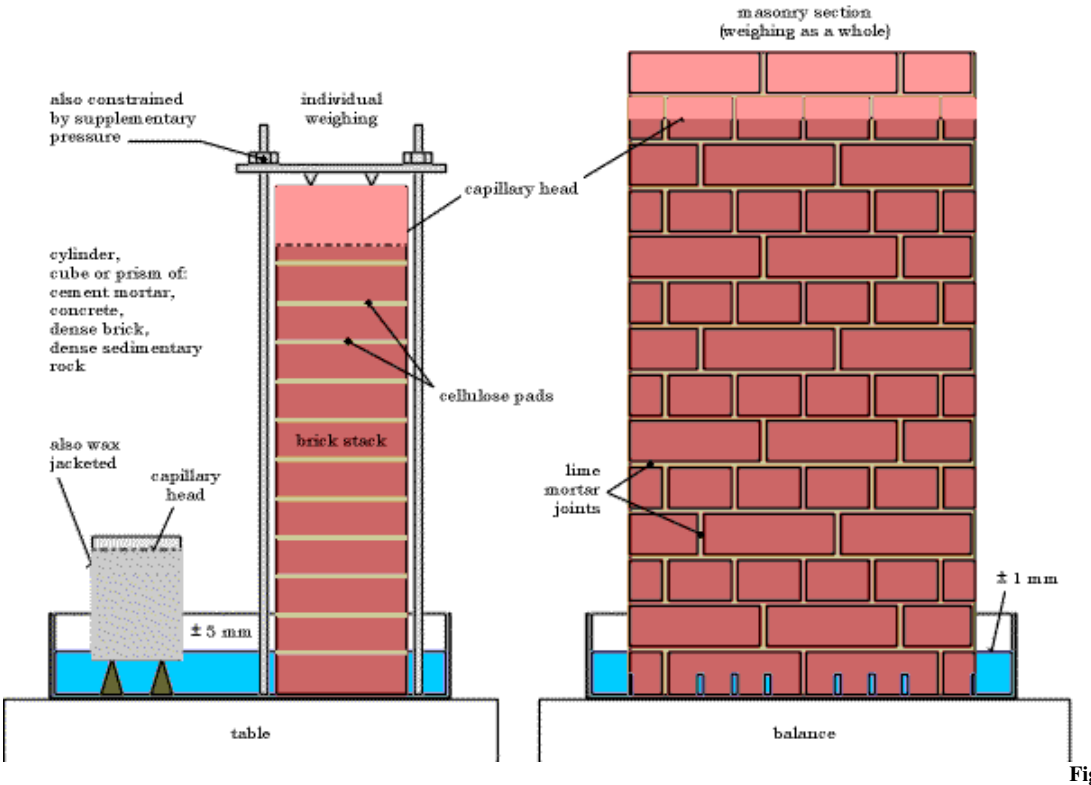

Fig.: 12a)

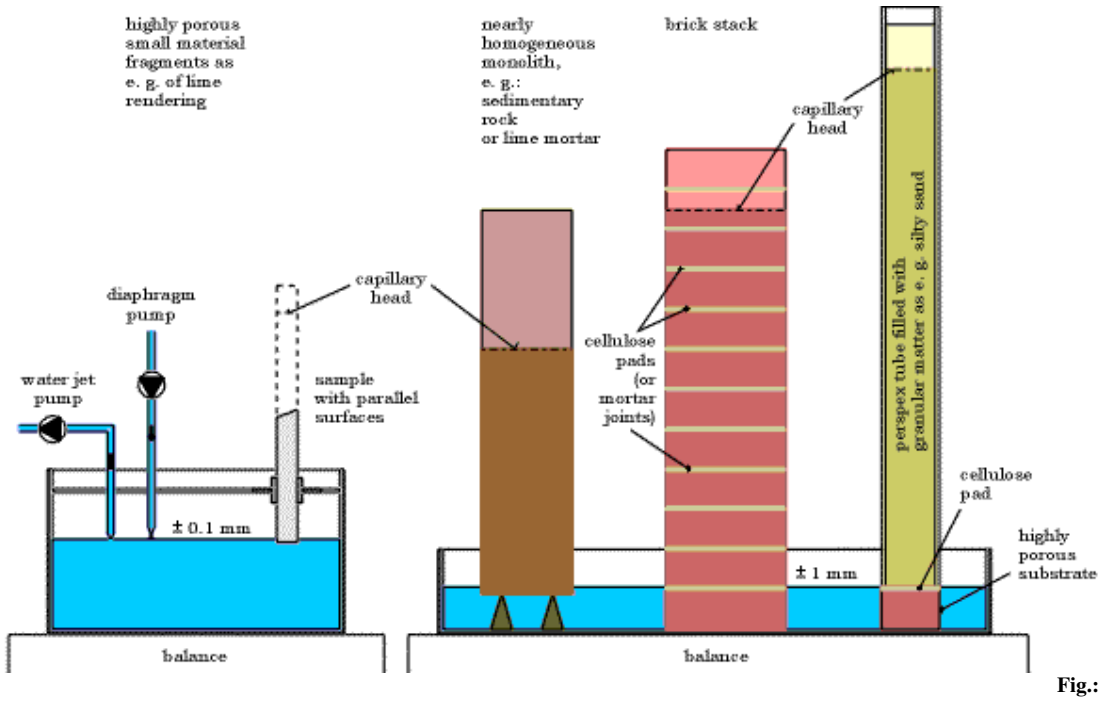

Fig.: 12b)

Fig. 12. Methods of periodic weighing: a) by hand b) automatic registration of the entire test setup

Thus it is advisable to choose corresponding procedures due to hydrometrical characteristics which are specific for each material.

The above-mentioned monolithic specimens as fragments of rendering, drilling cores of brick or blocks of natural stone and even masonry units (cf. section 5.8) do serve for gaining those basic capillary parameters as described, nevertheless by concealing the complete spectrum of obtainable information. Only such material in columns consisting of integrable single elements, as e.g. a natural stone block subsequently cut into slices or - for the present case - an assembled brick stack both of course coupled hydrometrically by inserted textile pads in

between, can moreover furnish some additional characteristics as maximum capillary absorption height, water capacity and diverse post-suction data, the corresponding formulas for their calculation being shown in Fig. 13.

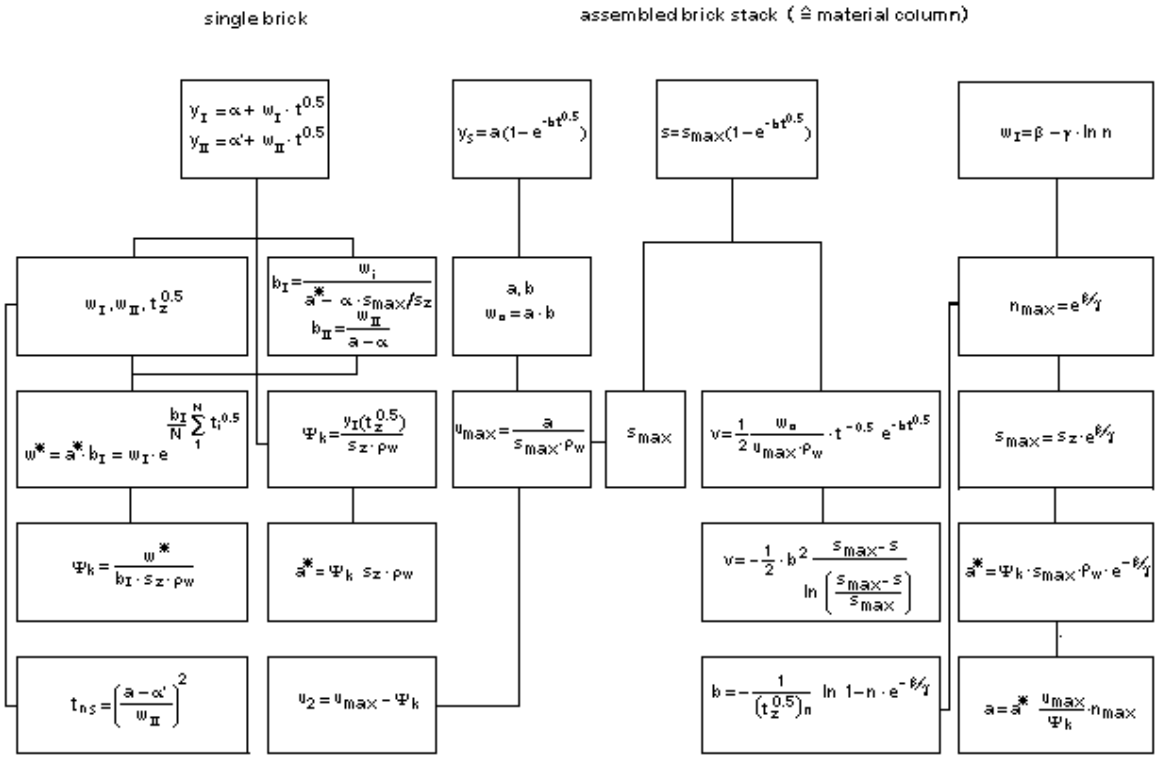

Fig. 13. Compilation of formula expressions deducible from experiment and describing liquid transport in bricks containing capillary-active pores

Formula signs: Symbols and units:

a - maximum liquid mass in a material column related to surface area in kg/m^2
a_1 - liquid mass related to surface area when s = s_{max}, in kg/m^2
a_2 - liquid mass related to surface area during post-suction phase in kg/m^2
a* - liquid mass in a single brick related to surface area when s = s_z, in kg/m^2
b - length-related water penetration coefficient in h$^{-0.5}$
b_I - length-related water penetration coefficient for primary absorption phase in h$^{-0.5}$
b_{II} - length-related water penetration coefficient for post-suction phase in h$^{-0.5}$
n, N - position number of bricks (n = 1 = most inferior position during measurement)
n_{max} - maximum position of brick just still achieved by moisture front
s - absorption height in m
s_{max} - maximum absorption height in m
s_z - height of single brick in m
t - time in h
t_{ns} - time of post-suction in a
t_z - time when $y_I = y_{II}$, in h
u_2 - moisture content based upon post-suction, in m^3/m^3
u_{max} - maximum moisture content in m^3/m^3
v - velocity with which moisture front migrates in m/h
w_o - a · b; water absorption coefficient of material column at t = 0, in kg/(m^2 · h$^{0.5}$)
w_I - water absorption coefficient for primary absorption phase in kg/(m^2 · h$^{0.5}$)
w_{II} - water absorption coefficient for post-suction phase in kg/(m^2 · h$^{0.5}$)
w* - water absorption coefficient of a single brick related to surface area when s = s_z, in kg/(m^2 · h$^{0.5}$)
y_s - liquid mass in a material column related to surface area in kg/m^2
y_I - liquid mass in a single brick related to surface area during primary absorption phase in kg/m^2
α,α' - constants in kg/m^2
β,γ - parameters specific to stack type in kg/(m^2 · h$^{0.5}$)
ρ - apparent density of brick in kg/dm^3
ρ_w - density of water in kg/m^3

Ψ_k - water capacity in m^3/m^3 as that moisture content at which a primary absorption front just reaches an upper limiting surface of a specimen

After all those complex relations of capillary liquid rise in such way could practically be deciphered without any gap.

Application field

Although one should principally monitor an anisotropy of a plaster's characteristics in the direction of stress, i.e. for a perpendicular-oriented brickwork horizontally, one can scarcely do it in the case of capillary moisture absorption from the surface exposed to rain, because such a short distance cannot, as a rule, experimentally furnish a stable approximation curve of capillary rise. If unwilling to give up a comparison of corresponding characteristics, one could however offer a test in the direction along a rendering shell, even when inhomogeneity given by stratification, i.e. caused "genetically", should be extensively equalized. Further adulterations moreover might be based on an unfavourable ratio between cross section and peripheral evaporation surfaces. The procedure variation presented is therefore mainly suitable for testing specimens of small thickness as e.g. rendering plates comprising only a relatively short distance for capillary rise, i.e. not much more than 10 cm, and being completely soaked within a few hours. Adulteration of results can occur by experiment in the case of geometric irregularities on a specimen, leaching of water soluble salts and swelling processes, especially though when a test duration is too brief. This method also does not furnish sufficient accuracy, if material by its nature indicates inhomogeneities or even if it is pretreated with water repellent or preservative.

Test method

Since such a procedure would promise a better insight into moisture transport phenomena in this material, however, a special weighing device was developed. The small gain in mass made it necessary to provide lightweight parts in order to construct a useful apparatus. Therefore permanent level correction of the liquid and its supply also had to be included into the system to be weighed as a whole. Although evaporation loss is considered already sensitive in the case of the thin-plate specimen concerned with such a large surface, its influence on weight at different times was neglected. For as a rule there was also no need to take it into account during test runs lasting less than 10 hours. Since in this special case difficulties arise in holding the test liquid's level constant when using a lateral overflow at the tank, it is safer to maintain the necessary equilibrium by evacuation through an air jet pump, which is provided with a narrow nozzle so that a suction curve can be plotted satisfactorily [32], [74]. Fig. 14 shows astonishing simplicity of this novel device which is nevertheless quite appropriate for this purpose while guaranteeing an interval of no more than 1/10 millimetre in height (cf. also Fig. 11 and Fig. 12b).

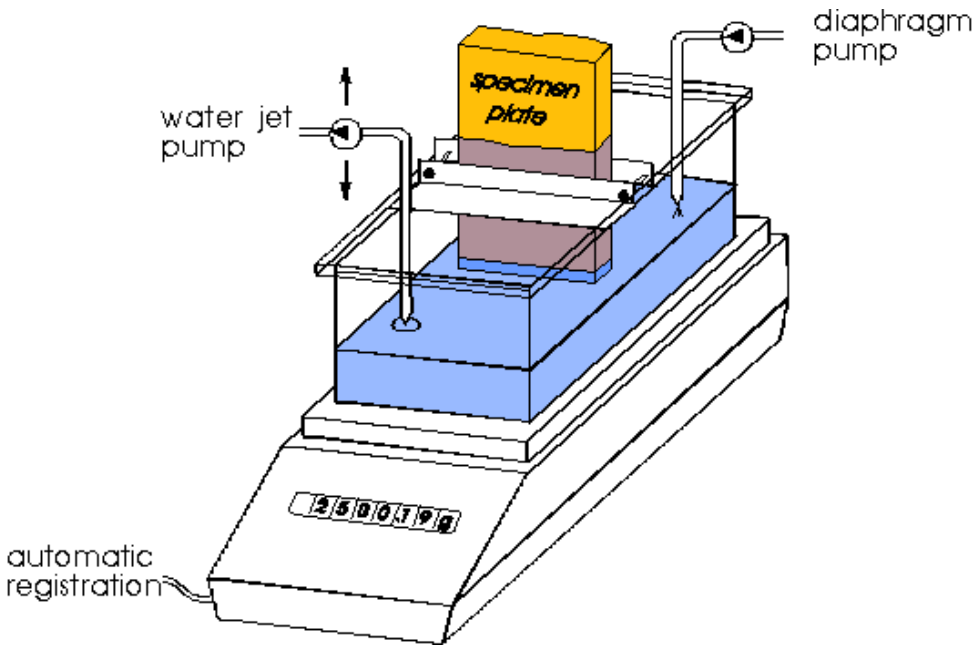

Fig. 14. View of a test setup for determining capillary rise on rendering fragments

The dried specimen plate is quickly submerged into the test liquid to a previously defined level; it succeeds at different intervals in obtaining readings of temporary weight which allow a continuous curve to be drawn following the formula discovered for capillary rise in porous media. Hereby, the curve stability is less as more water quantity is absorbed in a time unit approaching that which is required for maintaining the fluctuating liquid level constant.

4.2.2 Evaporation

Principle of method

An important contribution for quantitative characterization of porous building materials has been achieved due to their evaporative behaviour [38]. After dividing a curve's course into different phases as first mentioned by the B u i l d i n g R e s e a r c h B o a r d [5] and later defined by O. K r i s c h e r [58], one namely can describe the almost exclusively material-specific drying section following the climate-dependent practically linear portion of moisture release course by means of the exponential function shown:

$$y_e = a_0 \cdot e^{-b(t-t_0)} \qquad \text{eq. (4)}$$

As far as one holds a specimen's geometry comparable, however soaked of course by capillary action only, the remaining so-called equilibrium moisture content has to be considered, the amount of which can additionally be influenced by salt deposits when using a test liquid other than water, as e.g. a sulphate solution. So a building material can be characterized by means of parameter a_0, corresponding to moisture content at the boundary between both phases (t_0), and by evaporation parameter b as well. By forming differences, an inflection point in the velocity course - i.e. the curve's first derivative - at both sections' border commonly can be fixed (Fig. 15). Marking of the end of the original measuring values series linear portion by means of the "classical" formula according to Z a c h a r i a s and V e n z m e r

$$y_e = a \cdot e^{-b \cdot t^c} \qquad \text{[100], [107]} \qquad \text{eq. (5)}$$

can also be achieved considering shift by t_0 when optimizing of $c \rightarrow 1$, i.e. varying inflection-point coordinates (t_0; a_0). Because representation of this process formerly occurred by a unique value, i.e. just resulting from this function, that respective subdivision (cf.[40], [72]) was recalled anew under special consideration of its latter part. Admittedly the case may t_0 =result that practically parameter c in this no more up-to-date equation already became unity and therefore a linear portion no longer exists (0). A corresponding behaviour as a consequence of decelerating the process e.g. can be shown in specimens saturated with a salt solution.

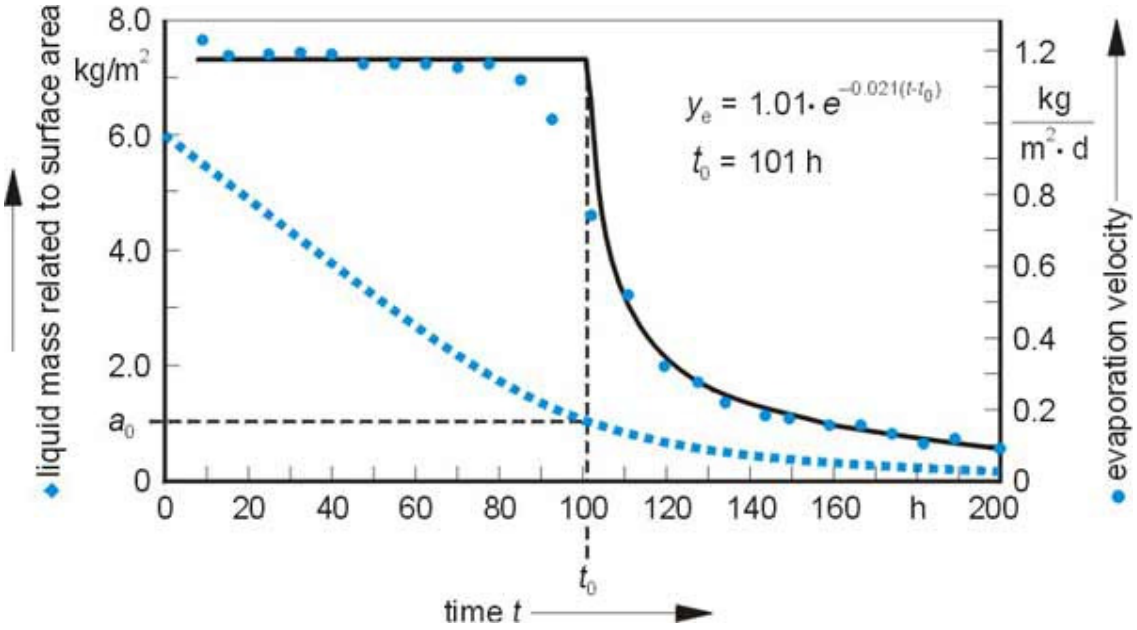

Fig. 15. Evaporative course and its velocity after capillary rise exemplified on a lime plaster column when using water as a test liquid at 20ºC and 50% relative humidity (sand <0.5 mm diameter as a mortar's aggregate, industrially hydrated lime, mix proportion 1 : 4.0)

As an experimental procedure to be proposed for characterizing a rock's evaporation behaviour the following one may serve as an example: A 7cm cube of the material meanwhile dried to constant mass is wrapped laterally, i.e. on four planes, into a self-adhesive aluminium sheet, which enables complete sealing towards ambience. Thereafter saturation with water takes place by capillary rise, viz. through that cube plane provided for evaporation. When soaking appears at the opposite plane, this one will be sealed in the same way and used after turning over as the supporting surface so that starting at this moment, evaporation can be recorded by mass loss over time. This therefore occurs exclusively through the remaining sixth cube plane upon which water mass released in a time unit has to be related. For the purpose of calculation, of course, weighing of relevant single components should not be overlooked. To extensively avoid an air circulation (convectional current being striven for), subsequent storage of specimens within a climatic chamber at 20°C and 50% rel. humidity is recommended, and that in an open plastic container (here: distance from its upper border ca. 12 cm), which is provided with a perforated covering plate removable during weighing. The minimum distance between the single cubes themselves and the container's inner wall is 4 to 5 cm.

Presentation of results

From liquid mass related to evaporation surface, a_0 (in kg/m^2), serving as a criterion for each material type and its orientation towards ambience, one can additionally determine the typical inflection-point moisture content. Although the physical meaning of b (in h^{-1}), which is influenced by capillary supply as well as water-vapour diffusion, has still not yet been exactly determined,one can understand it yet as a reciprocal value of time, which is - apart from pore structure - considerably affected by moisture-furnishing volume behind the evaporative surface. This parameter proves to be a dependable measure for a different evaporation behaviour which was found at the same material, e.g. when applying various test liquids. Under extensive consideration of the evaporative course described by Krischer [58], this provisional parameter obtained by experiment allows with all reservation an approach to the problem of quantitatively characterizing this process in porous materials. The test sample's geometry as it is given, e.g. by a brick located in the middle of stack's height used for determining the curve of capillary liquid rise, may simulate that brick situated at a building's corner but does not indeed expose to evaporation only one but two stretcher and header faces in each case. For comparative tests it seems however useful to retain the same thickness of each material's water-supplying volume behind the evaporative surface and also covering n - 1 planes of the specimen. A climatized storage in an ambient air having virtually immovable conditions (= convective flow) is hereby required. Although it sometimes would be difficult to localize exactly the inflection point, especially in a case of low evaporative velocity e.g. at a high salt content of the pore solution, when considering these facts the parameter b so obtained would compensate for the remarkable efforts. Nevertheless, it should not be forgotten that one has to omit a transition zone bordering directly at the linear portion of the curve.

The accuracy with which one can determine that salient point and so also a_0 sometimes leaves much to be desired. This is especially valid for measurement series which have their readings interrupted by an intervening weekend as well as for a material having a relatively small pore volume which is expressed only indistinctly. Finally the entirety also depends upon the respective position of a brick within the stack and its surface structure exposed to the ambient atmosphere. Comparisons one with another are therefore advisable just only when similar exposure conditions exist. When fitting such curves one has to mention that an actual inflection point is commonly not just immediately located at the end of linear portion in raw measuring values' sequence - a fact being of interest for cutting off curve path of the first drying phase according to Krischer properly. Rather because of an existing evaporation transition zone it is shifted to a later moment. To be able to verify its correct positioning, however, one should monitor the evolution of exponent c obtained by practically same formula (2) and provided that then achieving 1 as near as possible, it will be improved with each additional plot of new data. By the way, also for the function (1) containing evaporative parameter b, in which of course one has set c = 1, one can so attain an optimal approximation. In order to receive here the best solution sometimes several attempts can be necessary anyway. In our opinion, this unconventional characteristic however is more than a rough approximation for instance as attributed in the building materials field to concrete's uniaxial compressive strength. Possible evidence for its usefulness may also be seen therein that this nearly material-specific feature is independent from the soaking or saturation intensity of the involved test liquid. This way judging criteria and therefore promising tools for characterizing pore structure which were lacking for a long time have been made available to the material expert. In any case such features appear to be extremely useful for multiple linear regression analysis of pore-related and mechanical parameters.

4.2.3 Water vapour permeation

Principle of method

When referring to DIN 52 615 [13], the following measuring principle is the basis: The test device specimen forms the upper end of a hollow glass cylinder on which the rim is closed vapour-tight. In the receptacle prevails a defined air humidity originated - when using the dry-cup method - by a water-absorbent medium, whereby the entire set-up is placed into a climatic chamber in which a varying but higher constant humidity is maintained. In order to just avoid uncontrollable modifications of moisture content in material in case of hygroscopic behaviour, it should be stored a sufficiently long time in the climatic chamber provided for tests. The water increase of the sorbent will be measured in such way that the entire vessel is weighed periodically up to having reached a constant mass increment. This is monitored over several days and from the resulting straight line, the water-vapour diffusion current is determined. Instructions on the specimen's state and dimensions, climatic conditions, required sorbents and other technical details can be obtained from the standard mentioned.

Preparation of specimens

Permeability to water vapour can be used as a specific value in order to characterize a porous building material, the amount of which being a result of the passage of water vapour through the open pore space and depending on the open pore volume. Speaking of water vapour diffusion instead of water vapour permeability is justified insofar as the passage of vapour molecules through the pore space in fact occurs within the atmospheric air in the pores. Herein also lays the difference between water vapour diffusion and the so-called specific permeability to gas, which is also characteristic for a porous matter and results from measuring laminar flow of dry air through the specimen within a pressure-inducing device. In contrast to this, vapour diffusion will be tested under atmospheric conditions producing a constant vapour transmission caused by different partial vapour pressures at each end of the test piece, where the pressure difference is a tenth to a hundredth lower than that of compressed gas. Moreover the duration of an experiment on water vapour diffusion lasts several days, while the gas permeability procedure takes less than one hour. DIN 52 615 basically describes limiting conditions related to humidity, temperature, necessary absorbents as well as technical details.

Test method

For preparation rendering, samples exposed to atmospheric pollution on the rack previously mentioned and their equivalents stored in a climatic chamber, both after 17 years exposure, were carefully removed from their base plates as well as material sampled directly from a building. Circular disks slightly greater than 8 cm in diameter and of uniform thickness were cut out and used for the experiment. Prior to this such specimens were stored for a few days at humidity conditions in the climatic chamber. After sealing off their peripheric contours with wax and following air-tight insertion into an aluminium ring using wax and another sealing compound, this sample mounting was placed into the upper rim of a glass vessel containing silica gel and closed in the same way (compare Fig. 16). So the specimen forms the lid of a receptacle in the experimental arrangement. Tests followed at 20°C and 50% relative humidity in the climatic chamber and 0 - 3% r.h. generated above the silica gel in the container, which nearly corresponds to the experimental procedure of DIN 52 615 (dry cup method 23 - 0/50). Water vapour transmission is determined as an increase in mass of the absorbent medium by weighing the whole set-up at intervals until mass remains constant.

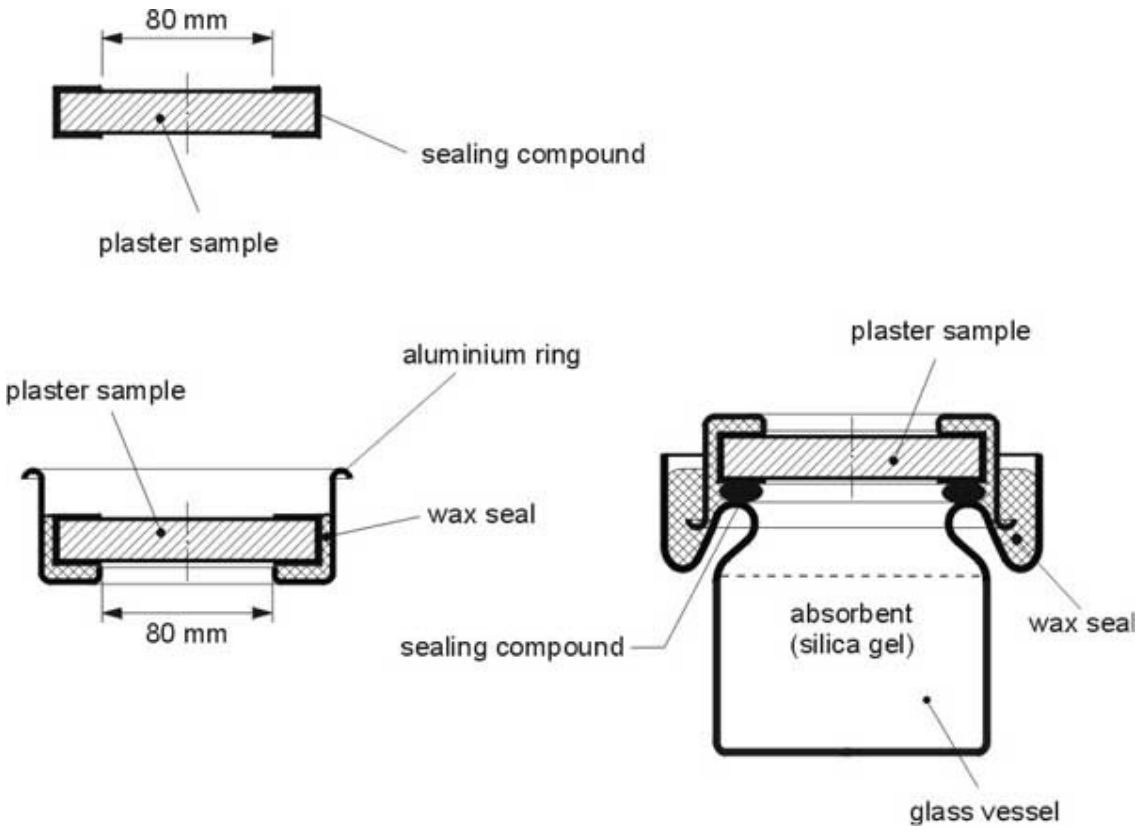

Fig. 16. Embedding device for plaster samples and test set-up for determining their water vapour permeability, shown as cross section

As a result of test conditions and specimen's dimensions, one calculates the diameter S_d of the air layer which is equivalent to the rate of diffusion through the sample, respectively the water vapour diffusion resistance index (moisture resistance factor), μ. Evaluation is done as follows:

$$s_d = \delta_L \cdot A \cdot \frac{p_1 - p_2}{I} - s_L \qquad \text{eq. (6)}$$

&

$$\mu = \frac{1}{s}\left(\delta_L \cdot A \cdot \frac{p_1 - p_2}{I} - s_L \right) \qquad \text{eq. (7)}$$

i.e.

$$\mu = \frac{s_d}{s} \qquad \text{eq. (8)}$$

In these equations mean:

μ - water vapour diffusion resistance index
A - effective surface of specimen,
p_1, p_2 -partial vapour pressure at each end of the specimen respectively,
I - water vapour transmission,
S - mean thickness of specimen,
S_L - mean diameter of the air layer underneath specimen
δ_L - water vapour permeability in air.

First of all, a few characteristic permeability data from comparative investigations of weathered and unweathered material already mentioned shall be presented.

4.3 Mechanical Strength (Grinding abrasion)

4.3.1 Introduction

In the course of work on rendered surfaces, the question inevitably arises, how to characterize the mechanical resistance of such material. The choice of method depends on whether one seeks connection to data already available or better information on structure. The appropriateness of the choice is determined by the skill of the researcher making the decision. In this regard a paper by O. G r a f [26] may serve as an example how structural cohesion or manufacturing and storage conditions find their expression in classical mechanical characteristics. In the present study quantification of bending strength, e.g. on specimens not especially made for this, was not carried out. The main reason for this was that one has to reckon with the material's brittleness and the sensitive effect of notched spaces which, among other factors, are promoted by the preparative steps. Therefore tests were restricted to investigation of grinding abrasion.

4.3.2 Principle and objective of abrasion procedure

For assessing strength of a rendering, it is advisable to choose a type of stress which reveals the stability of grain boundaries, i.e. a bond between hardened binder and aggregate can be expressed, for instance, by abrasion. This way one can obtain information on a material's cohesion which confers resistance against expansion of freezing water or crystallizing salts. So a procedure with a grinding disk according to B o e h m e serves to characterize the behaviour of hard to exceptionally hard rocks, corresponding to the description in DIN 52 108 [12]. This test is not appropriate, however, in the case of structural cohesion of materials which are not so strong, because this then results in too elevated wear rates for each test cycle. Therefore the development of a suitable procedure [39], [65], [66], [89] was necessary in order to ensure a more sensitive evaluation of resistance against grinding and subsequently the amount of wear per time period, test cycle or abrasion depth. Such a method is especially interesting for monitoring profiles having different strength as they are formed as a result of weathering effects coming from the specimen's surface.

The P.E.I. Abrasion Tester, developed by the Porcelain Enamel Institute of America for characterizing glazes of ceramic tiles (cf. ASTM C 448-88 [2]), was used as a starting point. The square-shaped test specimens fastened on its oscillating table are engaged in an eccentric and horizontal motion. Using loose boron carbide grains as an abrasive, a plane disk of tungsten carbide produces progressive wear of the sample surface while it is moving as in a vibrating disk grinder (Fig. 17).

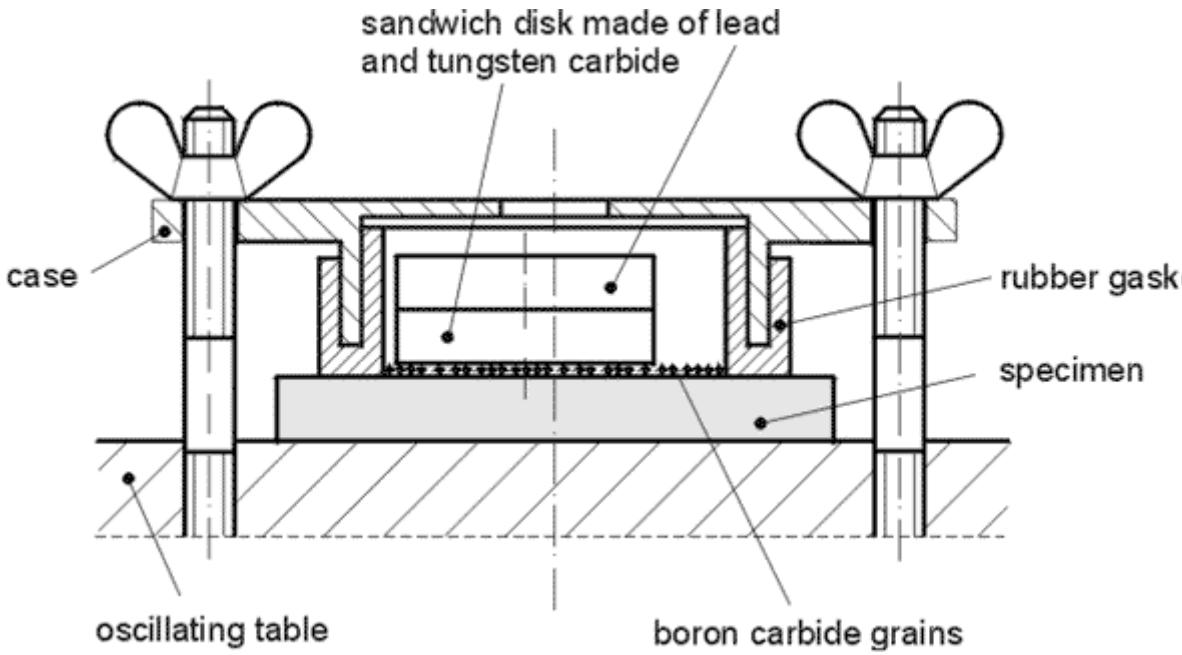

Fig. 17. Test device for surface abrasion

In addition, one has to modify the drive for that platform in order to avoid during test a jerky and therefore undesirable tumbling motion of the disk. This can be achieved by using an electronic soft start module. After each stress cycle the abrasion surface is cleaned by a compressed-air stream. The course of the abrading disk is such that the abrasive particles are carried along hypocycloid-shaped paths over the specimen. The free selection of revolutions of the apparatus eccentric allows the removal of small quantities of material. A necessary requirement though is the availability of an even surface of the sufficiently dimensioned specimen, i.e. with a minimum size of 10 cm by 10 cm, a maximum thickness of about 3 cm, and a circular abrasion plane 8.6 cm in diameter on its upper surface. The rendering for test must neither be too friable nor have very coarse grains or voids, but should have a character as uniform as possible. The abrasive grains should not be substantially smaller than either the structural grains (which above all become the abraded particles) or the pores of the material. In addition the chosen number of revolutions of the eccentric per stress cycle must be adapted to the test piece in such a way that the linear proportionality of the method does not suffer through a reduction of the boron carbide grains or an excessive dilution of the abrasive by the abraded substance. The best evaluation criterion under the given conditions turns out to be the determination of the thickness difference between two stress cycles. During the test a dial gauge with a probe having the annular contact surface fixed by a ball bearing (Fig. 18) is used to measure this difference. However its operation is rather time-consuming, especially since numerous single measurements are necessary. Sometimes deviating values are also obtained when the probe makes contact with larger pores.

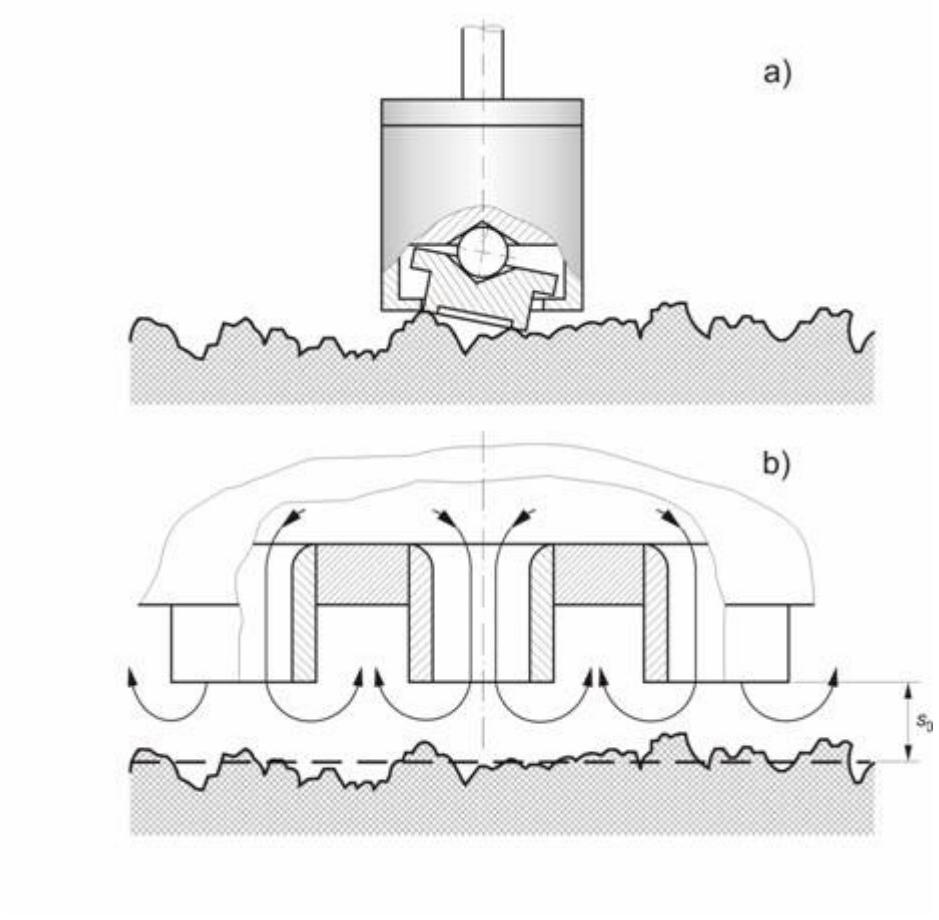

Fig. 18. Methods for sensing rough surfaces:
a) mechanical contact with a movable probe
b) contactless with a pneumatic multi-nozzle probe(s_o = distance to average surface plane)

In this case it is better to use contact less sensing by means of a pneumatic multi-nozzle head [65], [66]. During measurement its height will be so adjusted that the total cross-sectional air flow is equal to a constant, and that at each determination the same distance to the average surface plane s_o is maintained. For this purpose the face formed by the tips of single nozzles has to be vertically shifted until the pressure read on the gauge has reached the value "zero", which occurs at a distance of about 0.8 mm from the mentioned plane, which of course depends upon multi-nozzle's inner geometry (Fig. 19). This corresponds nearly to a plane which would be formed by abrading the elevations over the mean surface and filling up the hollows in such a way that it is located between the highest "hills" and the deepest "dales". Thus the determination of the average height decrease of the rough surface

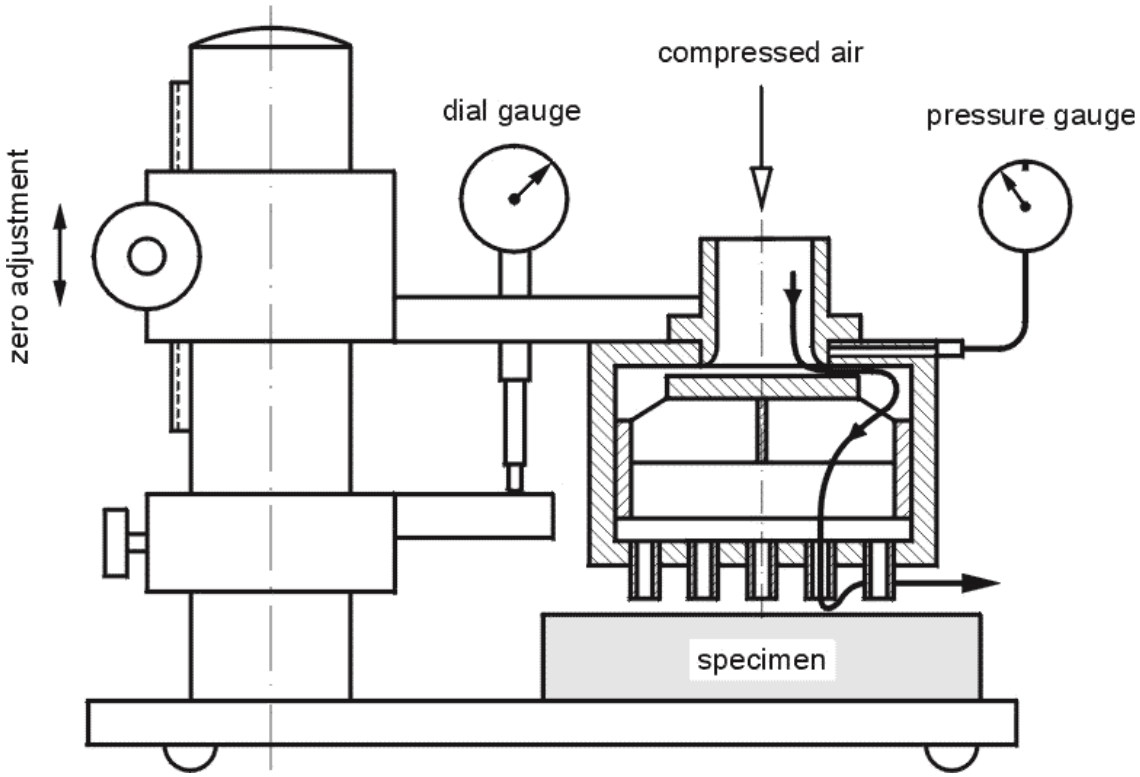

Fig. 19. Thickness measurement by pneumatic sensing

can be reduced to a single measurement of the position of the multi-nozzle probe which is read on another dial gauge in order to guarantee manual compensation of the distance. The time expended can be therefore decreased to less than 5% of that which is necessary for the mechanical method. This allows the sensing of surfaces with a maximum profile height of about 1.4 mm, so long as the average plane to be measured runs parallel to the face of the nozzle tips (19-fold-nozzle head as shown in the figure). For sensing material surfaces with a maximum profile height up to 5 mm a 7-fold-nozzle head is used. A useful secondary effect is that the abrasion surface always remains free from abrasive and abraded particles by the air flow of the pneumatic probe. Comparative tests do not show any essential differences between results obtained with both methods. The wear is calculated here as the quotient of the abrasion depth divided by the number of revolutions of the apparatus eccentric shaft. With regard to an interpretation of such depth profiles, it must be stated that when the test is first started a surface roughness is caused which depends on the method as well as being specific for the material. This so-called “break-in” abrasion, as e.g. shown in Fig. 20 and the following, obtained by adaptation to the stressed surface plane cannot be distinguished from the actual wear and leads to a higher measuring uncertainty. The diagram also shows that at a later stage, hardening of the dolomitic component runs parallel to carbonation. Apart from this, the method is able to demonstrate **characteristic values** of building materials almost homogeneous.

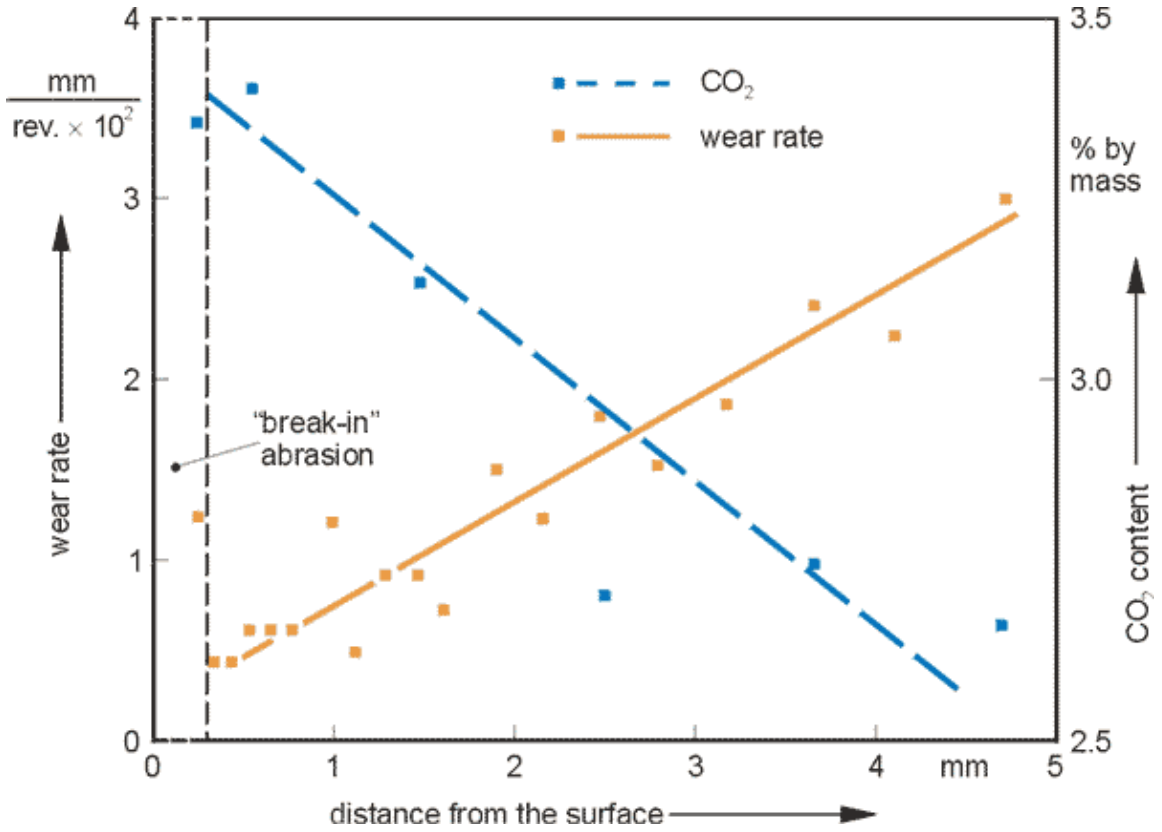

Fig. 20. Abrasion profile of a laboratory prepared dolomitic rendering: wear rate and CO_2 absorption for comparison

4.4 Chemical composition

The chemical modification of rendering - leaving aside a carbonation process - is in many cases a concomitant rather than being able to considerably influence its structure. The physical process of dissolution increasingly plays a role, since it commonly represents the main cause of a mineral phases' rearrangement, which is as a rule responsible for plaster's dispersivity. Therefore - deviating from ranking order as usual in building materials science when describing properties and characteristics - chemical analyses should be initially treated here.

4.4.1 Analytical methods

In order to assess the kind and extent of influence, which sulphur and nitrogen oxidic and chloride-containing air pollutants exert on above-ground surfaces of rendering and natural stone, it is necessary to quantitatively determine the typical constituents such as sulphate, sulphite, carbonate, nitrate, nitrite and chloride. For these determinations gravimetric, coulometric and ionchromatographic methods as well as energy-dispersive X-ray analysis have been used whose particular characteristics are the subject of the following description.
Concerning samples from buildings, an established scheme of chemical analysis was available for this scope in the case of finish layers of rendering, whose block diagram is shown in Fig. 21.
This procedure serves for characterizing the kind of binding agent of a plaster and its mix proportion provided that the aggregate portion soluble in hydrochloric acid is known or may be neglected. Sometimes particular determinations will be necessary.

4.4.1.1 Gravimetric analysis

Principle of method

In addition to volumetry, gravimetry belongs to classical quantitative chemical methods. Its nature consists therein that a sulphate ion SO_4^{2-} to be determined is converted into a less soluble compound of defined composition (barium sulphate $BaSO_4$) whose precipitate is released from adherent impurities and finally weighed. The reaction occurring during precipitating with barium chloride solution ($BaCl_2$) fulfils conditions coupled to a gravimetric determination of a less soluble precipitate specific for a component to be analyzed and completely filterable, which can be converted additionally into a stable well-defined compound, the "weighing form", in a simple and reproducible manner. By the aid of such a method, quantitative recording of sulphur in the form of sulphide, sulphite and sulphate is possible. When these compounds are simultaneously present, one can determine total sulphur content via sulphate after corresponding oxidation.

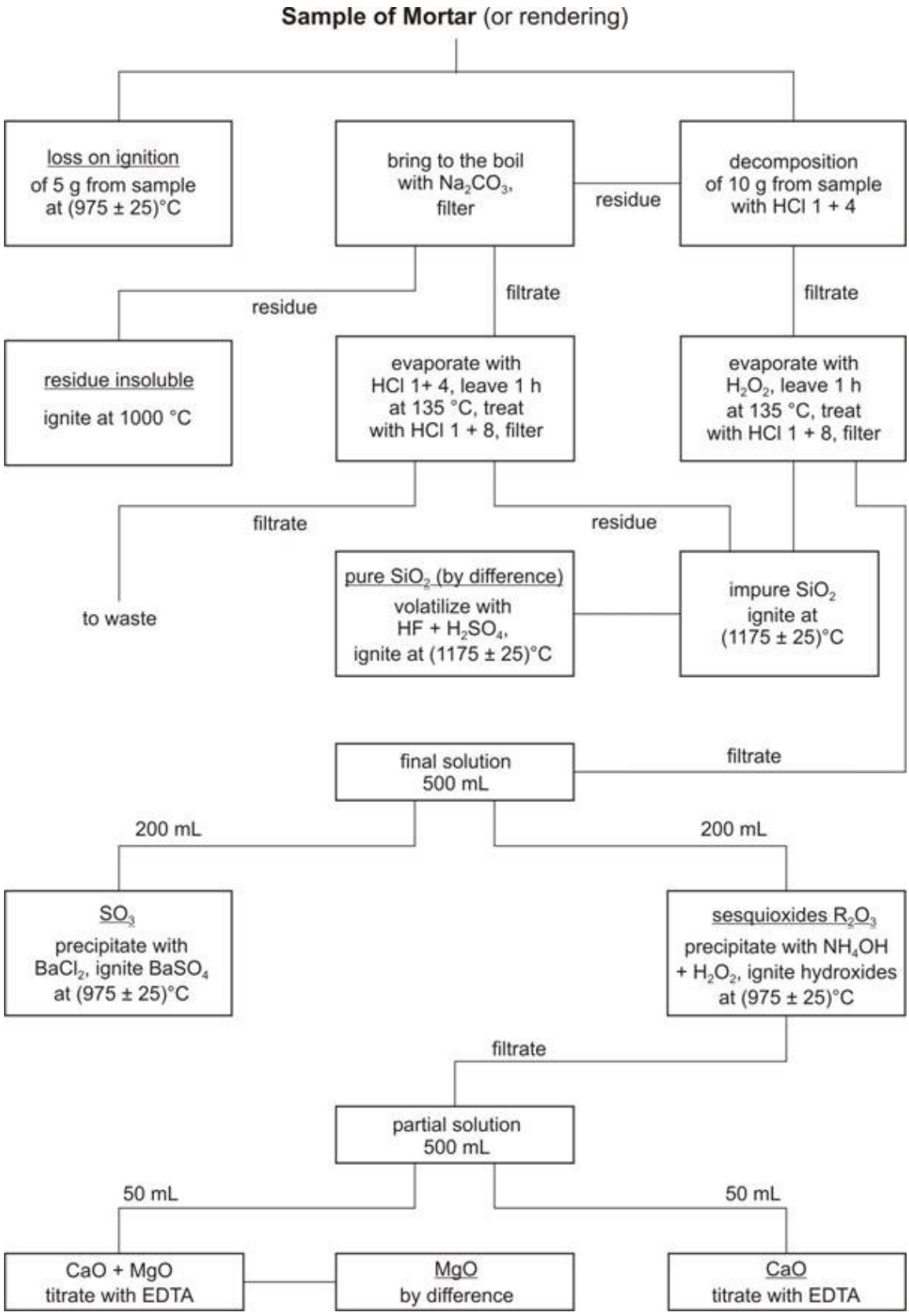

Fig. 21. Block diagram for chemical analyses of mortars and renderings

Application field

The gravimetric method finds use for analyses of inorganic non-metallic building materials, e.g. binder, plaster and concrete, but predominantly also of sulphide, calcium and magnesium oxides (compare DIN EN 196-2 [17] and DIN EN 459-2 [18]).

Preparation of samples

Chemical composition can be determined on plaster samples previously crushed and dried between 40 and 105°C to constant mass depending on the type of binding agent to be expected before complete passing through a gauze wire-mesh cloth according to DIN 4188 part 1 [10] with 0.63 mm mesh width. There the maximal grain should measure only slightly below 0.63 mm, because solubility of aggregate in acid increases remarkably with elevated grinding fineness.

Mode of operation

This method requires that the component to be determined is placed into solution, which is acidic in the case of sulphate in plasters. This depends thereupon that a sulphate ion exists in the form of calcium sulphate if there is an excess of calcium whose solubility in dilute hydrochloric acid is essentially higher than in deionized water. Precipitation of sulphate ions occurs with a hot barium chloride solution in filtrate from the determination of insoluble residue. After standing several hours at room temperature, the precipitate is filtered and washed out. Then follows incineration of the filter and ignition of residue to constant mass.

Presentation of results

From precipitate's mass and its composition, one can calculate e.g. quantity of sulphate the result of which is expressed in % related to mass or in ppm.

4.4.1.2 Coulometric titration

Principle of method

Hereunder one understands measuring electric charge by means of a quantity of substance converted according to Faraday's law. The prerequisite for this is a quantitative current yield, i.e. uncontrollable secondary reactions should not occur. Since one works with a constant current strength, the substance's quantity converted in a given time is a measure for quantity of charge, whereby quantitative analyses become possible.

Application field

Coulometry has been proven for performing quantitative analyses. According to the OELSEN-ABRESCH method, one can determine total carbon as CO_2 and total sulphur as SO_3 by coulometric titration. It has since been applied for determining carbon dioxide in limestones and building limes [84] and in rocks [34]. It is suitable for CO_2 contents from ca. 40 ppm up to 73%. By means of this application, one can also analyze lime- and sulphate-containing material rapidly with sufficient accuracy.

Preparation of samples

Generally a pulverized sample dried to constant mass is applied having a preferred grain size of ≤ 0.125 mm. In the case of coarser material, uncertainty exists that a quantitative conversion of sulphate into SO_2 or carbonate into CO_2 respectively cannot be ascertained in a reasonable time period. A prolonged post-titration would moreover falsify the result. If a material contains only carbonate, one can pre-dessicate it at 105°C. In case of additional sulphate (in samples mostly as gypsum $CaSO_4*2H_2O$), 40°C should not be exceeded. The mass of a test portion is accordingly dependent upon the contents of carbonate or sulphate.

Mode of operation

The sample should be decomposed at 1000°C in a dry air stream free of CO_2 and SO_2, whereby existing carbon escapes as carbon dioxide and carbonate is also released as CO_2. Burning gases are conducted over a perhydrite absorption bulb which takes up oxidation products contained in the sample. The gas stream then enters a titration vessel filled with barium perchlorate. By absorption of CO_2 the pH value of the solution set to alkalinity decreases during simultaneous formation of barium carbonate. By means of electrolytically produced barium hydroxide, one titrates automatically back to the pH starting value. The electrical charge used is a measure for carbon content in the sample based upon Faraday's law. This method works without an external standard.
The procedure is similar for determination of an SO_3 portion. However the sample has to be ignited to ca. 1350°C, in order to guarantee quantitative decomposition of calcium sulphate. Released sulphur dioxide is introduced into an acidic sodium sulphate solution mixed with hydrogen peroxide. By means of electrolytically produced sodium hydroxide, an automatic back-titration to the pH starting value occurs. One obtains a sulphite portion by release of SO_2 with the aid of dilute phosphoric acid. So by subtraction of this from total sulphur, the sum of sulphate and sulphide is derived.

Presentation of results

According to respective requirements, one can indicate results as total carbon or carbon dioxide content in %, related each to mass of the test portion. Correspondingly one obtains for sulphur after converting as a percentage portion the total sulphur, sulphate (SO_4^{2-}), and sulphite (SO_3^{2-}) as SO_3 or SO_2.

4.4.1.3 Ion-exchange chromatography

Principle of method

The conventional column chromatography was significantly advanced in the mid-sixties due to the development of "High Performance Liquid Chromatography" (HPLC). A similar system improvement began in 1975 which led to the methodology of ion chromatography [97]. Common to both methods is a better separation of substances or ions respectively, a shorter analysis time, and a direct combination of chromatographic separator systems with various suitable detectors. These also determine analytical performance. The basis of separation is ion-exchange processes on corresponding columns having low capacity with weakly dissociated eluents [57]. The measuring arrangement mainly consists of a conveying pump, an ion-exchange column and a detector. According to modern technical state-of-the-art, the pump operates with one or two pistons, whereby its pressure-related conveying

characteristic has to be free of pulsations. When choosing an appropriate separator column, one is not tied to one product, since all technical parts have been manufactured according to the HPLC standard. Employed are conductivity, UV or UV/VIS refractometer, amperometric, potentiometric and electrochemical detectors, which are applicable to the kind of ions to be determined. Through the system pump is steadily conveyed a solution, named eluent or mobile phase, from a reservoir with a certain pressure, which varies depending on a given flow rate. The sample's feed takes place via a chemically inert connection loop representing a respectively defined volume over its length.

Material changes find, among others, their expression in the chemical depth profile. To characterize this there was available an ion-exchange chromatograph with computer-aided data evaluation by means of which one can also find small concentrations of cations, and anions as well as what might be of special interest for characterizing the immission of some reactive air pollutants. The following schematic diagram (Fig. 22) gives insight into the method. One can determine ions quantitatively by means of appropriate equipment of the H i t a c h i and M e r c k firms, operating according to analytical procedures slightly modified. This device comprises M e r c k columns of both types RT Polyspher IC AN-1 with a bead size of 12 µm and IC CA for the separation of fluoride, chloride, nitrite, nitrate, bromide and sulphate as well as sodium, ammonium, potassium, rubidium, cesium, magnesium and calcium. For the mentioned anionic groups a mixture of aqueous solutions of phthalic acid (c = $1.5 \cdot 10^3$ mol/L), tris-(hydroxymethyl)aminomethane (c = $1.38 \cdot 10^3$ mol/L) and boric acid (c = 0.3 mol/L) serves as an eluent at a flow rate of 1.5 mL/min and at 30 bar pressure. For cations an aqueous solution of cerium(III)sulphate with a concentration of 10^{-4} mol/L was applied as a mobile phase; the flow rate was 1.5 mL/min at a pressure of 143 bar. Detectors for analyzing anions are based on conductivity measurement, whereas determinations of cations utilize the principle of UV photometry at a wavelength of 254 nm. Rendering for preparation was sampled layer-by-layer, dried to constant mass at 45°C and milled in such way that it passed a test sieve with wire-mesh openings having a width of 0.5 mm according to DIN 4188

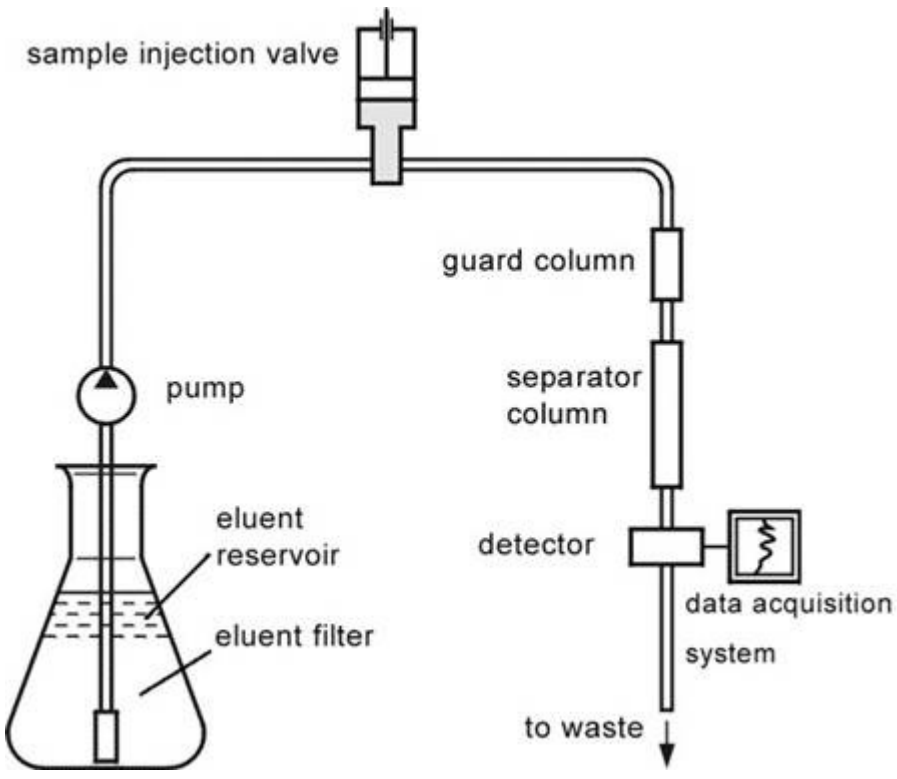

Fig. 22. Schematic diagram of the ion-exchange chromatography method

part 1 [10]. Extraction of an average sample in a ratio of 1 g to 50 ml was subsequently conducted in deionized and then distilled water at room temperature during a 2h shaking process. A filtered solution served for performing the chemical analysis.

Application field

The method described is appropriate for selective and simultaneous determination of uni- and bivalent ions in mixtures. Because of high sensitivity in the ppb range, reduced analysis time, and the mostly simple preparation of samples, it represents an important supplement to classical chemical and voltametric methods of analysis. Hereto belong analyses of samples containing ions of chloride, nitrate, nitrite, sulphate, sulphite, alkali and alkaline earth as they occur inter alia in the analyses of food and water, but also during chemical characterization of building materials. For confirmation of results, alternate classical chemical procedures are applied.

Preparation of samples

Here one can either get an insight into optional and only semiquantitative local element distribution by energy dispersive X-ray microanalysis, or by removing layers of defined depth and thickness it is possible to acquire integrated values for chemical composition or any pore characteristic. Nevertheless, an optimal solution would consist - technical facilities provided - of a method to choose depth of layers for analysis so freely that the typical regularities can be recognized. In contrast to this, a global investigation of an average behaviour, e.g. over the entire profile, may be no more than an expedient, although it could by all means deliver a useful contribution.
The sample obtained by abrasion of defined material portions millimetre-by-millimetre, finely ground afterwards in an agate grinding dish and homogenized, is passed completely through a sieve with mesh width of 0.63 mm according to DIN 4188, the required quantity weighed, brought into an Erlenmeyer flask and extracted with bi-distilled water for about one hour. Then one quantitatively transfers the flask's content over a white ribbon paper filter into a volumetric flask and fills this up to its mark.

Mode of operation

Salts of alkali and alkaline earth compounds occurring in a completely dissociated state are added by means of a syringe over a loop to the eluent stream which leads it then through a selected exchange column. The separator material used carries a functional group with a fixed charge. Close by is the corresponding counter-ion so that the group appears electrically neutral outwardly. In the case of anion chromatography, the exchange function generally originates from a quarternary ammonium group, on which a basic portion of eluent is adsorbed. This again is displaced by negatively charged ions of the test solution. So different ions in a sample can be separated because of their distinct affinity to the stationary phase and registered by its conductivity change in comparison to a quiescent current during subsequent passage through a corresponding detector (W e i ß and G ö b l [104]).

Presentation of results

The exchange process of the column and the result obtained therefrom can be illustrated by a compensation recorder or optically on a screen. Such "chromatograms" called recordings show how, in the course of analysis, the detector current compensated before to zero or its voltage respectively is modified as a consequence of varying values for conductivity. While

recording this process, one conventionally obtains symmetrically shaped curves according to a type of Gaussian distribution (peaks), because of time dependence (abscissa) of voltage modifications of the detector (ordinate). When including a basic line, one can planimetrize a concentration of a corresponding chemical compound or ion respectively. The area proportional to this results from the formula for an isosceles triangle a = h·w, where a denote area, h height and w half width of triangle. In this case all calculations can be retrieved from a printer. The principle of presentation and achievable sensitivity can be seen in Fig. 23 and Fig. 24.

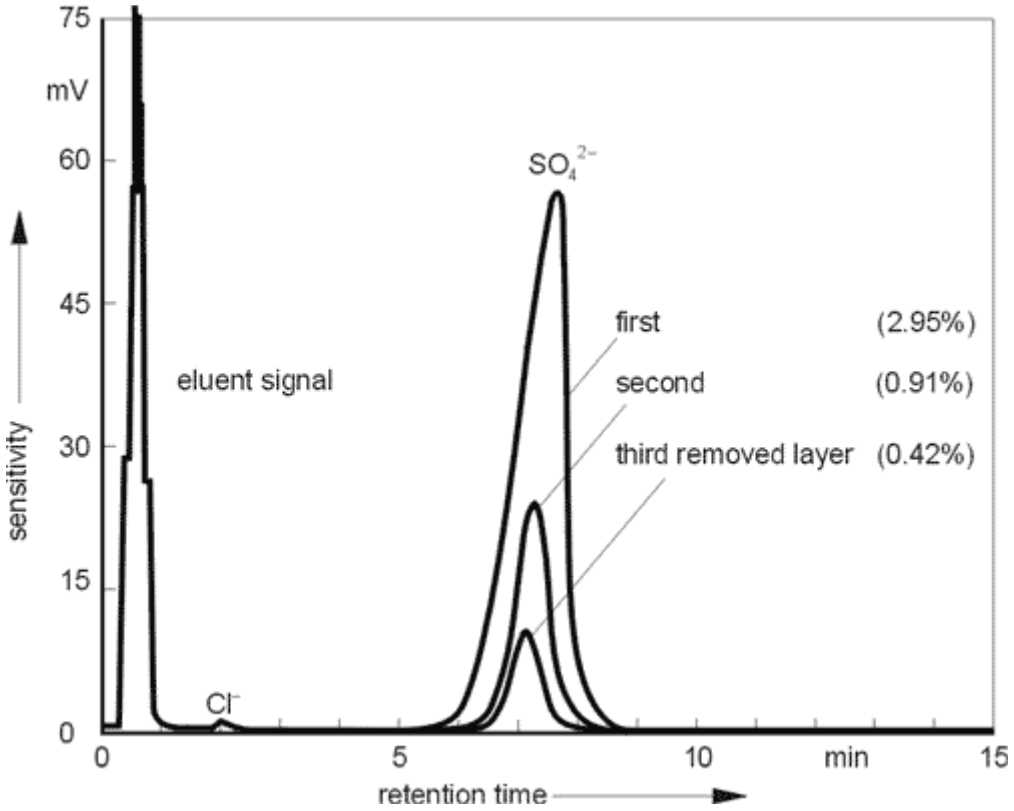

Fig. 23. Superposed ion chromatograms of three consecutive layers of a weathered lime plaster taken from its surface area (scheme)

Three samples taken from the depth profile of a lime plaster demonstrate the principle of this analysis (Fig. 23) and represent a decreasing sulphate content - from 2.95% by mass in the surface layer to 0.91% in the second one, and 0.42% in the third.
A very small chloride peak can also be detected in these diagrams. If altering the sensitivity setting, one can observe not only an increased chloride reading, but also a trace of nitrate. However, it is not yet possible to make any comments on its origin, i.e. standard sand which is used for production of rendering samples also contains traces of nitrate. Since one of the objectives of this project was to find out whether there are hints for reaction products with NO_x, this method has been proved as a rather good instrument to detect such anion group (nitrate or even nitrite). The diagram this way obtained (see Fig. 24) shows a small peak at the retention time for NO_3^- corresponding to a quantity less than 0.01%

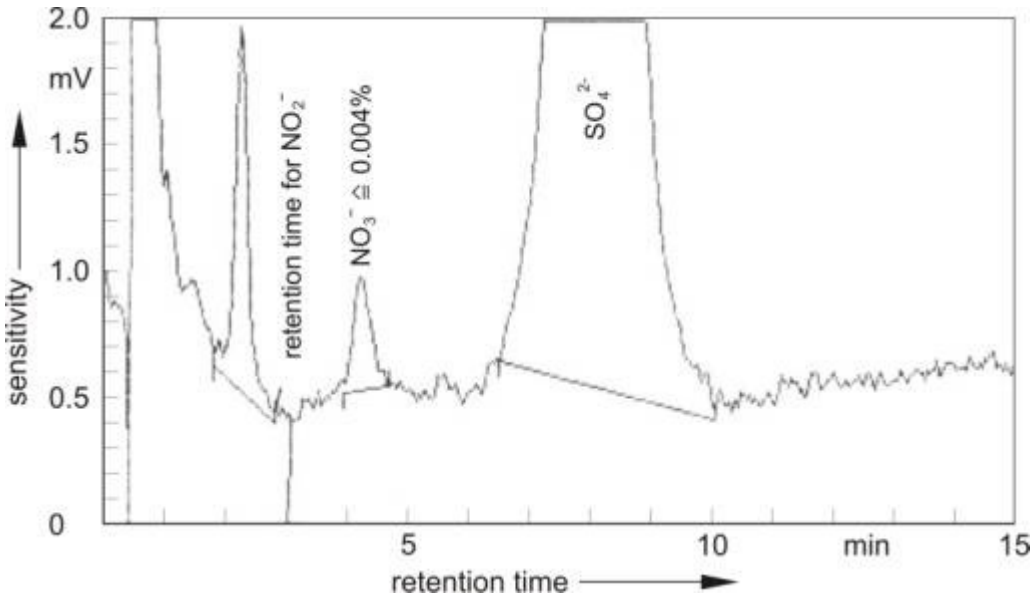

Fig. 24. Chromatogram of a weathered lime rendering with an increased sensitivity range allowing to show traces of nitrate (original plot)

5 Results

Rendering exposed outdoors and such from a building as well primarily served as material for the test programme. Because of air-pollutants' concentration in the Berlin region, meanwhile however considerably reduced, there resulted a shift of research focus in the direction of façade material. Samples taken from exposure racks show only slight changes in chemistry and structure after half or one and a half years respectively compared to starting material. Fortunately one could gain important indications as to their behaviour and the effect of pollutant gases by means of rendering plates originating from a former programme where they were exposed over 17 years to atmosphere. A further reason to intensely direct one's attention on material taken from a building was that - surprising for the moment - one could find a dependence on orientation to cardinal points [31], [93] and on sampling height as well [31], [37]. Nevertheless treated here initially, in addition to difficulties having occurred during sampling and preparation, are test results obtained for deposition rate of SO_2 on samples performed at commission by a staff member of the University of Hamburg (cf.[105]).

5.1 Sampling and preparation

For sampling material in order to establish corresponding depth profiles, a milling cutter was used which allows defined portions to be removed from the specimen's height, millimetre by millimetre. A precondition for this is that a rigid drilling frame is used on which the milling head is fastened so that it has practically no chance of giving way when aggregate grains of that brittle matrix are grasped by its cutting edges. But first one should bring the rendering's surface into such a position that its main parts run parallel to the cutting plane. However, this way it is impossible to spread over the whole surface at the same level. So one should sample the most projected regions only to establish the first layer of the profile and should confine further sampling to these regions.

At this point, it should be noted how much effort must be made in order to obtain the planned results. In the case of weathered rendering, this starts with the selection of a building. When finally a façade with scaffolding in the city area was found, the old external rendering has sometimes been already chiselled off. Or as has recently become the rule, it simply concerns an attic expansion for living space, or the rendering is over coated with paint. When a suitable location has been found, however, one has to act immediately by taking samples, because perhaps this is no longer possible the next day. The sampling should yield flat fragments - as large as possible - of that brittle and sometimes crumbly material which often adheres tenaciously to its plastering subsurface. Patience and persistence are necessary here. When carrying samples from the building to a vehicle and later on to the laboratory, there is a need for instinctive feel to avoid damaging these samples. In the case of two-coat work, the weather-exposed outer layer must be carefully separated from the layer beneath without causing damage. For taking samples by abrading, rendering plates of large size were used, embedded by means of epoxy resin in a frame made of plastic in order to level out differences in thickness and to facilitate sampling parallel to the original surface, where in fact it matters to the millimetre. The epoxy resin hardening time is 24 hours, during which the sample must remain fixed. For the actual work, a machine with rotating, grinding, and cutting tools is available which gives the assurance to obtain - as far as allowed by the material - layer fragments of defined thickness with sufficient accuracy.

There is some problem with the scraped finish because of its certain unevenness in some cases, and since it indeed contains coarse quartz grains which should be removed before by using tweezers to avoid pulling out the matrix from the actual surface at the same time. So controlled abrading is not satisfactory if such a procedure is not followed. During abrasion of defined material portions, millimetre-by-millimetre, however, an additional problem may arise: since the milling shaft is rigid regarding torsional action, it cannot deviate under load

and the tool mills easily through the material and sometimes brittle parts situated below the level just abraded are grasped by its cutting edges and break away; consequently one has to dispose of these unwanted fragments. In a former contribution [32] the principle of preparative measures concerning specimens for the determination of water vapour diffusion was already described. Material provided for the present study is occasionally in a friable state, since it succumbs to weathering processes and is then available in limited quantity anyway. Preparation of specimens is very time-consuming, especially if they have to be reduced to uniform thickness and separated from adjacent material such as undercoat or even splatterdashcoat, and if one wishes to remove heterogeneous parts containing voids or wood inclusions. To guarantee tightness between sample and mounting in spite of irregular contours of rendering surfaces, an additional sealant was used in a procedure normally requiring remelting of the wax mass which was found necessary in order to close shrinking cracks produced during the first embedding phase. To avoid intrusion of molten wax into rendering and to favour recovery of specimens already tested without damaging them, a supplementary mask of adhesive tape was applied below the wax mass.

Nevertheless, preparation of climate-stored rendering plates and especially those exposed outdoors over years and originating from a former test series is quite difficult because of their reduced thickness and friability. Since one cannot separate them from their substrate by sawing that thin and rather crumbly material, one is obliged to strike it off by numerous cautious blows with a plastic hammer. The same is true for the relatively brittle specimens of the present series which have not yet had sufficient time for consolidation by hardening and alteration during their 6-month storage period. On the one hand there is the necessity of providing a good adherence of rendering on the fibre reinforced cement plate. This is desirable so that the sand wiches can endure the whole exposure duration without separation and fall of their upper layer. On the other hand it is rather difficult to shear it off for preparation purposes in a non-destructive way near the interface marked by the splatterdashcoat. However, it cannot be separated without damage at this surface, for instance by hammer blows. Therefore it becomes necessary to remove the carrier plate from behind in slender strips after sawing them perpendicularly to this bearing plane. Although it is a time-intensive procedure, it is nevertheless considered as a rule to be the only successful method.

5.2 *Material on a building: Modification of renderings depending upon orientation to cardinal points*

It is just not easy to pin-point the causes of the distribution of the soluble constituents within the pore system. It is even more difficult, however, to detect their influence on structural characteristics of that building material. Changes at boundaries between aggregate grains and agglomerates of the binding agent caused by local reactions and enrichments as well as by physical processes are not always significant, and sometimes are even superimposed by the scattering of measured values. Pore space composed mainly of open and permeable cavities causes changes in chemistry, principally parallel to the rendering profile faces. It represents after all the negative between different-size aggregate grains and the local enrichments of binding agent. As a consequence of hardening, both form together a kind of framework granting mechanical strength to a rendering layer, which enables buildings to really withstand weathering.

Samples were taken at nearly the same height from several parts of a free-standing three-storey-dwelling near the Federal Institute, representing its four façades. Because the samples originated from sides of a building diversely orientated and also somewhat varying in their composition, one cannot assume a systematic sequence of properties. The essential similarities would be their common existence for more than about 30 years. Nevertheless, it should be considered that when producing a scraped finish at a building, gravel grains of about 2 - 5 mm diameter are usually introduced into the raw mix, which then gives the decorative effect intended. This admixture, sometimes constituting a volume of up to 20%, was removed by sieving before starting chemical analysis in order to assure comparability of the mass of its binding substance with e.g. that of any smooth finish.

Tab. 7 shows the mix proportions for the rendered finish sampled from four sides of a house nearly at the same height. By subtracting sulphate contents originating from atmospheric SO_2 reaction, one obtains in all cases the composition of a lime plaster with cement admixture.

Tab. 7. Composition of ca. 30-year-old external wall rendering samples taken from all sides of the building

Rendered Finish	M = proportions by mass V = proportions by volume	Ratio of Components		
		lime	cement	sand
ENE façade	M	1.0	0.2	9.7
	V	2.0	0.2	7.4
SSE façade	M	1.0	0.6	12.6
	V	2.0	0.5	9.7
WSW façade	M	1.0	0.6	11.2
	V	2.0	0.5	8.6
NNW façade	M	1.0	0.6	12.4
	V	2.0	0.5	9.6

For mercury porosimetry they were divided into layers of the upper 5 mm and the portion below. Roughness and irregular appearance of the finish layer led to difficulties in preparation as well as to influences on the results obtained. Data determined and values calculated therefrom are given in Tab. 8 (cf. Fig. 25).

Use has been made of the Ravaglioli interval and the microporosity. Leaving aside the mean critical diameter d_{10m}, which was found to be too near the outer border of the range tested, there occurs a variation of discrete values with a tendency from one to the next layer abraded that is independent of cardinal point. The specific pore volume, R interval and micro porosity

increase systematically with depth, whereas the median or 50% fractile does the opposite. This means a decreasing porosity and a prevalence of coarser pores in the outer layer than in a rendering's interior. A likely explanation may be the clogging of fine pores by neoformation of mineral phases from reaction or by recrystallization. Influences according to respective cardinal points can be possibly expressed by differences in or amount of corresponding values.

Tab. 8. Characteristic values for pore-size distribution determined in a ca. 30-year-old rendering and their change due to differing exposure conditions being dependent on cardinal points

Sampling Place	Façade (rough and irregular surface)								Gable (smooth surface)			
Orientation	ENE		SSE		WSW		NNW		SSE		NNW	
Height in m	4 – 6		6 – 8		6 – 8		6 – 8		8 – 12		8 – 12	
Depth in mm	0 - 5	> 5	0 - 5	> 5	0 - 5	> 5	0 - 5	> 5	0 - 5	> 5	0 - 5	> 5
Specific pore volume in cm^3/g	0.16	0.16	0.13	0.18	0.17	0.20	0.16	0.17	0.17	0.16	0.19	0.20
d_{10m} value (diameter) in %	1)	62.0	1)	52.5	1)	68.3	1)	70.0	1)	1)	37.5	1)
Ravaglioli interval in %	14.6	29.7	20.2	30.0	14.6	18.6	15.7	22.1	20.2	23.0	23.8	16.4
Microporosity in %	49.0	68.5	61.9	75.0	53.2	67.9	53.2	59.8	58.4	62.7	75.0	66.0
Median (radius) in µm	2.7	0.6	0.6	0.5	1.6	0.6	1.0	0.8	1.0	0.8	0.4	0.6

1) achieving or exceeding upper limit of method's working range at 75.0 µm pore diameter

Since concentration profiles prove a weathering process occurs in the upper 4 to 5 millimetres, a comparison of surface layers requires special attention (Fig. 25).

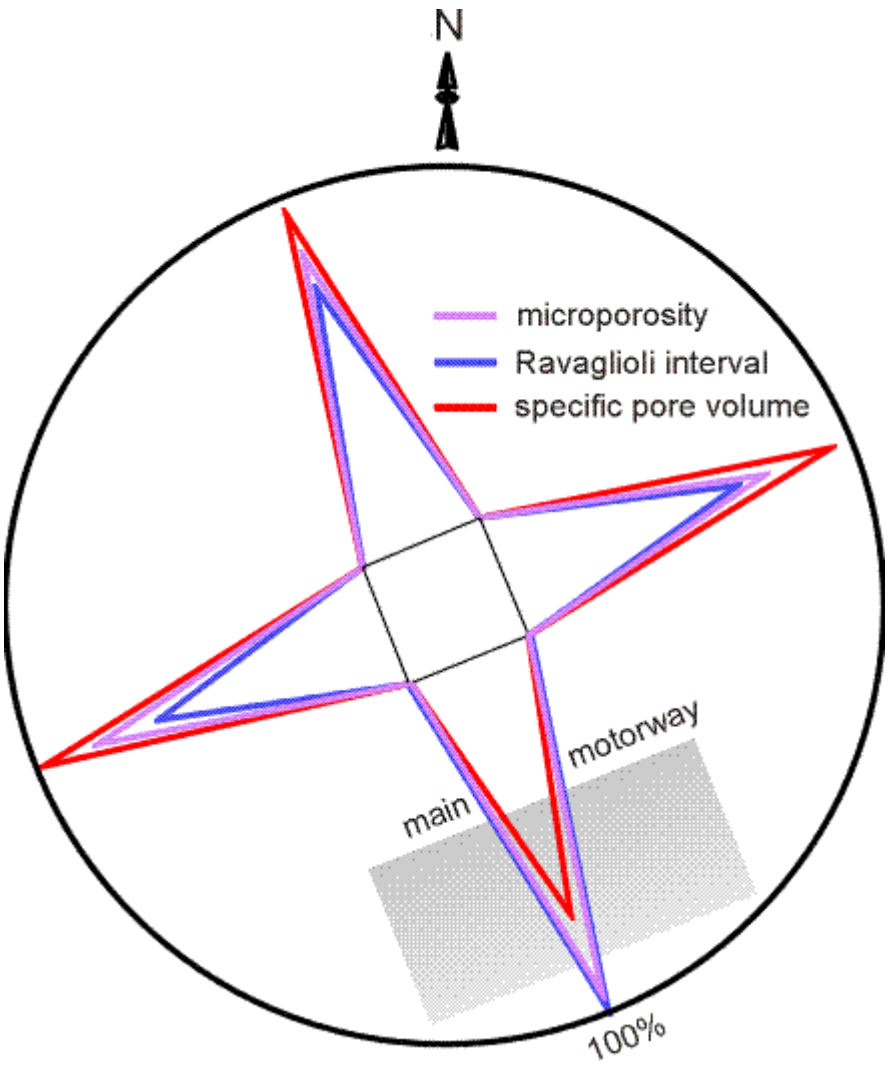

Fig. 25. Pore-size distribution of surface layers (0 - 5 mm depth) in external wall renderings: discrete values whose maxima were set to 100%, as represented for the façades of a building

Therefore structural data of the SSE façade vary substantially from those of other sides. Besides filling of the pore space with reaction products, orientation to one of the most crowded Berlin motorways "Unter den Eichen" and also greater exposure to sunlight, temperature differences and dew probably play an important role here.
Moreover, one can also satisfactorily estimate available pore space by the water absorption coefficient, w_o, or water vapour diffusion resistance index, μ. Provided that heterogeneity and irregular cross-section is taken into account, both of which determine capillary liquid absorption of the specimen concerned, the fitted model obtained includes some parameters with sufficient accuracy. Although practically dominating the measuring problems for renderings, there however result difficulties to shaping such a brittle and crumbly material to specimens which have fairly rectangular contours. So for capillary behaviour are obtained integrated average values and that also on material being a multi-layer type because of its manufacture. Though one can only perform capillarity measurements on plaster fragments over a total cross section - corresponding to their absorption surface - and after a relatively short but material-specific time period of about six hours or one day, the curve's validity is not yet satisfactorily guaranteed. However one can gain information on the important water absorption coefficient. This gives insight into dynamics of rain-water movement penetrating from outside and is one of the driving forces for redistribution of migrating salts within the profile, which nevertheless depends upon the cardinal point. By automatically recording gravimetric values in this way, plausible curve plots were obtained.

On samples taken from the cited building, circular-shaped slices having a uniform thickness were examined with the objective to determine water vapour diffusion. The low resistance of plaster against deformation during mechanical stress as a consequence of temperature cycles can nevertheless be explained by its open structure going hand-in-hand with a relatively high porosity. Among other things this promotes a high permeability for fluids, bringing in this way reactive constituents in close proximity to each other, and similarly favours the conversion of reaction products. Water absorption coefficient, as well as water vapour diffusion resistance index, are highest in samples from an ENE façade, decrease in those of SSE and NNW and finally achieve their minimum at a building's side pointing towards WSW. When plotting both characteristic values against each other, a linear dependence results (see also Fig. 41).

Chemical analysis indicates in all samples a continuous decrease of sulphate content towards the rendering interior. Maximum enrichment of more than 2% related to mass of the dried substance was found at the surface of the scraped finish, especially at ENE and SSE façades of the building (see Fig. 26). In contrast to this, the lowest amount was detected at its NNW side, which may be ascribed to partial leaching caused by elevated rain incidence. As can be expected, the calcium fraction in an aqueous extract decreases with increasing depth of profile. Therefore, in the upper layer of a rough finish from ENE and SSE façades, one can certainly expect a maximum of water-soluble calcium and sulphate fractions, whereas the lowest amount was met at the NNW side. Generally found at traces of 0.03% down

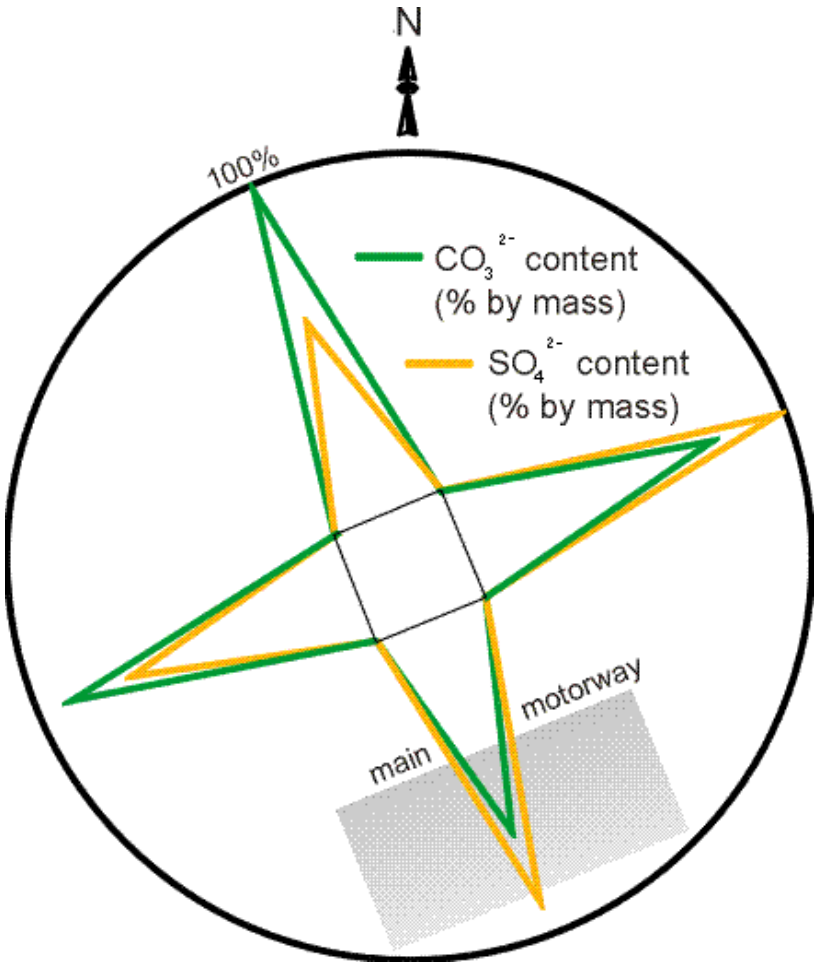

Fig. 26. Sulphate and carbonate concentrations at the surface (1 mm depth) in external wall renderings: contents whose maxima were set to 100%, as represented for the façades of a building

to less than 0.01%, nitrate was not detected in all outer layers of a profile but appeared distinctly in the scraped finish of ENE and SSE sides (see Fig. 27).

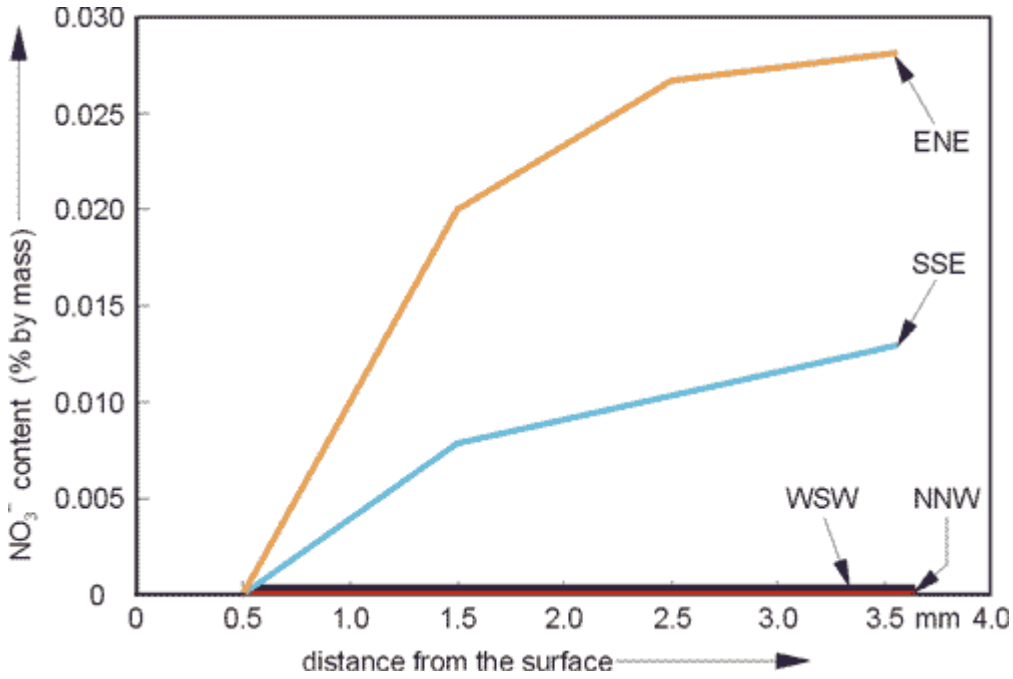

Fig. 27. Comparative depth profiles showing nitrate distribution in ca. 30-year-old external wall rendering samples taken from all sides of the building

This nitrate occurrence may obviously be attributed to the proximity to one of the most crowded motorways in Berlin, whereas the smooth finish shows at both gable-sides, as expected, small nitrate amounts only at SSE. Nitrite could not be detected. Chloride concentrations - here ranging from 0.02% to less than 0.01% - seemed to be distributed not as systematically as usual for the other anions already cited. In some circumstances there exists a prevailing orientation to SSE and ENE as being the main direction to the source of pollution. pH-values measured in aqueous extracts were always situated above the neutral point, having their maximum at 10.9. They consequently increase with diminishing calcium sulphate content, above all rather clearly in deeper layers in material of SSE and ENE façades. In aqueous extracts of experimental rendering exposed outdoors, lower pH values have been observed than in their indoor equivalents. This evidently finds its explanation in more intense carbonation and sulphation at an unobstructed contact with the atmosphere.

As expected, there is a steep decline of sulphate content within the first millimetres of depth profile of a lime-containing porous building material. It is also not surprising that its absolute value in one and the same material can be variable with the cardinal point (compare Fig. 26 and Fig. 28). Regarding such a representation, however, one should consider the obviously systematic change in the sequence of amounts over the entire profile. One must reflect so far that low values for the abraded first millimetre accordingly go hand in hand with relatively elevated values of the fourth millimetre, while conversely high sulphate contents at the surface are associated with low ones in the profile depth.

Calculating the arithmetic mean of the four contents belonging to each profile, it was uniformly close to 0.8% by mass. If one assumes comparable material at all building sides at the same height and a satisfactory moisture supply for solution transport, by no means must a unilateral immission be taken into account as a possible explanation for the mutual intersection of the individual concentration curves, as conditioned by the orientation of a building towards its source. On the contrary, one can imagine that - proceeding from a nearly homogeneous distribution in the first four millimetres of the profile - a supplementary enrichment of this salt would merely have taken place, in the long run, in the sense of neo-precipitation originating by a more or less intense evaporation.

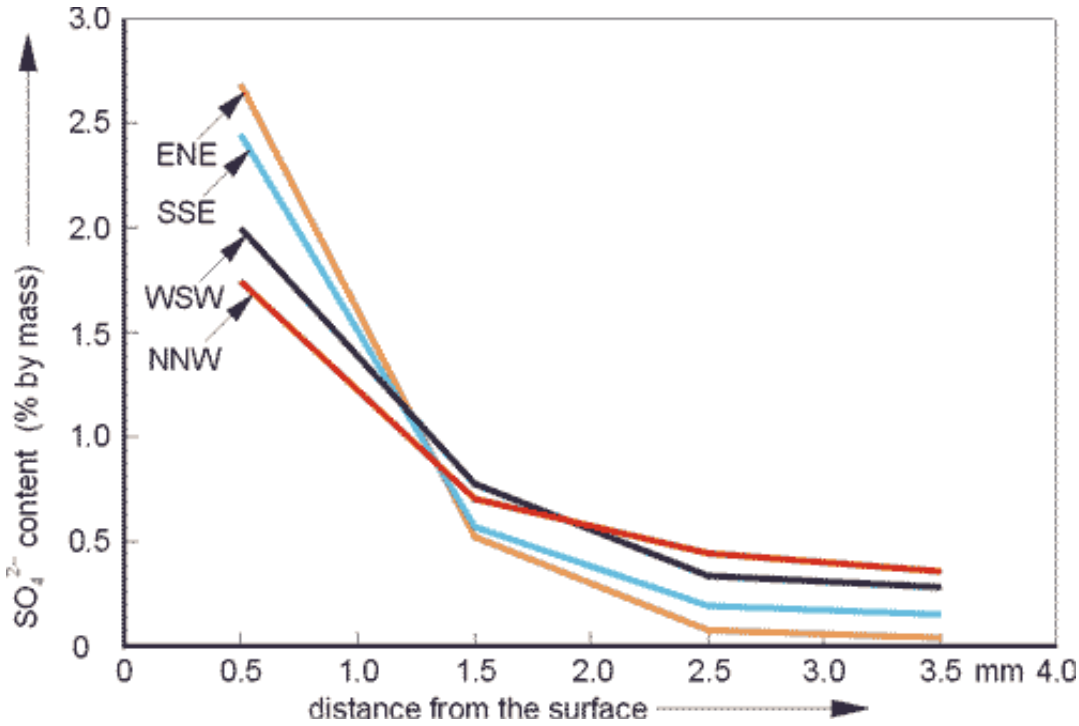

Fig. 28. Sulphate distribution in ca. 30-year-old external wall renderings sampled from all sides of a house at the same height

As far as this finding can be confirmed by additional analytical data obtained at other buildings sampled at all their façades, one can overturn a long-standing conception. This would mean that, at least in the case of sulphate, one has to understand the entire building's rendering surface at one and the same height as a practically uniform reaction face, at which - depending upon microclimate - the formation of different concentration gradients would have taken place afterwards as a consequence of the cycles of dissolution, transport and reprecipitation.

Unfortunately chemistry only permits one to determine concentration profiles caused by different air pollutants and graded in millimetres for the powdered material or aqueous extracts that are needed. Structural changes can be detected integrally in ranges between 0 - 5 mm distance from a sample's surface or from a depth greater than 5 mm, since for mercury porosimeter test a certain quantity of material in solid pieces must be available, which can only be arduously obtained from the friable sample. As was expected, the abrasion behaviour indirectly yielding information on structural changes in this range also shows considerable differences related to the direction of outdoor exposure (Fig. 29).

Plainly visible is a distinct hardening in the layer carried out as a scraped finish down to about 2 cm depth at the SSE façade, which occurs much less at the NNW side, and does not appear at all on the ENE side. In the last case, one observes a comparable resistance near the surface and also in a 3 to 5 mm depth, corresponding to an almost linear increase of the cumulative curve. This behaviour can also be deduced from structure: the SSE side presents the highest number of fine pores and at the same time the lowest pore volume, whereas at the ENE side the conditions reverse (high specific pore volume, low portion of micropores). In the course of this, the influence of carbonation or sulphation, which took place at its expense, does not seem to be so significant.

A smooth finish (rubbed surface) present at the gable region of this building shows on the other hand a comparable abrasivity on the SSE and NNW façades down to about 2 cm depth (Fig. 30). At a greater distance from the surface, the rendering of the NNW side is stronger, which also reflects a higher amount of fine pores and a shift of the median to smaller pore radii in contrast to material of the opposite exposure direction (cf. Tab. 8).

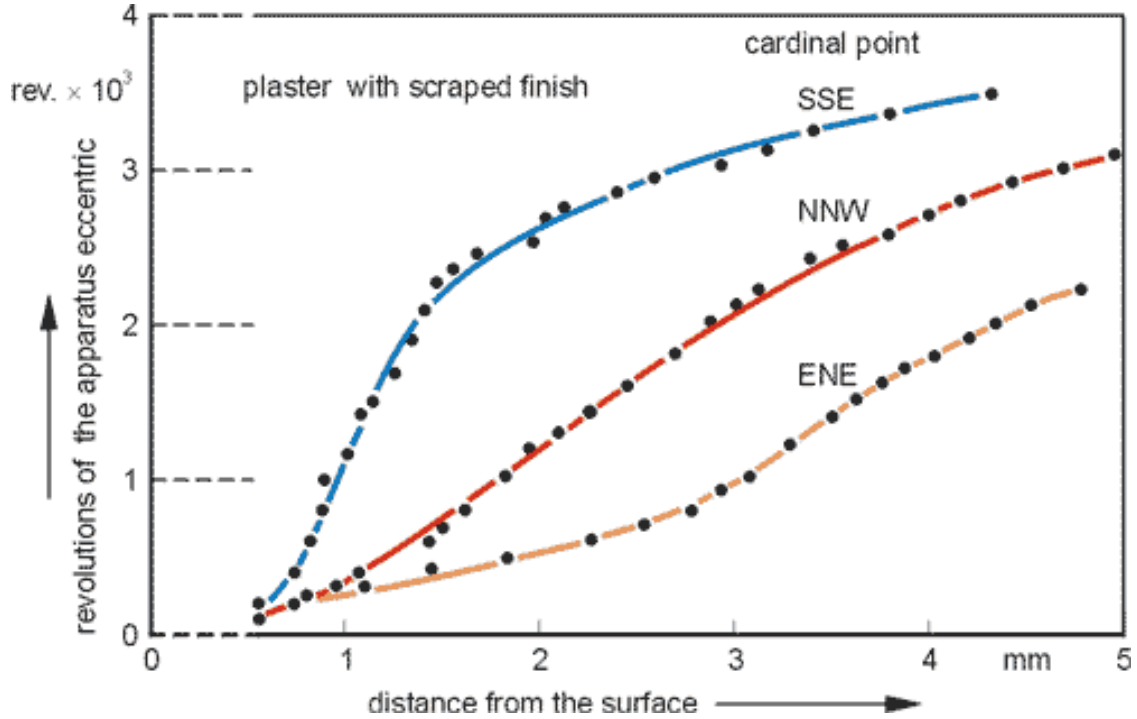

Fig. 29. Abrasion behaviour of a wall rendering, depending upon the respective cardinal point: cumulative curves of single amounts of wear of specimens taken from the same height

Generally, however, differences between scraped and smooth renderings can be determined with regard to structure and other data, which are clearly expressed by abrasion behaviour and sulphate absorption. The surface layer rich in binder always found in this type of finishing, which is inevitably obtained by a rubbing procedure, is responsible for this. Although largely remote in this case, it has possibly exerted a kind of protective function for underlying material and offered resistance to hardening by carbonation, sulphation and recrystallization.
It can be stated that weathering intensity at rendered façades at a certain height caused by air pollutants such as SO_2 is not determined to such a degree by the direction of the emission source, but rather by the micro-climatic circumstances at the exposure site whereas others like nitrate or chloride show clear dependence. This can also be concluded from results of a more recent survey [95] on façades with limestone called “Caen stone” at the same-named town in France, where sulphates from traffic and industry, and chlorides from the marine environment of the nearby Atlantic coast are causing corresponding deterioration.
It should be emphasized that in such a way only water-soluble constituents are captured and not those already fixed by precipitation and having formerly participated in profile formation. Although this instantaneous view of a continuing evolution is subjected to the seeming disadvantage that monitoring of former stages is no longer possible, it yields information of material behaviour with regard to present absorption and solution transport. Previous depositions and conversions characterized merely by a summarizing effect can be investigated by an acid digest or better directly with a scanning electron microscope combined, for instance, with an energy-dispersive X-ray analyzer.

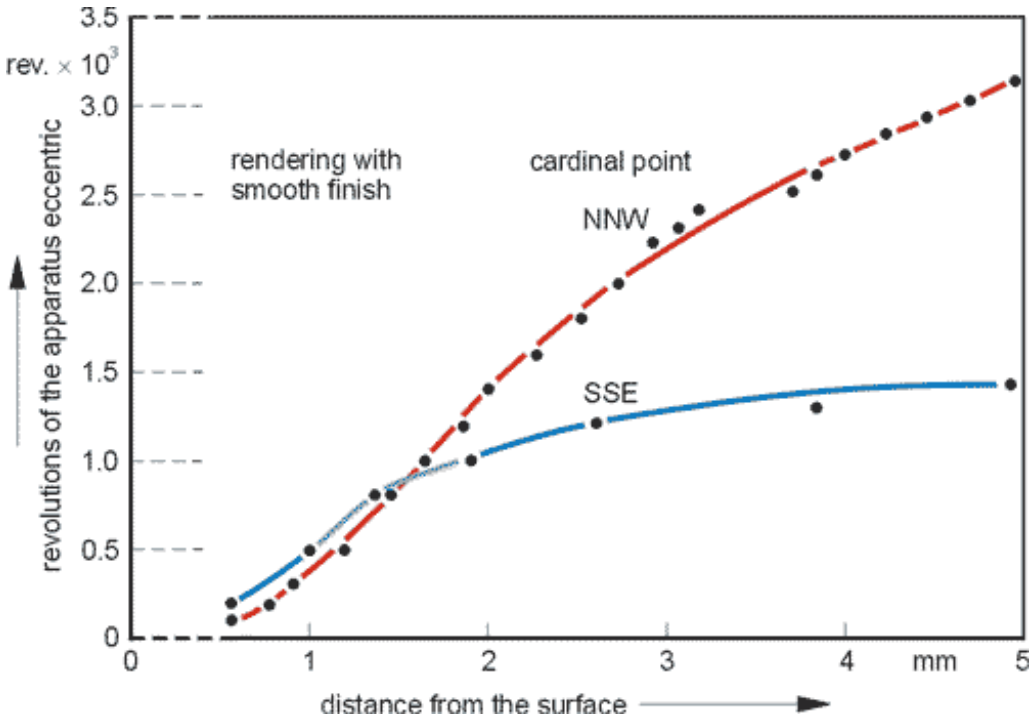

Fig. 30. Abrasion behaviour of a wall rendering, depending upon the respective cardinal point: cumulative curves of single amounts of wear of specimens taken from the same height

5.3 Material on a building: Height-dependent modifications

During visual evaluation, care was taken so that rendering fragments were sampled from regions situated as far as possible perpendicularly one above the other. For structural characterization, water absorption coefficient as well as discrete values of pore-size distribution and vapour diffusion resistance index was utilized. Fig. 31 shows curves for the platy fragments sampled from different heights of a dwelling house on a rendered external wall facing west at the yard side. In this case trees and shrubs were present around the building.

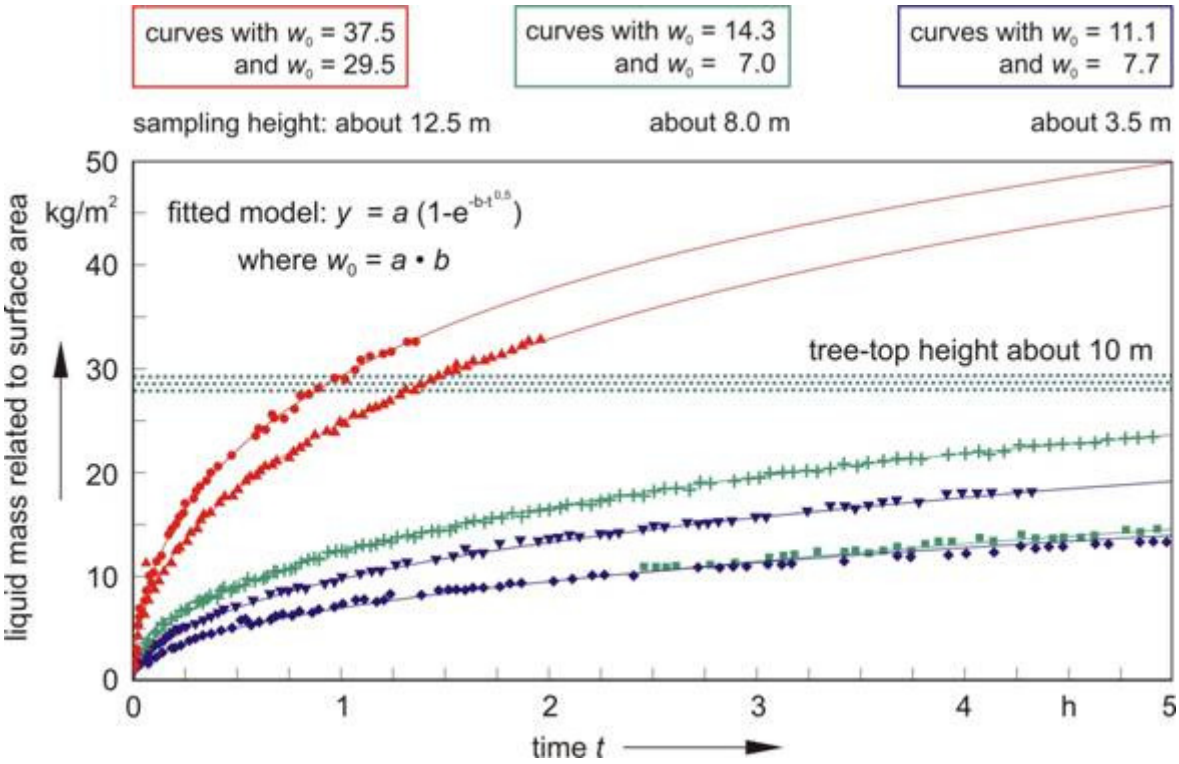

Fig. 31. Capillary absorption behaviour of six ca. 40-year-old rendering fragments (lime plaster with cement admixture) taken from western façade of a dwelling house at different heights

With increasing elevation from ground level, one can find a considerable rise in the water absorption coefficient, which could be an indication that the degree of weathering or structural damage due to corresponding attack was augmented. Also the sulphate content increases with building height, which is seen in Fig. 32. Plotting average sulphate content across the whole profile versus elevation from ground level, one can find an almost linear increase with height. The distribution in samples taken from 12.5 m height further indicates leaching in the first millimetre.

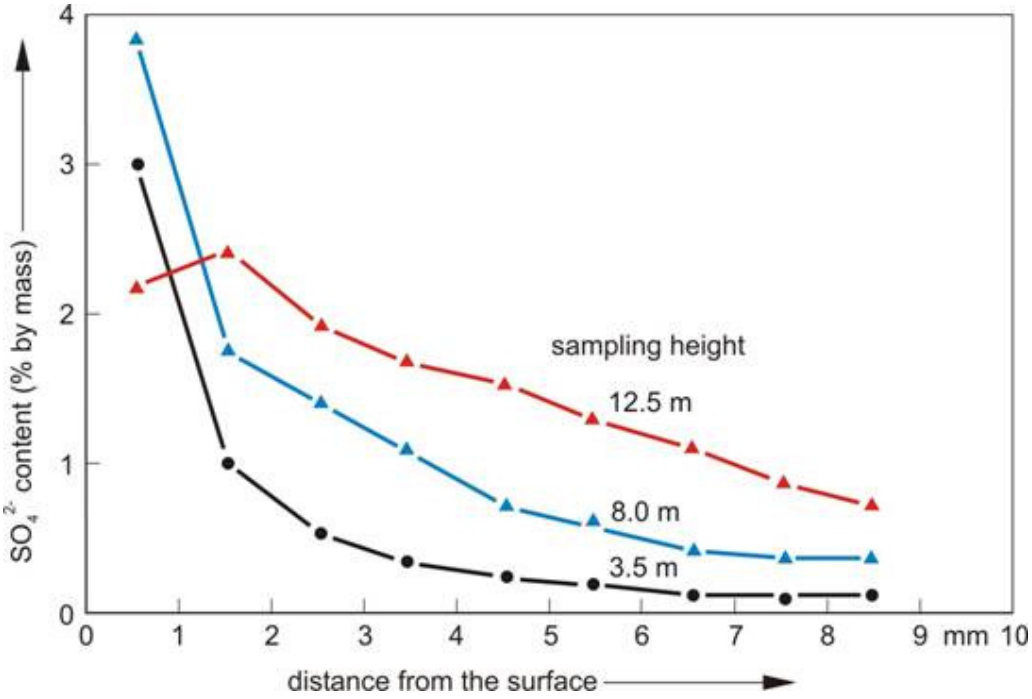

Fig. 32. Sulphate distribution in ca. 40-year-old external wall renderings sampled from different heights of a dwelling house

Nitrate and chloride appear only at lower parts of the building, i.e. they are detected only at 3.5 m. Also as found previously, the distribution is characterized by a gradual increase with depth, where these ions are missing in the outer 2 to 3 mm. It remains doubtful, however, whether maximum values of 0.018% for nitrate and 0.012% for chloride could exert significant influence on weathering progress. Calcium runs parallel to sulphate, potassium probably too, but at 0.01% it cannot be taken into account. From this building, samples were also taken at different heights for determining porosimetry by mercury intrusion.
Integrating results across the whole thickness of the plaster, one also can deduce the influence of exposure height upon the discrete values of porosimetric data already mentioned (Fig. 33). For this purpose the same parameters as before were used, and furthermore the water absorption coefficient and water vapour diffusion resistance index, by plotting them all versus sampling heights on the building. So one can clearly observe that the specific pore volume and also w_o grow with increasing distance from ground level, whereas microporosity, R interval and μ decrease, meaning that the small pores will be shifted to larger diameters.

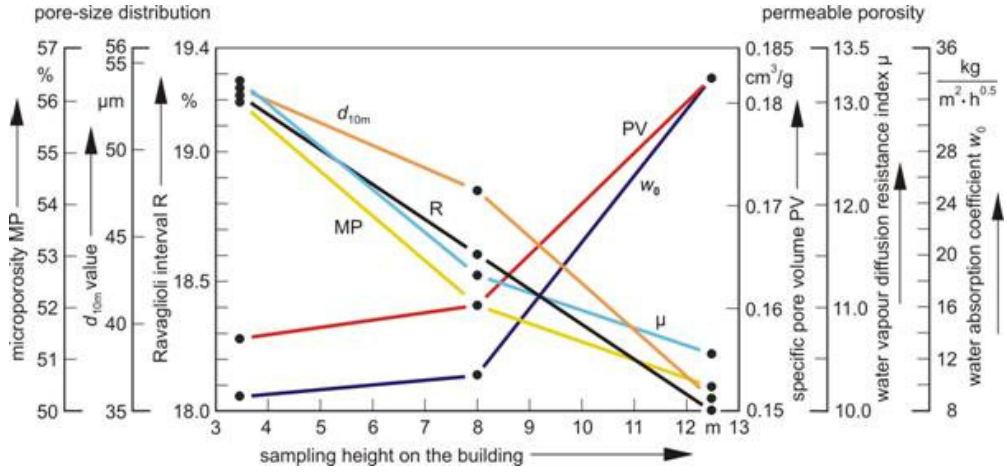

Fig. 33. Pore characteristics of a ca. 40-year-old rendering and their change by means of differing exposure height, western façade, yard-side

This finding can even be expanded, considering for example a change of d_{10m} value for the single plaster courses with increasing elevation. One can monitor that weathering, starting from the surface, affects increasingly deeper layers of rendering, so that at 12.5 m fitting of this parameter was almost fully attained over the whole plaster cross section. Specific pore volume shows a corresponding behaviour (compare Tab. 9). From these results the conclusion is drawn that a diminution of coarse pores will be first caused for example by filling up with reaction products from sulphuric air pollutants. Such a conversion leads to a narrowing of the pore channels to about a third and consequently a lowering of d_{10m} to a smaller diameter. Fine pores are in fact

Tab. 9. Characteristic values for pore-size distribution determined in a circa 40-year-old rendering and their change by means of differing exposure conditions dependent on building height

Sampling Place	Façade (smooth surface)					
Orientation	W		W		W	
Height in m	2 – 4		6 – 8		12 – 16	
Depth in mm	0 - 5	> 5	0 - 5	> 5	0 - 5	> 5
Specific pore volume in cm^3/g	0.15	0.17	0.15	0.16	0.18	0.19
d_{10m} value (diameter) in µm	52.7	53.7	37.4	57.7	35.1	37.8
Ravaglioli interval in %	20	18	20	17	18	17
Microporosity in %	57	54	54	50	51	48
Median (radius) in µm	1.2	1.5	1.7	2.5	2.2	2.8
Water absorption coefficient w_0 in $kg/(m^2 \cdot h^{0.5})$	9.4		10.8		33.4	
Water vapour diffusion resistance index µ	13.1		11.3		10.6	

also subject to systematic change, i.e. here a decrease of the micropore portion of the whole profile is found with increasing height, but differences between both layers (from 0 to 5 mm and greater than 5 mm in depth) are not remarkably reduced. From all this follows a pore-size distribution characterized by a steeper development of the cumulative curve, which corresponds to a pronounced maximum of pores during simultaneous narrowing of their range. Thereby pores between 2 to 100 µm diameter are principally concerned, whereby the distribution curve shows a distinct maximum at 10 µm.

Since capillary effects occur in pores between about 0.1 and100 µm diameter [64], the water absorption coefficient as a representation of this behaviour of a material will be also influenced by this convergence. Sources in the literature reveal that vapour diffusion takes place in pores larger than 0.1 µm in diameter. According to the results obtained, the resistance to water vapour diffusion decreases with sampling height. The corresponding process is practically not influenced by coarser pores but more by finer pores, since once their fraction decreases, the specific pore volume simultaneously increases. This could mean that through a weathering process, fine pores were enlarged and coarser pores narrowed by recrystallization and neoformation of mineral phases (Fig. 34). This is in accordance with changes of d_{10m} (compare Fig. 33).

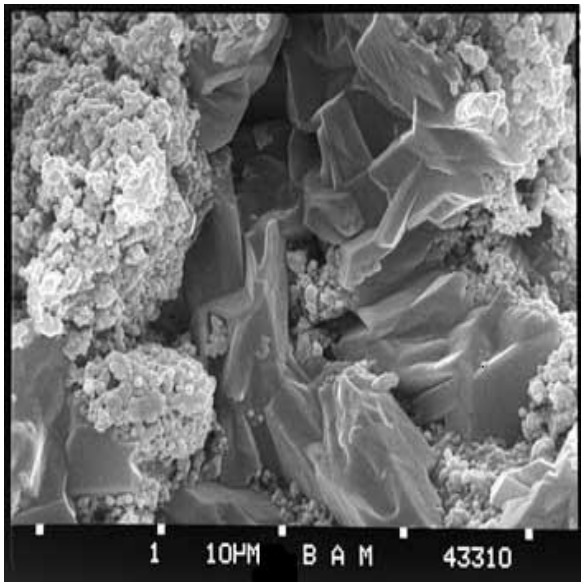

Fig. 34. A coarse pore in a rendering, filled with sulphate reaction products causing size reduction (SEM micrograph)

In accordance with the corresponding findings, this causes an elevated porosity and results in the vapour diffusion behaviour as well. Therefore one can, at least in the case of samples tested, amplify the statement in such a way that this phenomenon is not essentially affected by more intense weather attack on the higher situated parts of a building. Another factor for structural change would be contributed by plant growth, especially found at a greater building height and seen as traces in coarser pores of surface samples taken there.
The influence of sampling height at a building is also evident as shown by the grinding abrasion curves determined on rendering fragments (Fig. 35). With an increasing height position, strength decreases in accordance with pore data being equal to smaller portion of micropores, shift of median to coarser pores and increase of pore volume.

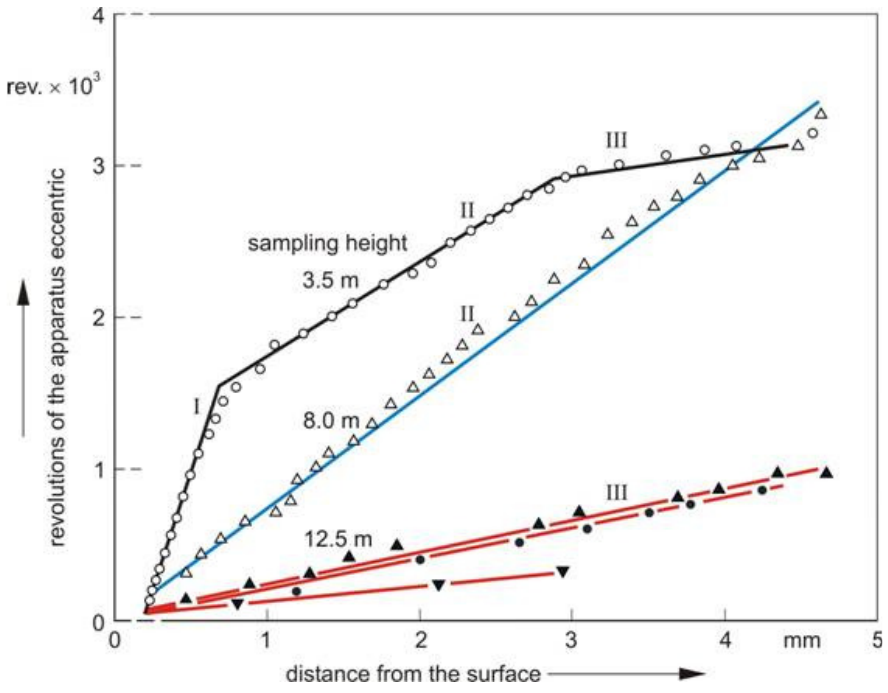

Fig. 35. Modification of abrasion behaviour of rendering fragments with sampling height: cumulative curves of single amounts of wear (Roman numerals indicate layers of same strength.)

Here also an elevated intensity of weathering at upper building parts compared to lower ones clearly emerges. It is obvious as abrasion behaviour of a sample from 3.5 m height assumes a tripartite curve course. The first part down to about 1 mm depth (I) is characterized by a steep slope of the cumulative curve (about 1700 revolutions of the eccentric per mm of depth; crust indication). It is followed by a second section (II) with about 600 rev./mm ranging between 1 and 3 mm distance from the specimen's surface. The next part (III) then finally shows no more than 200 rev./mm. A similar slope as in the last part is found in material from a greater height. So rendering obtained at an 8 m height reflects approximately curve section II at 3.5 m, whereas rendering at 12.5 m height corresponds to that of section III of the same materials. Thus with increasing building height, an impression emerges not only of a structural breakup but also that due to erosion, one can no longer find the original rendering surface - a suspicion which increases by visual assessment of corresponding samples.
If vegetation is absent around a building, nearly the same behaviour is observed. So an elevation of the water absorption coefficient w_o with increasing distance from ground level is found, whereas the μ value shows a countercurrent behaviour (Fig. 36).

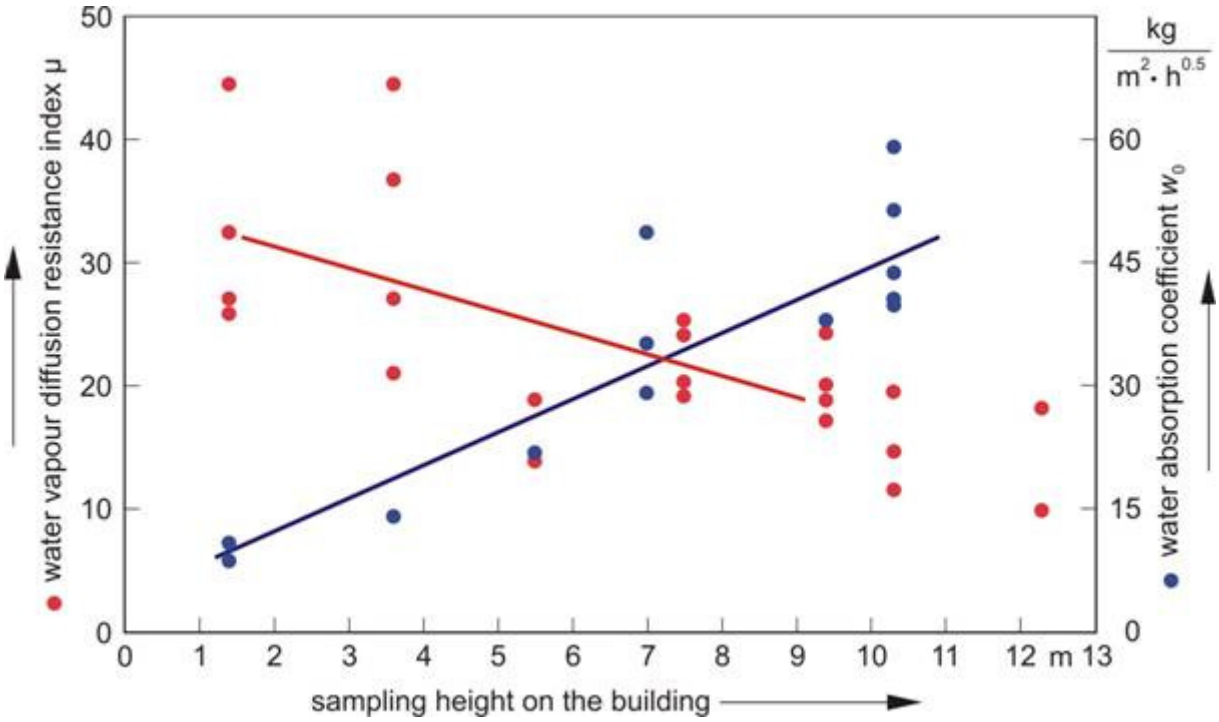

Fig. 36. Capillary absorption and water vapour diffusion behaviours of rendering fragments taken from the façade of a ca. 50-year-old dwelling house at different heights

If a diagram analogous to Fig. 33 is developed for such a building from discrete values of the mercury porosimeter test, water absorption coefficient and μ value, they indicate the same course - with one exception - as values plotted against sampling height (Fig. 37). Because of intense degradation of the surface and its roughness, only such characteristics could be taken into consideration which represent results of material sampled at least at a depth of more than 5 mm. They together with w_o demonstrate a dependence upon building height. Based on the weathering degree, specific pore volume and w_o increase, while microporosity as well as μ simultaneously decrease. Contrary to previous experiences [36], however, the d_{10m} value expresses an inverse tendency. Showing a clear displacement, this parameter behaves as a measure for modification of the coarse pore range.

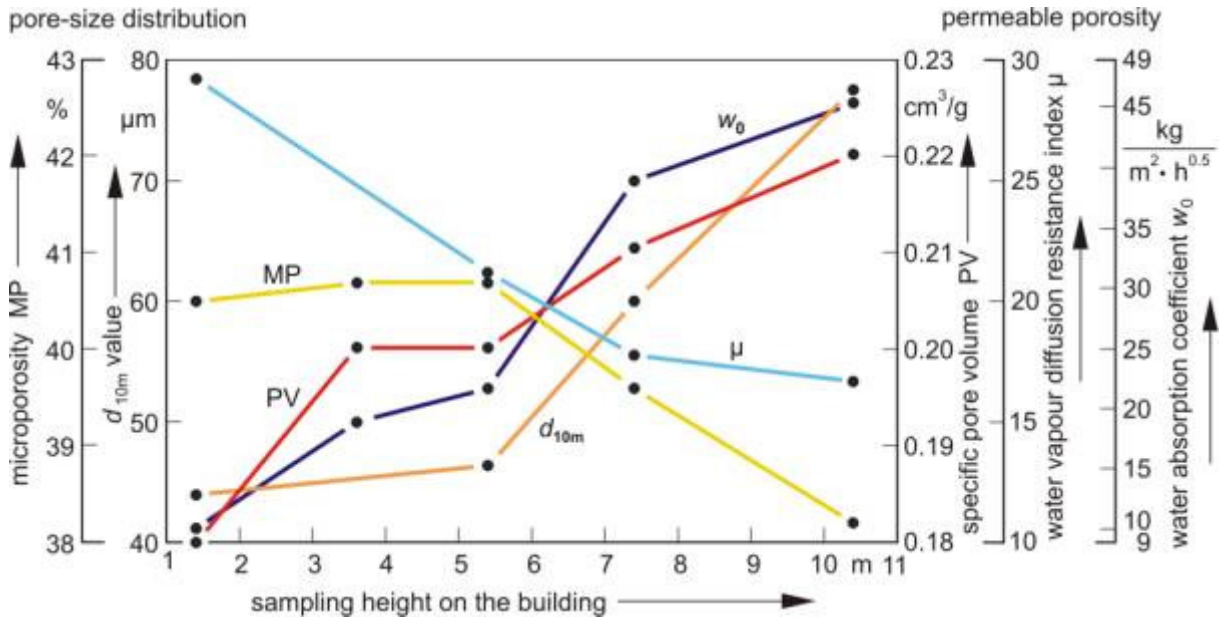

Fig. 37. Pore characteristics of a ca. 50-year-old rendering with hydrated lime and cement admixture and their modification by means of differing exposure height

It can be seen by comparing test results at the heights of 1.4 and 10.5 m. Such a remarkable phenomenon, exhibiting a narrowing and then widening of pore space can find an explanation with the countercurrent dependence of sulphate content (Fig. 38).

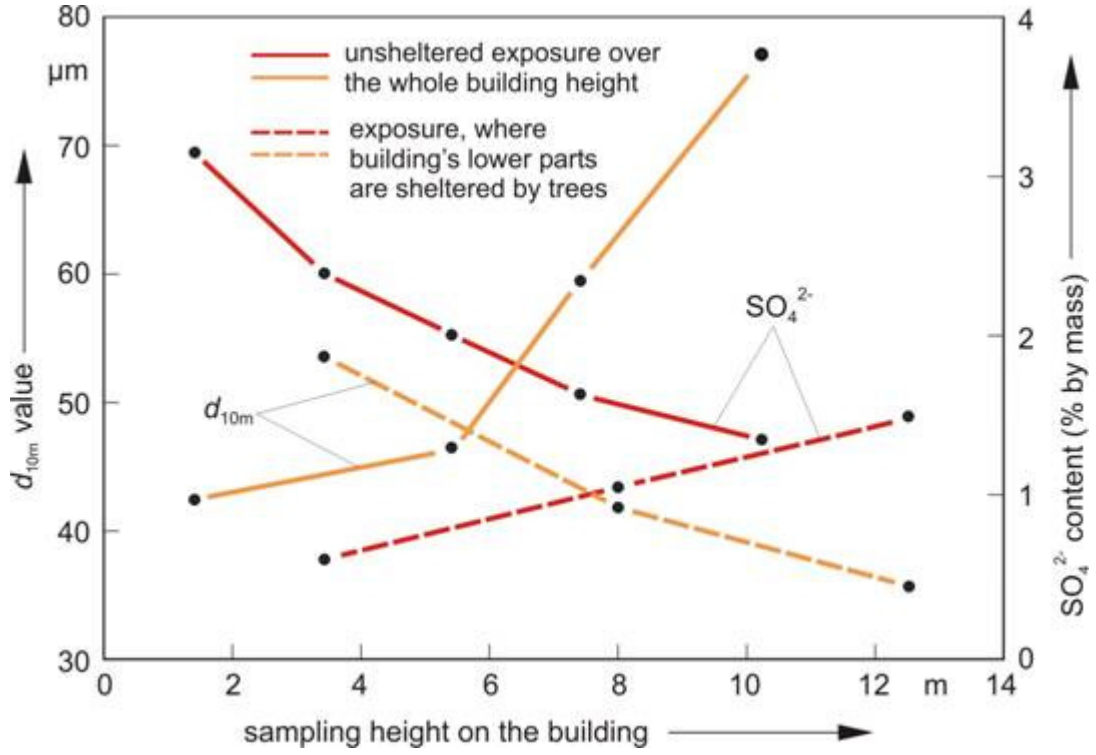

Fig. 38. Countercurrent dependence in each case of sulphate content and portion of coarse pores d_{10m} in external rendering from two walls facing west (circa 40 and 50 years old), plotted versus building height

If diminution of pores with increasing building height could be formerly ascribed to a neoformation of clogging salt precipitates, in the present work it is the case of decreasing sulphate with height attributable to leaching and thinning of the profile during erosion, so that the original surface was hardly available for analysis. In the previous case, protective and

absorptive behaviour by plant growth as e.g. trees at lower levels could have an opposite influence. On the present plant-free site, however, total sulphate amount originating from the external 5 mm abraded layer of greater than 3% by mass at a height of 1.4 m diminishes to 1.7% at the 7.4 m level where the d_{10m} value coming, however, from samples taken at a deeper layer shifts simultaneously from 40 to 80 µm. This equating is permissible since the observed tendency also remains constant in deeper parts of a rendering profile. So at a distance from the surface of >5 mm a sulphate content of >1% still exists at 1.5 m height, whereas 7.4 m samples show no more than 0.5% at a corresponding depth. As already mentioned, contrary to previous work, here one has stated a decrease of total averaged sulphate content with building height, which corresponding depth profiles may reflect (Fig. 39). So a common feature is the diminishing of sulphate with increasing depth.
In this way a zonal formation on a building takes shape which finds its expression in a different weathering intensity after the same exposure duration, either as a sulphate enrichment as reported by G r ü n in 1933 [29] and later on [3] or in an elevated immission by air pollutant precipitation [19], [63].

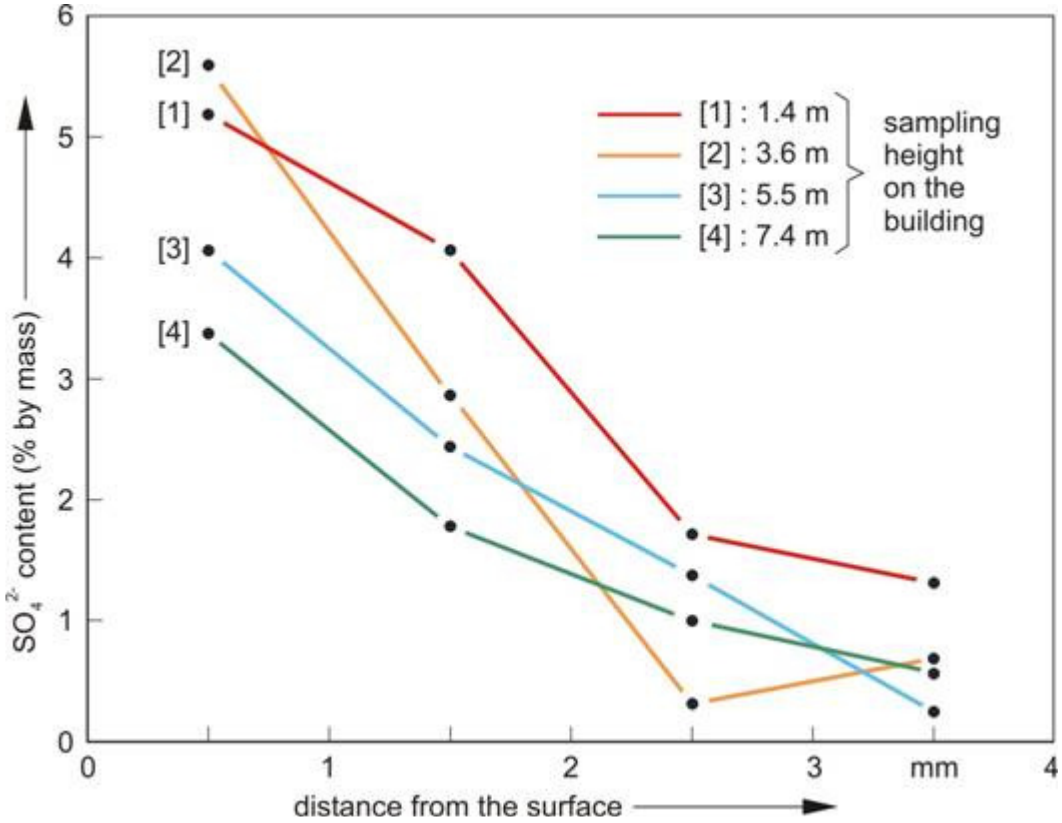

Fig. 39. Sulphate distribution in a ca. 50-year-old rendering sampled from the western façade of a dwelling house at different heights

Earlier statements that nitrate and chloride are enriched in the rendering's interior, as described in section 5.3, could be confirmed. At that time the NO_x reaction was conspicuously linked to the cardinal-point orientation and the close proximity to an emission source of a main motorway; one can now transfer this finding additionally to a building's height (Fig. 40). As also exemplified formerly [36], detectable quantities appear predominantly in the building's lower parts up to 4 or 5 m.

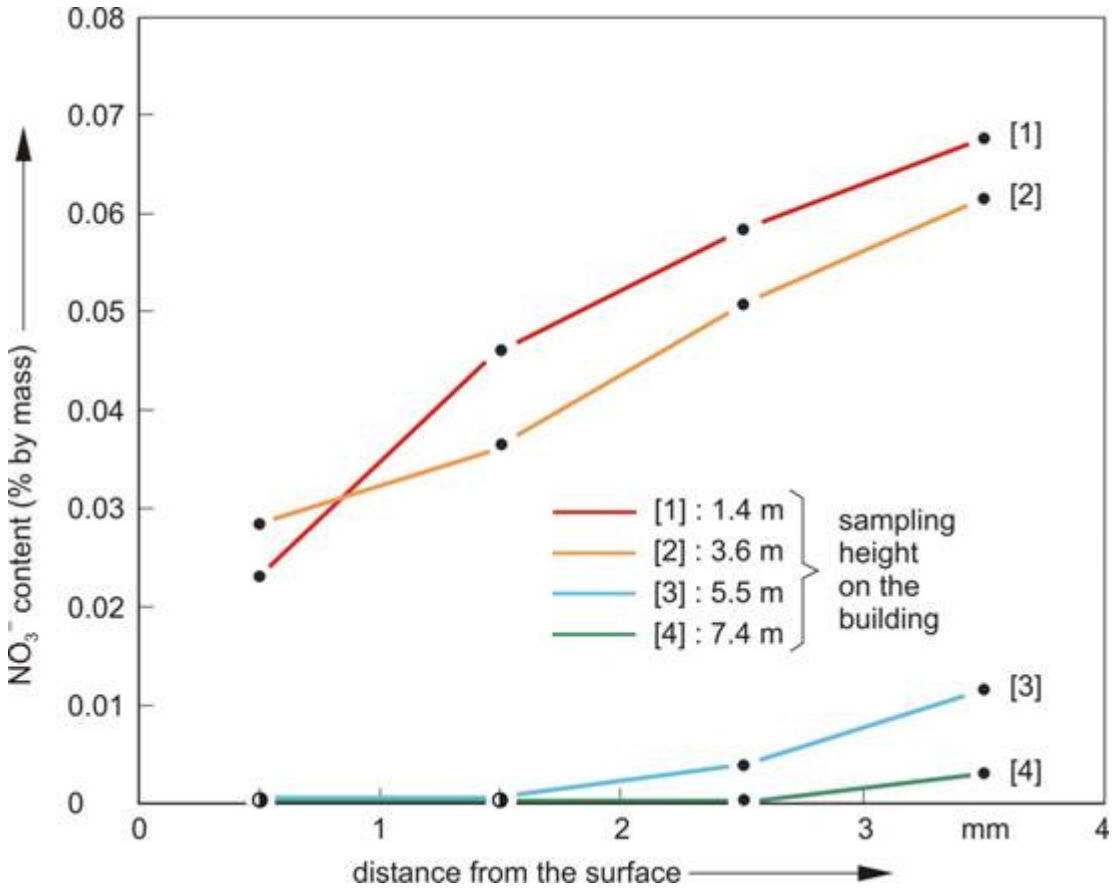

Fig. 40. Comparative depth profiles showing nitrate in a ca. 50-year-old external wall rendering, sampled at different building heights

5.4 Former outdoor exposure of rendering specimens over a period of 17 years

To determine the effect of air pollutants on rendering as accurately as possible, comparative examination of weathered and unweathered plasters, which in their original state should be identical, is useful alongside the examination of samples taken from older buildings as well. For this kind of investigation, rendering plates were available which had been specially produced during an earlier research project consisting of lime plaster and a dolomite equivalent and installed on the flat roof of a building of the Federal Institute for Materials Research and Testing, where they had been left exposed to atmospheric pollutants over a period of about 17 years. Others of the same type were stored in a climatic chamber at a temperature of 20°C and a relative ambient humidity of 50% for the same time interval. Chemical analyses and other methods were used for detection of change in the weathered plates compared with those in the sheltered samples.

When considering change in the surface layer down to 5 mm in contrast to a rendering's interior, it seems surprising that at both kinds of exposure the specific pore volume is larger in the first area. The same is true for the critical diameter d_{10m} and the microporosity compiled in Tab. 10. Furthermore, use is made of the R interval and the median, the latter being distinctly smaller. This means that in the outer layer a larger pore space exists while at the same time smaller medium diameters prevail. The reason for this indoor development is probably based on a carbonation process and on SO_2 attack during atmospheric exposure.

Tab. 10. Characteristic values of 17 years' stored renderings and their change outcomes at different exposure conditions, calculated from their pore size distribution

Sampling Depth	Characteristic Pore Value	Dolomitic Plaster		Lime Plaster	
		stored at 20 °C/50% r.h.	exposed outdoors	stored at 20 °C/50% r.h.	exposed outdoors
Surface layer (0-5 mm depth)	Specific pore volume	0.159 cm^3/g	0.144 cm^3/g	0.146 cm^3/g	0.157 cm^3/g
	d_{10m} in µm	2)	1)	1)	53.1
	Ravaglioli interval in %	13.8	13.1	20.2	19.0
	Microporosity in %	46.8	46.2	51.6	52.0
	Median (radius) in µm	3.6	3.1	2.0	1.1
Interior of plaster (0-5 mm depth)	Specific pore volume	0.155 cm^3/g	0.139 cm^3/g	0.141 cm^3/g	0.146 cm^3/g
	d_{10m} in µm	2)	2)	2)	1)
	Ravaglioli interval in %	12.6	12.3	16.4	16.5
	Microporosity in %	45.6	45.0	45.0	49.2
	Median (radius) in µm	3.8	3.5	3.9	2.7

1) achieving upper limit of method's working range at 75.0 µm pore diameter

2) exceeding method's working range

On the other hand, in surface areas one can generally find structural changes. In the case of lime plaster, one can state a decrease of d_{10m} to 53.1 µm in diameter and of the median from 2.0 µm to 1.1 µm in radius. This effect may be obviously caused by neo-formation of mineral phases, as e.g. by reaction of the lime component with atmospheric SO_2 to gypsum via dissolution and reprecipitation. Referring to dolomitic plaster, other circumstances are responsible insofar as specific pore volume was comparably lowered by exposure. This can be ascribed possibly to a leaching process in the surface layer area [93], since highly soluble magnesium sulphate was formed as a reaction product.

Whereas a comparison of water absorption coefficient w_o in both cases does not display any unambiguous trend, which could depend on unsuitable test material because of difficult preparation, one can record considerable differences in corresponding µ values. It turns out that such values of these specimens exposed outdoors are higher than those stored in the climatic chamber - a phenomenon which can be attributed to sulphate deposition in the pore system leading to a hindrance for vapour passage. Although for w_o alone not allowing information, together with µ it indicates an orientation. This shall be illustrated in the following diagram (Fig. 41) through a relationship where one can connect measuring points for an individual series of one and the same type of plaster by straight lines. So in the case of material exposed outdoors, an increase of w_o is always coupled with an elevation of µ.

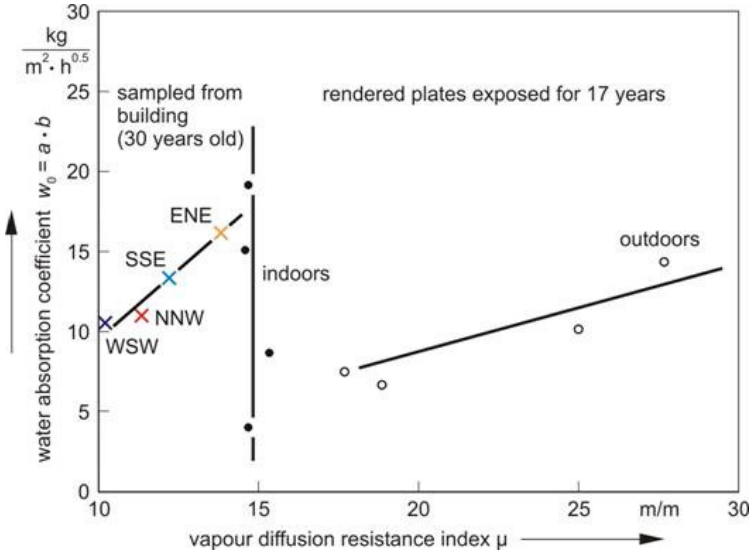

Fig. 41. Relationship between water vapour permeability and capillary behaviour: groups of similar renderings distinguished by their respective positions

Sulphate and carbonate contents of layers of these rendering samples abraded millimetre by millimetre were determined by means of coulometric titration. Fig. 42 shows corresponding concentration profiles for one lime and one dolomitic plaster. Samples are compared which were exposed 17 years in a climatic chamber with those exposed for the same time in an industrial atmosphere contact. According to results obtained, a dolomitic plaster shows a remarkably greater sensitivity towards SO_2. Of crucial interest is also the time course of its absorption.

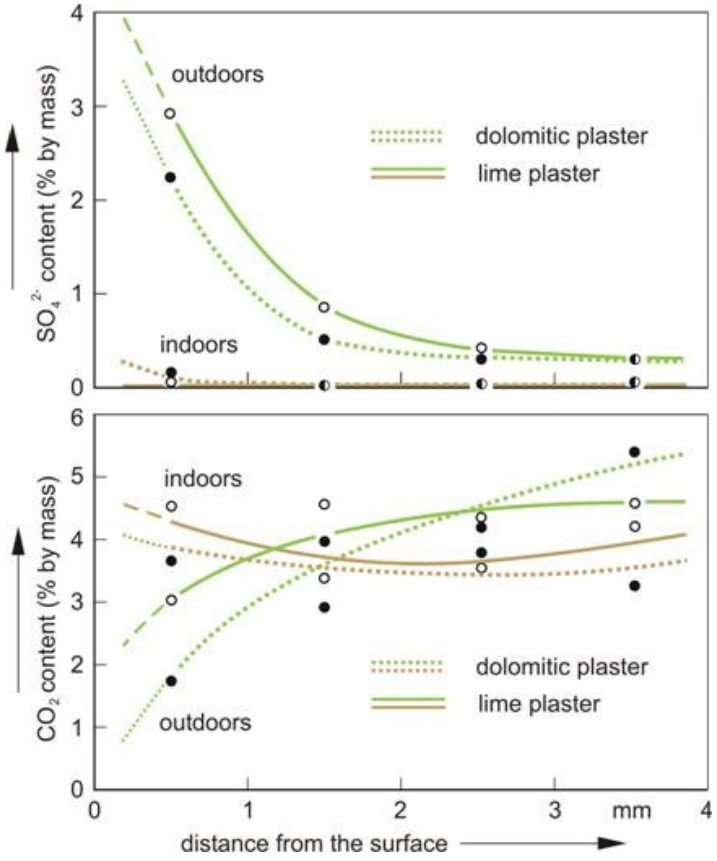

Fig. 42. Comparative depth profiles showing sulphate (top) and carbonate distribution (bottom) of weathered and unweathered samples of two rendering types after 17 years' storage

The distribution of carbonate (Fig. 42, bottom) determined by coulometric analysis, however, is not as well defined. But in the surface layer there is a lowering of carbonate in the weathered samples compared with the unweathered. This results from the SO_2 attack which causes substitution of carbonate by sulphate. In Fig. 43 a rendering exposed over 4 years is compared with one of corresponding composition but 17 years old.
If one would here plot the contents of the first millimetre of each plaster against exposure time, an almost exponential increase of sulphate absorption would be found. This however is because only two values are available next to the zero point which can be arbitrarily connected with one another. It is to be expected that absorption decreases with increasing duration, since the SO_2 portion ha consid- erably diminished during the last 20 years in ambient air.

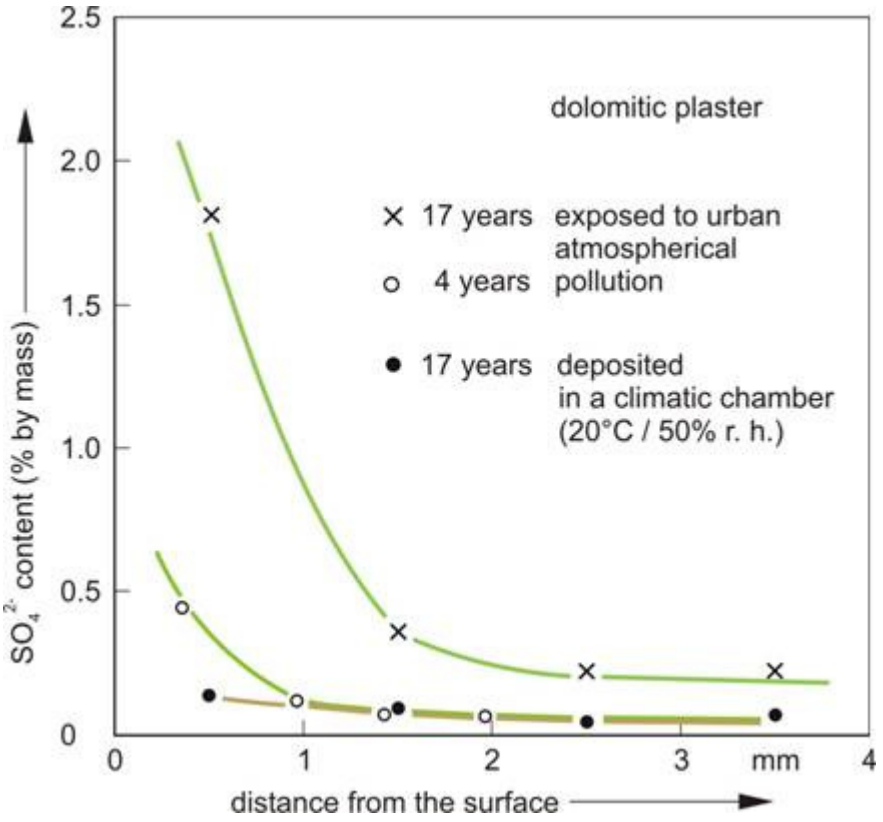

Fig. 43. Sulphate enrichment in dolomite hydrate plaster after different exposure times compared with indoor storage

In contrast to those specimens stored at room-climate conditions, rendering plates exposed outdoors were subjected to an enrichment of nitrate up to 0.06% although original material was free of it. Nitrite could not be detected. Another method for the information on distribution of elements is provided by scanning electron microscopy with energy-dispersive X-ray (EDX) analysis. This method can give information on distribution of elements on a submicroscopic scale. In most cases one can demonstrate the distribution of sulphur, which is clearly representative for sulphate deposition as a consequence of SO_2 reaction in the surface area of rendering.
On a secondary electron image of a lime plaster sample (Fig. 44), the surface edge of fracture is visible at the top where the specimen was directly exposed to the atmosphere. On the basis of sulphur and calcium distributions, one can recognize a distinct enrichment of sulphate in the region immediately below the surface corresponding to a Ca decrease. (Black spots in S and Ca distributions sometimes represent shadow effect areas where electrons rebounded and

scattered and could not be received by the detector, as well as quartz grains appearing as white areas in the Si distribution.)

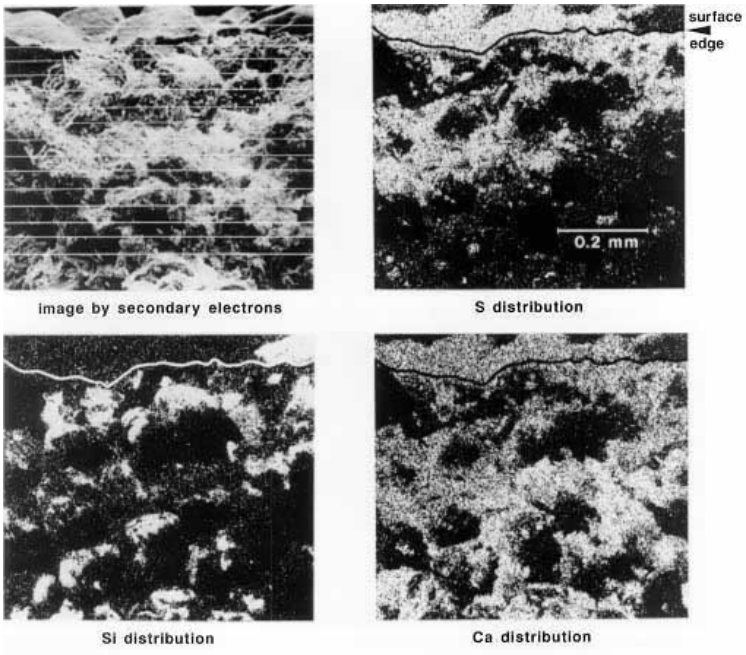

Fig. 44. EDX analysis of Ca, S and Si distributions in the surface layer of a lime plaster exposed to atmospheric pollutants for 17 years

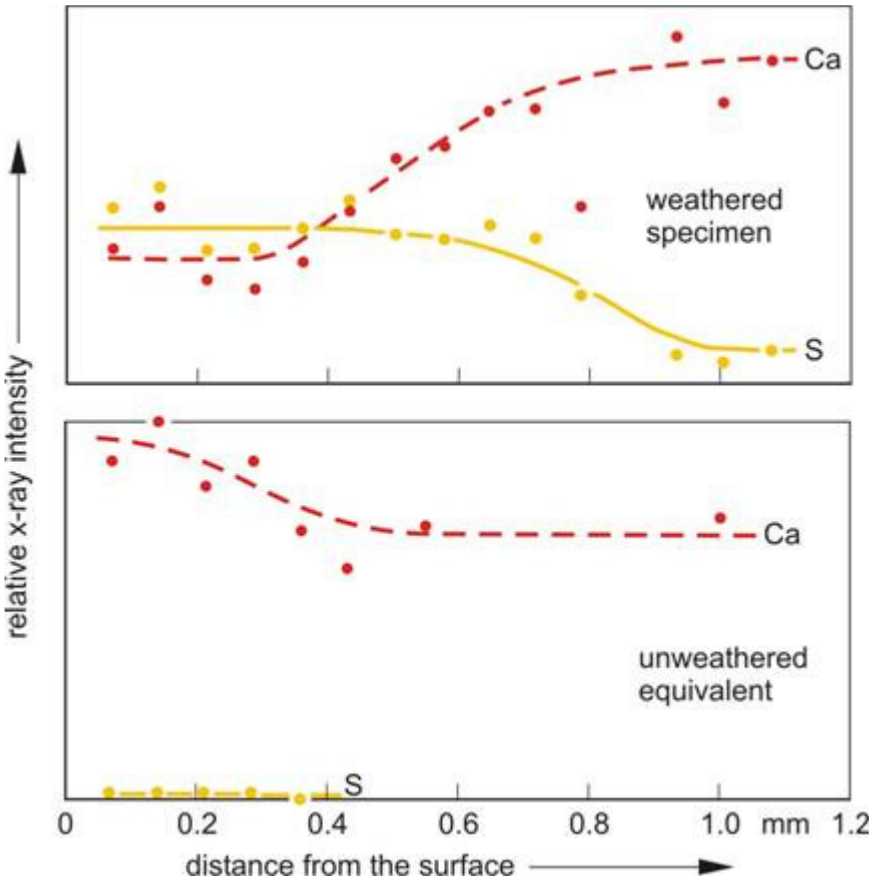

Fig. 45. Sulphate enrichment in a 17-year-old lime plaster stored under different conditions

X-ray scanning data, taken along the lines in the first photomicrograph of Fig. 44 and shown in a diagram plotted as function of distance from the surface, agree closely with the element

distribution of Fig. 45, top. There is a uniform level of sulphur at the surface layer, which decreases with depth at about 0.6 - 0.8 mm. Lime plaster stored in a climatic chamber, however, was found to contain a very small portion of sulphur (Fig. 45, bottom). One of the most striking features is the boundary between aggregate grains and binding matrix where as a rule only a point-by-point contacting area has been found. This is inter alia the reason why one has to search carefully for appropriate regions when using any microscopical method.
Some hope was directed to variations in specific surface area as also being a criterion for the reaction stage between binding substance and atmospheric components. Concerning this, one has to realize, however, that it could ultimately be no more than a summarizing result of carbonation, sulphation and original texture of the material. Specific surface area of a dolomitic plaster exposed outdoors decreases with rising profile depth, whereas indoor samples show the opposite effect. In the first case, the course is parallel to that of sulphate distribution; in the second case carbon dioxide distribution acts one against another (Fig. 46).

Specific surface of outside plasters is generally 2 to 3 times larger than their indoor equivalents, which means that carbonation and sulphation occur at the same time.
Although this determination deals only with a "one-point" method according to H a u l and D ü m b g e n, and preparative inconsistencies can introduce errors, there is no doubt about this finding. Here the question also arises on what influence a mix proportion exerts on a plaster's structure and the consequences this has for its behaviour on buildings.

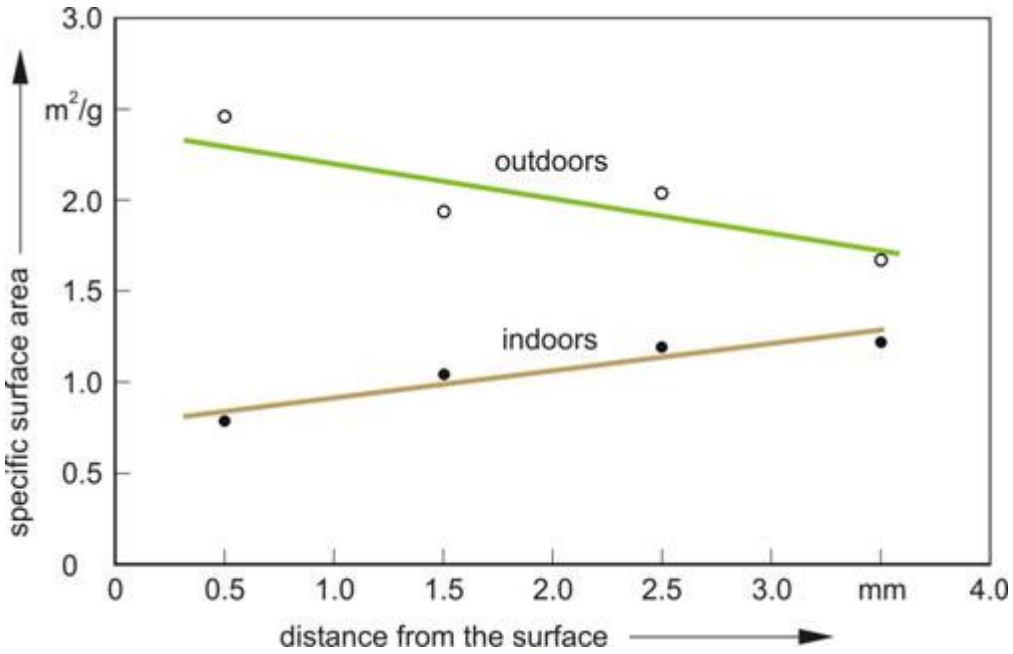

Fig. 46. Comparison of depth profiles showing specific surface of a 17-year-old rendering with a dolomitic hydrate-to-sand ratio by volume of 1:2.7, based upon different exposure conditions

Now one can obtain more information on pore structure and material properties of four-year-old room-stored plasters (see Tab. 11); so it was found that a cement addition of only 3.5% by volume to a dolomitic or a lime plaster leads to a remarkable increase in fine pores. This results in the first case in an elevation of microporosity from 40 to about 60% and in the second one from 40 to 77%. The higher the cement content the greater is the effect. Among others, this means practically that by such steps one can displace pore volume towards the region of the critical small diameters where sensitivity against frost damage is elevated as far as one can assume this criterion is also valid for this type of material. The same effect was brought about by increasing the binding agent. This could be proved when raising the dolomitic hydrate-to-sand proportion from 1 to 4.5 by volume to a ratio of 1 to 2.7, whereby

microporosity rose from 40 to 60%. With regard to SO_2 absorption, however, a leaner mix having a larger fraction of coarse pores unexpectedly absorbed more sulphate into its uppermost surface layer than that being richer in binding agent, since the absorptive ability of that with an elevated portion of fine pores does not seem here to be decisive. Cement-containing rendering behaves similarly. Accordingly as the portion of fine pores increases, despite a nearly constant specific pore volume, the uptake and penetration depth of sulphate decrease. This trend is observed as well in 4- and 17-year-old weathered plasters.

Tab. 11. Characteristic values of 4-year-old room-stored renderings having different mix proportions, calculated from their pore-size distribution

Characteristic Pore Value	Dolomitic Plaster				Lime Plaster	
	1 : 4.5 [1]	1 : 2.7 [1]	1 : 0.2 : 4.5 [2]	1 : 0.5 : 6.5 [2]	1 : 4.5 [3]	1 : 0.2 : 4.5 [4]
d_{10m} value (diameter) in µm	[5]	35	40	26	[5]	17.2
Ravaglioli interval in %	22.5	29.5	27.5	26.3	23.5	36.5
Microporosity in %	40.0	61.5	62.5	72.5	42.0	77.0
Median (radius) in µm	9.0	1.0	1.0	0.9	4.7	0.8
Specific surface area Σ_m (m^2/g)	0.8	1.2	1.2	1.1	0.6	1.2

[1] ratio of components (proportions by volume) of dolomitic hydrate and sand

[2] ratio of dolomitic hydrate, Portland cement and sand

[3] ratio of lime hydrate and sand

[4] ratio of lime hydrate, Portland cement and sand

[5] exceeded upper limit of method's working range

5.5 Characterizing starting material for exposure

5.5.1 Physico-technical features

For atmospheric exposure tests plasters were made with lime putty, industrially hydrated lime, industrially (completely) calcined and hydrated dolomite, hydraulic lime, and sand standardized according to EN 196 as an aggregate (cf. section 2.2). To one lime and one dolomitic plaster each were added mixed small portions of white Portland cement.

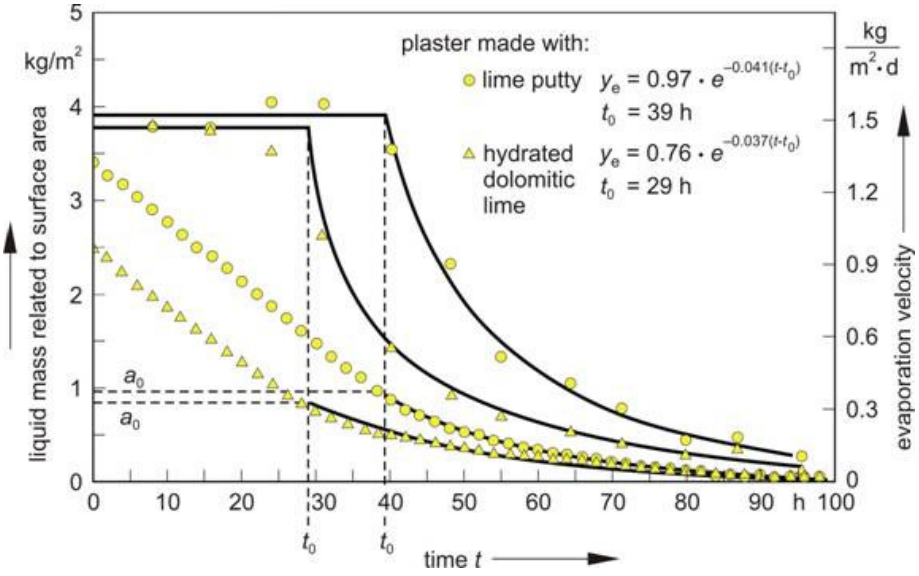

Fig. 47. Evaporative course and velocity of two selected laboratory prepared renderings before exposure

Tab. 12 lists data determined prior to exposure. Because of coulometric test results, one could assume that lime plasters were carbonated uniformly and thoroughly, whereas cement admixture because of its tightening effect (increase of fine pore portion impeding CO_2 diffusion) would probably have allowed only an unsatisfactory carbonating reaction. Additionally one can characterize plaster plates also by means of their evaporation behaviour. Because of reduced thickness (2 cm) problems could result when the inflection point between both evaporative phases was established (cf. section 4.2.2). Nevertheless, in individual cases one can achieve a satisfactory accuracy as presented in Fig. 47. Having an almost identical geometry, both specimens show different values for a_o, which are also transferable to residual water content. So evaporation parameters b reflect material-specific differences in this part of the curve.

Tab. 12. Characteristic values of room-stored pre-carbonated renderings having scraped surfaces, calculated from their pore-size distribution and other parameters (0-5 mm depth)

Rendering types	Specific pore volume in cm^3/g	d_{10m} µm	Ravaglioli interval %	Micro-porosity %	Specific surface area m^2/g	Sulphate content % by mass	Carbonate content % by mass	Vapour diffusion resistance index µ	Water absorption coefficient w_0 $kg/(m^2 \cdot h^{0.5})$
Plaster made with lime putty	0.125	–[1)]	6.3	45.7	0.53	0.02	3.15	9.5	25.7
Plaster made with industrially hydrated lime	0.135	–[1)]	16.9	48.6	0.63	n.d.[2)]	2.76	11.0	13.9
Plaster made with industrially calcined and hydrated dolomite	0.126	–[1)]	9.6	39.2	0.52	n.d.[2)]	1.34	10.9	26.7
Lime plaster mixed with Portland cement	0.143	9.79	44.9	80.7	1.48	0.02	4.32	11.5	21.1
Dolomitic plaster mixed with Portland cement	0.123	16.33	34.8	82.4	1.37	0.04	3.24	12.7	11.9
Hydraulic plaster	0.117	–[1)]	19.3	53.9	1.11	n.m.[3)]	3.72	13.7	9.5

[1)] exceeded upper limit of method's working range
[2)] not detectable
[3)] not measured

By considering their abrasion behaviour (Fig. 48) it is obvious that renderings with lime putty and industrially hydrated lime has the lowest strength, followed by those with a cement

admixture. Plaster made with dolomitic hydrate shows the highest resistance and is known to furnish an elevated early strength comparable to that of hydraulic rendering.

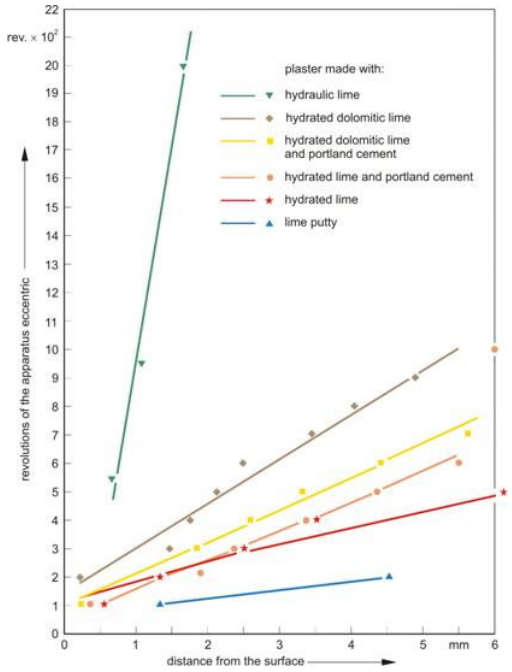

Fig. 48. Abrasion behaviour of laboratory prepared renderings before exposure, depending upon their composition

Quantifying this behaviour, the following values are obtained for renderings made with

- lime putty	ca. 50 rev./mm of depth (amount of abrasion)
- lime hydrate	ca. 70 rev./mm of depth
- lime hydrate and cement admixture	ca. 110 rev./mm of depth
- dolomitic hydrate and cement admixture	ca. 130 rev./mm of depth
- dolomitic hydrate	ca. 180 rev./mm of depth and
- hydraulic lime	ca. 2000 rev./mm of depth

The cumulative curves of amounts of wear show nearly a linear course for the relevant material. These points to the fact that there is a comparable abrasion resistance at each depth position making it possible to detect changes due to the influence of atmospheric pollutants.

5.5.2 Deposition velocity and uptake of SO_2 for plasters according to the chamber method

Till the present there has been no method for quantifying the SO_2 uptake by a building material. Samples from a façade can indeed deliver data as e.g. the rate of uptake of a gas related to a time unit, even though defined environmental conditions are lacking. Different processes such as dissolution of neo-formed phases by rain or dew water, their reprecipitation at another place, recrystallization and frost action can modify the material to an unknown degree and reinforce weathering effects. Beside this, the exposure height and direction are additional variables. Such data therefore represent no more than a stage of deterioration

arbitrarily selected. Problems arise when comparing building materials with each other. An experimental device developed by the Institute for Inorganic and Applied Chemistry of the University of Hamburg, enables determination of deposition velocity or uptake of SO_2. Across the reaction chamber of this device a gas of known concentration flows. From its reduction one can calculate the deposition velocity and also the uptake, by considering the surface area available for reaction.

Corresponding to the load or stress during a smog situation or a moderate in winter, SO_2 concentrations of 150 ppb (405 µg/m^3) and 37 ppb (100 µg/m^3) were respectively chosen in order to simulate an averaged stress during months of winter. Tests were carried out at a temperature from 20 - 22°C and 50 - 60% relative humidity over a period of 20 hours. The specimens were five different renderings provided also for outdoor exposure in the form of plates after a 90-day pre-storage at 20°C and 90% r.h. and the so-called Baumberger sandstone as well. The calculation formulas applied are reported by C. W i t t e n b u r g [105], who also performed all necessary experimental work. In Fig. 49 both absorbing features of a plaster made with lime putty are plotted versus time.

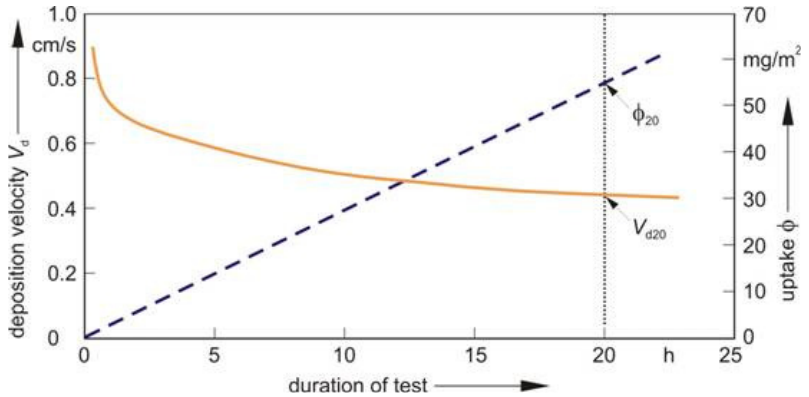

Fig. 49. Time course of SO_2 deposition velocity V_d and uptake Φ, monitored on a plaster made with lime putty

The test results obtained give a ranking order shown in Tab. 13.

Tab. 13. Deposition velocity V_{d20} and uptake Φ_{20} for SO_2 after 20 h, determined on specimen plates made of different renderings (SO_2 concentration 405 µg/m^3)

Binder type	V_{d20} in cm/s	Φ_{20} in mg/m^2
Dolomitic hydrate with cement admixture	1.71	74.8
Industrially hydrated lime with cement admixture	0.54	59.5
Lime putty	0.45	54.6
Baumberger "sandstone"	0.40	51.0
Hydraulic lime	0.20	32.1
Industrially hydrated lime	0.11	29.1
Dolomitic hydrate	0.09	24.6

As can readily be recognized, the cement admixture increases deposition velocity V_{d20} and uptake Φ_{20} as well. Therefore renderings with dolomitic hydrate or hydrated lime would be least sensitive towards an SO_2 effect, whereas their equivalents with cement admixture show an almost doubled uptake. Plaster made with lime putty takes an intermediate position. A decrease of gas concentration down to 100 $\mu g/m^3$ leads as expected to a higher velocity and a correspondingly lower uptake. In this sequence, plasters with hydrated lime alone indicate lowest values. Dispersivity of binding agent possibly exerts a significant influence on this behaviour. In any case, one cannot deduce definitely the ranking order from the pore-related data. Reserve samples corresponding to those used here show that values for specific pore volume lie close to one another, but in the case of both cement-containing renderings the values for R interval and microporosity are obviously higher and for the median many times smaller than in batches without admixture.
When comparing these data as material parameters with those obtained from lime-bond sandstones (compare [105]), it is noticed that under the effect of the elevated gas concentration, none show a higher velocity or uptake than the cement-containing plasters. Nevertheless the values for lime renderings are in the same order of magnitude as the sandstones. Tests were also carried out on plates saturated with distilled water by capillary rise at the high gas concentration. Tab. 14 lists the results obtained. It turns out, as expected, that V_{d20} of wet specimens is considerably higher than those in a dry stage (compare Tab. 13).

Tab. 14. Deposition velocity V_{d20} and uptake Φ_{20} for SO_2 after 20 h, determined on water-saturated specimen plates made of different renderings

Binder type	V_{d20} in cm/s	Φ_{20} in mg/m^2
Dolomitic hydrate with cement admixture	6.9	81.1
Industrially hydrated lime with cement admixture	9.3	81.2
Lime putty	5.1	79.8
Industrially hydrated lime	9.3	81.3
Dolomitic hydrate	7.5	81.1

Whereas SO_2 uptake of all plaster types is nearly the same, small differences in velocity appear - a result influencing their ranking order. Under these circumstances lime plaster namely shows the highest values. So it can be concluded that only SO_2 absorption data obtained in dry stages represent material parameters, while wetted samples absorb the admitted SO_2 quantity almost quantitatively. Transferring such a finding to conditions at a building, one can realize that the absorptive ability of this gas depends mainly on a material's moisture content. In other words: conditions of exposure determine a rendering's behaviour towards SO_2.

5.6 Outdoor exposure of building materials at locations with differing stress by pollutant gases

5.6.1 Time-dependent modifications

Up to mid-1992, five different rendering types had been stored outdoors over 1.5 years on racks. The sixth one previously, a hydraulic lime plaster, was however mounted at a later date. Consequently three stages can be compared with one another: initial state, half-year and 1.5 years exposures. Regarding both materials having dolomitic hydrate as a binder, the cement-containing mix also after 1.5 years shows no change in sulphate content of its uppermost millimetre layer at any location, whereas that without admixture showed slightly elevated amounts compared to the starting material remaining constant over the course of time. Only lime renderings with and without cement took up measurable quantities of SO_2 (Fig. 50).

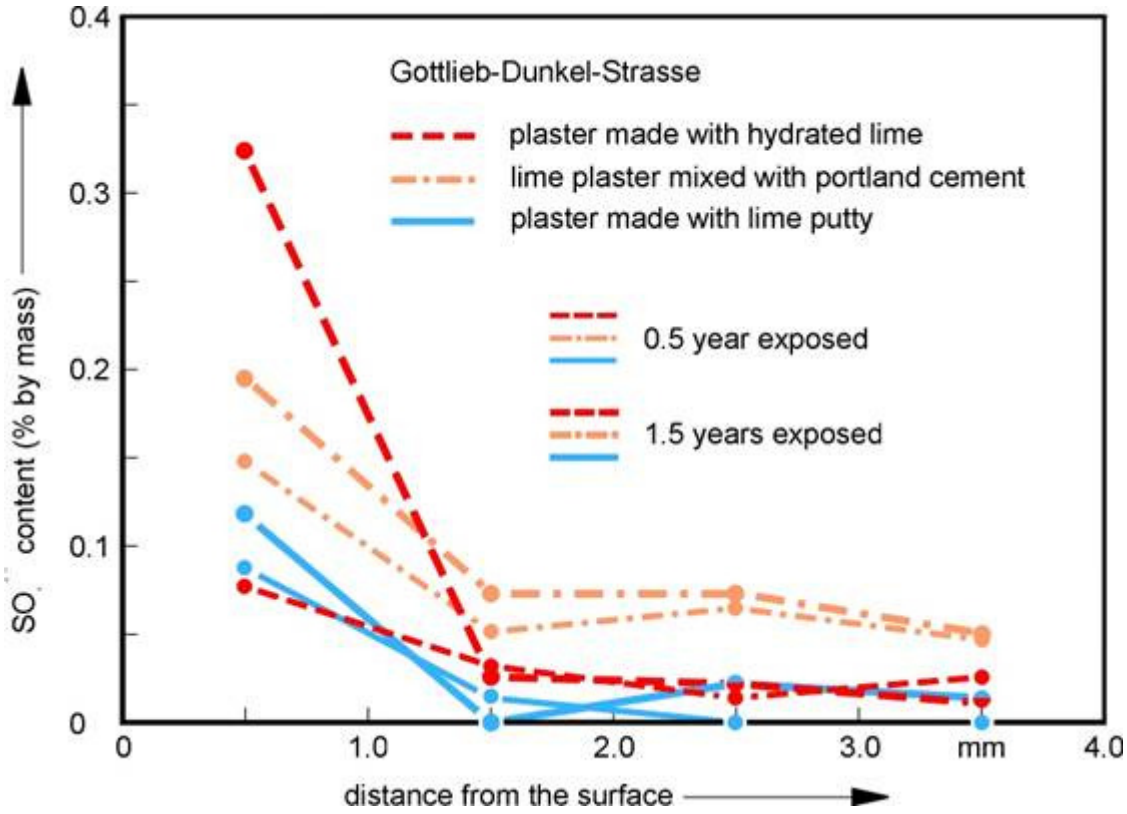

Fig. 50. Sulphate enrichment in the uppermost layer of various rendering types after different exposure periods

For the location of Gottlieb-Dunkel-Strasse, as an example, this means that material made of lime putty and having a starting SO_4^{2-} content of 0.06% by mass contains 0.09% after six months and 0.12% after 1.5 years. This value correspondingly increases in plaster with industrially hydrated lime from 0% over 0.04% to about 0.33% respectively. Material from other exposure locations furnishes similar values. One can only find a plausible ranking order in their reaction with the air pollutant, because the maximum SO_4^{2-} content in samples was also found as far as at Lerschpfad (highest pollutant concentration in air near the highway). Since such results are always related to the outermost rendering layer, a subsequent frustration occurs when penetrating to a greater depth. Apparently only the first millimetre is directly influenced by atmospheric SO_2, since the values in 2 mm depth are situated insignificantly above those present at the test start (Fig. 51).

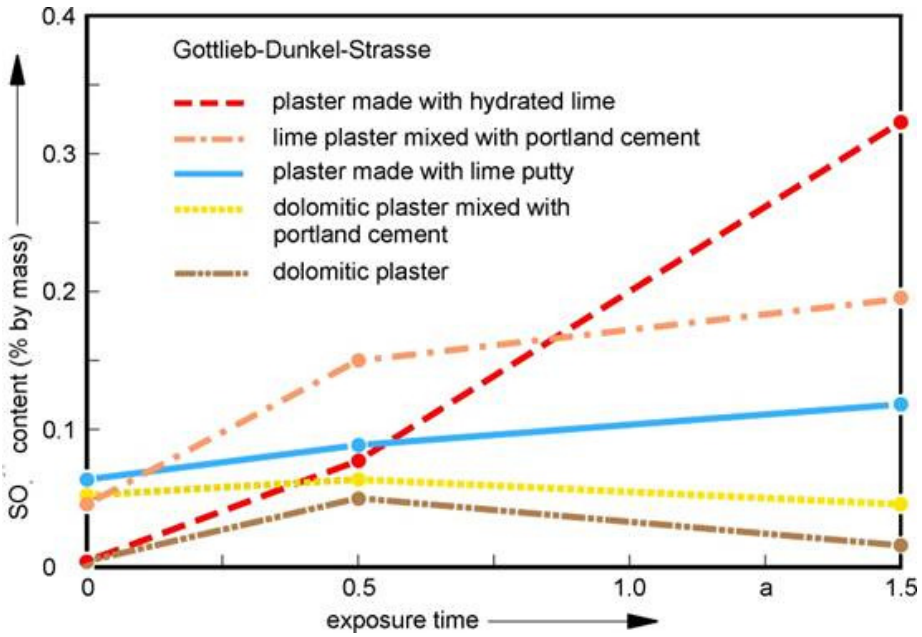

Fig. 51. Comparison of sulphate concentration profiles in renderings after 0.5 and 1.5-year exposure periods

In this connection it should be nevertheless noticed that differences of 0.02% are within the scattering range where even preparation of a 1 mm thick layer at its best (accuracy in abrading, mass of the test portion, extraction, etc.) still yields the 0.02% difference in sulphate content related to mass. Therefore the chemical reactions are obviously extremely weak, so it is to be expected that structural modifications also take place to a small extent. Only the outer 5 mm of rendering could be affected. This represents the layer used for corresponding comparisons.

Both plaster mixes with dolomitic hydrate are those with the smallest change in chemical composition, and therefore show no trends concerning structural data related to exposure duration. The water absorption coefficient of the dolomitic plaster merely rises with time at all locations (Fig. 52).

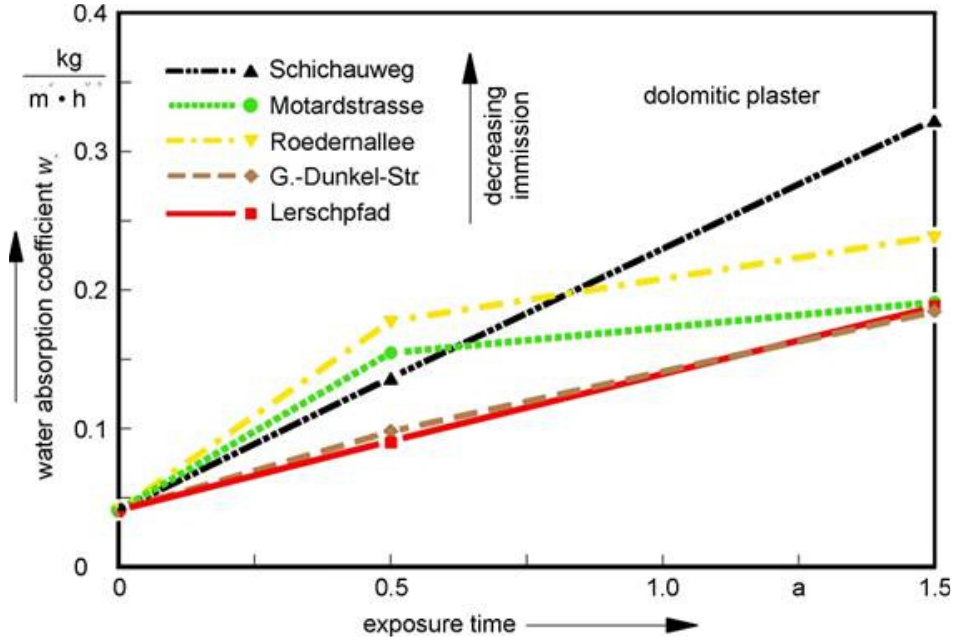

Fig. 52. Increase in water absorption coefficient, w_o, of a dolomitic plaster referring to locations and exposure time

After 1.5 years' exposure at the location with the lowest noxious gas concentration, the greatest value was found (w_o = 26.1 kg/($m^2 \cdot h^{0.5}$)) and at the location with the highest concentration the smallest value was determined: 19.6. Also in the case of lime plaster with cement admixture, there are no pertinent systematic changes in w_o or μ. Probably one can state rather an extremely small decrease of specific pore volume but not at all locations, suggesting subsequent hydration or carbonation and consequently showing structural compaction. The same is true for pure lime plaster, whereas that made with lime putty points to clear dependencies. So the median of pore sizes increases to coarser pores and microporosity decreases at three of five locations. Slightly fluctuating w_o values increase with time at all locations.

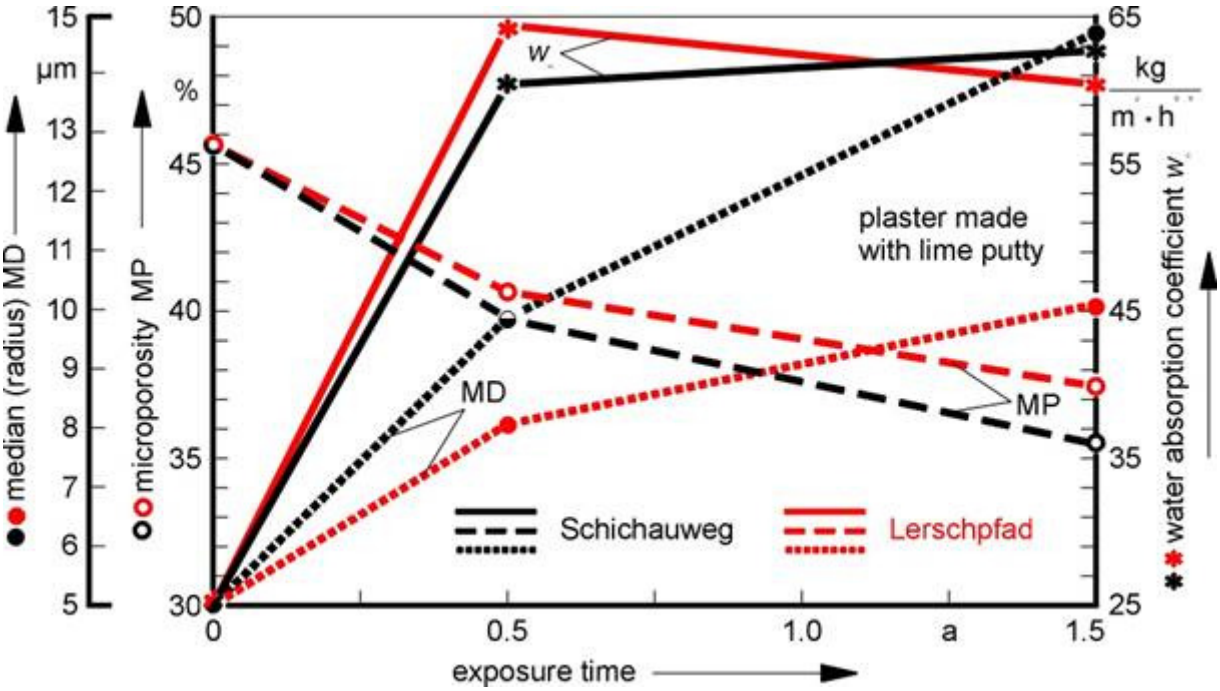

Fig. 53. Variations on pore-related parameters in a plaster made with lime putty after different exposure times

In Fig. 53, these parameters are plotted for both extreme conditions of samples taken from Schichauweg with the lowest SO_2 concentration and Lerschpfad with the maximum value. For this part of the program, one can summarize that at given exposure conditions, 0.5 (compare [36]) and even 1.5 years are simply too short in order to produce systematic structural modifications even in renderings. Therefore results obtained should be considered with utmost caution, since the trends found could partially lie within a scattering range of the results, and sometimes be made visible only by a corresponding spread of the coordinate system.

Due to the slight chemical modifications, renderings made with lime putty or industrially hydrated lime show in contrast to their nonexposed equivalents nearly identical abrasion depth profiles after 0.5 as well as 1.5 years (Fig. 54). This is valid for exposure locations with high (Lerschpfad) and also low gaseous pollution (Schichauweg). Lime plaster with cement admixture displays an increased strength only near the highway (Lerschpfad). There all sample surfaces have become dark-coloured, probably caused by deposition of such pollutants as abraded tire rubber and other grime originating from traffic. Only tiny modifications in dolomitic materials also appear up to 0.5 years, which are expressed solely in a barely detectable surface

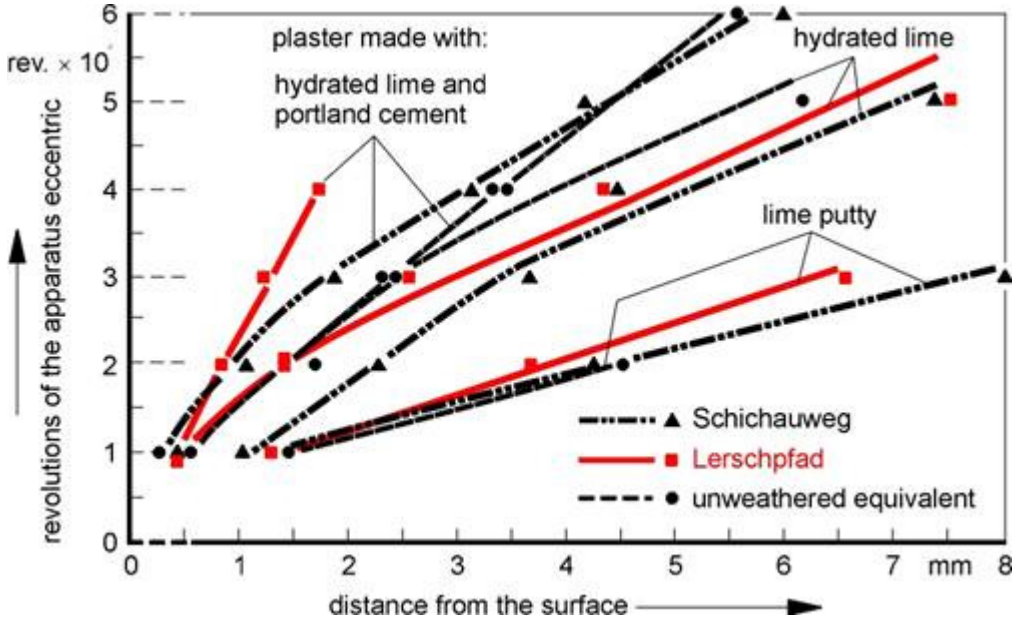

Fig. 54. Abrasion profiles of lime renderings after a 1.5-year exposure: cumulative curves of single amounts of wear

consolidation. Nevertheless, after 1.5 years, drastic differences can be observed in comparison to rendered lime material, which is also evident in the case of a cement admixture (compare Fig. 55).

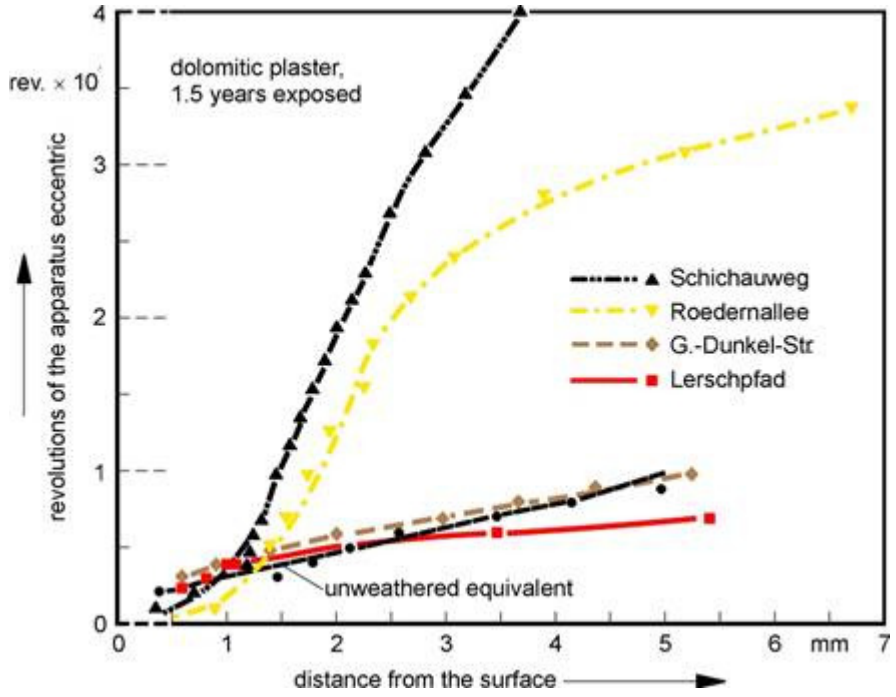

Fig. 55. Abrasion profiles of dolomitic rendering at different locations after a 1.5-year exposure: cumulative curves of single amounts of wear

Although the behaviour of materials from Lerschpfad is quite similar to those stored indoors, corresponding samples from Schichauweg exposed to low NO_x and SO_2 concentrations show a very high abrasion resistance (about 1800 rev. per mm depth progress). But this result cannot be explained merely with their higher carbonate content. Still other influences may rather have been effective, e.g. a higher average relative humidity or an increased tendency of dew formation at this location.

Such a material [initially such not slightly soluble phases as $Mg(OH)_2$ and MgO besides amorphous magnesium carbonates, and of course the calcium component are present] requires an increased moisture content for its optimal strength development more than does lime rendering (cf. [50]). This may also explain the similarity of abrasion characterizing unweathered samples, although the latter contain twice the carbonate content. Pore data can be considered as well for an explanation. Thus pore volumes differ remarkably down to 5 mm profile depth: material from Schichauweg shows 0.106 cm^3/g and that from Lerschpfad 0.121 cm^3/g, which indicates a higher compactness of the first one. In comparison one can find no interpretable differences in the discrete values of pore-size distribution.
Renderings with dolomitic hydrate and admixed cement show in contrast to their equivalents without a hydraulic portion a completely different abrasion behaviour. Here conditions obviously reverse (Fig. 56), so that samples from Schichauweg correspond to those which are unweathered, whereas those from Lerschpfad are distinctly stronger despite more intense SO_2 immission at this location. The cumulative curve of amounts of wear even has an almost linear course, indicating a comparable structural cohesion in each depth position. The pore characteristics can also explain the different abrasion curves, whereby only pore volume exhibits definite tendencies (0.122 cm^3/g in Lerschpfad material and 0.138 cm^3/g in such from Schichauweg). Therefore this type is closely similar to that made with hydrated lime and cement; the sample of the latter, however, allowed an abrasion test only to 2 mm distant from its surface (cf. Fig. 54).

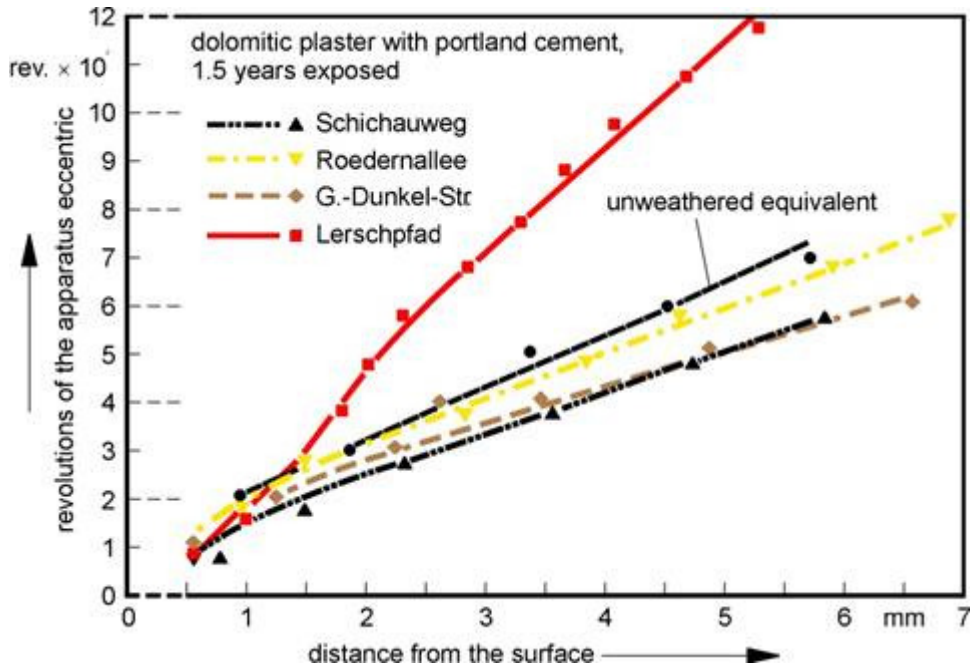

Fig. 56. Comparison of abrasion profiles in a dolomitic rendering with cement admixture after 1.5-year exposure: cumulative curves of single amounts of wear

At Lerschpfad, better hardening conditions prevail for cement-containing material, since drizzle presumably occurs there by spray from the highway during and after a rainfall. At this location one additionally finds the highest fraction of suspended particulates. At Schichauweg the supply of such media for an intensified hydration was apparently insufficient. Here dolomitic hydrate with admixed cement did not become so hard, although there exists a high moisture level which still requires a plausible interpretation.

5.6.2 Influence of exposure conditions on material behaviour

As already pointed out, load or stress by pollutant gases was reduced in the course of time at single exposure locations. It seems probable that in the urban area of Berlin, different climatic factors other than atmospheric SO_2 attack can strongly affect building materials. Nevertheless, despite all the rather small time-related dependences, one rendering made with lime hydrate was apparently subjected to systematical variations proportional to immission intensity.
Fig. 57 shows several structural parameters such as the median and microporosity of pore-size distribution as well as the water absorption coefficient of test samples exposed over 0.5 and 1.5 years, plotted for the respective locations which were ranked in the order of atmospheric SO_2 concentration. It turns out that an increasing SO_2 and NO_x immission causes a decreasing portion of micropores and a shifting of the median towards coarser pores, being in such way coupled with a reduction of w_o. The time

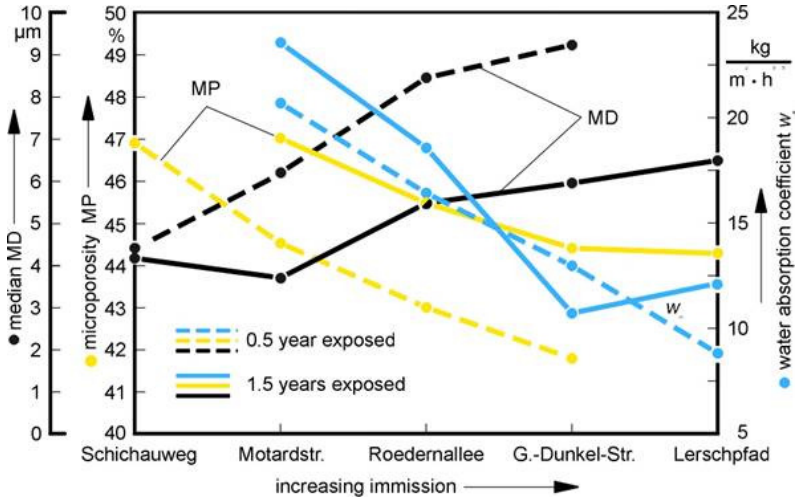

Fig. 57. Some structural variations of pore-related parameters, determined on plaster made with lime hydrate and referring to locations and exposure time

influence may be so expressed that a portion of micropores after 1.5 years exposure is noticeably more strongly developed in proportion to that of a half-year exposure, whereby the 50% fractile of pore-size distribution (MD) is correspondingly decreased. The water absorption coefficient is apparently not significantly affected by these structural changes.
Both extreme outdoor-exposure locations do scarcely furnish hints on differences in the effect of climatic-conditioned factors, because they show comparable values for specific pore volume, median and pores < 5 µm. Principally all plasters become denser with increasing exposure duration because of reduction in pore volume (see also Tab. 15).

Tab. 15. Changes in physico-technical characteristics due to exposure sites and time

Material	Plaster made with hydrated lime								Plaster made with lime putty							
Exposure site	Schichauweg				Lerschpfad				Schichauweg				Lerschpfad			
Exposure time (a)	0	0.5	1.5	4.5	0	0.5	1.5	4.5	0	0.5	1.5	4.5	0	0.5	1.5	4.5
Specific pore volume (cm³/g)	0.135	0.121	0.126	0.104	0.135	0.124	0.125	0.107	0.125	0.117	0.130	0.113	0.125	0.116	0.119	0.096
Median (µm)	3.19	4.20	4.78	11.4	3.19	5.10	5.01	10.0	5.13	9.79	14.58	18.03	5.13	7.20	11.98	11.13
Microporosity (%)	48.6	46.8	45.2	36.0	48.6	46.8	46.2	37.0	45.7	39.6	35.7	27.4	45.7	42.0	37.7	37.0
w_o (kg/m² h$^{0.5}$)	13.9	10.2	14.1	–	13.9	12.3	8.7	–	25.7	60.5	64.4	–	25.7	64.5	59.5	–
µ value	26.7	10.0	10.8	–	26.7	10.1	9.7	–	9.5	9.3	9.5	–	9.5	8.6	8.2	–

Simultaneously, from discrete values for pore-size distribution, the median tends to coarser pores, whereas microporosity and water vapour diffusion resistance index, μ, as well diminish, whereas water absorption coefficient, wo, especially in the case of mortar made with lime putty, increases. However, only insignificant differences between single locations are present. The found differences between renderings on a lime basis by industrial slaking and as a putty can possibly be caused by the double amount of specific surface area of the putty.
This is also valid when a small quantity of white Portland cement is added to plaster mixes representing a widely used coating of external walls. Such plasters taken from Schichauweg and Lerschpfad show some differences after 1.5 years of exposure. However, they are nearly levelled off after 4.5 years. Microporosity and median are almost the same at every moment (Fig. 58).

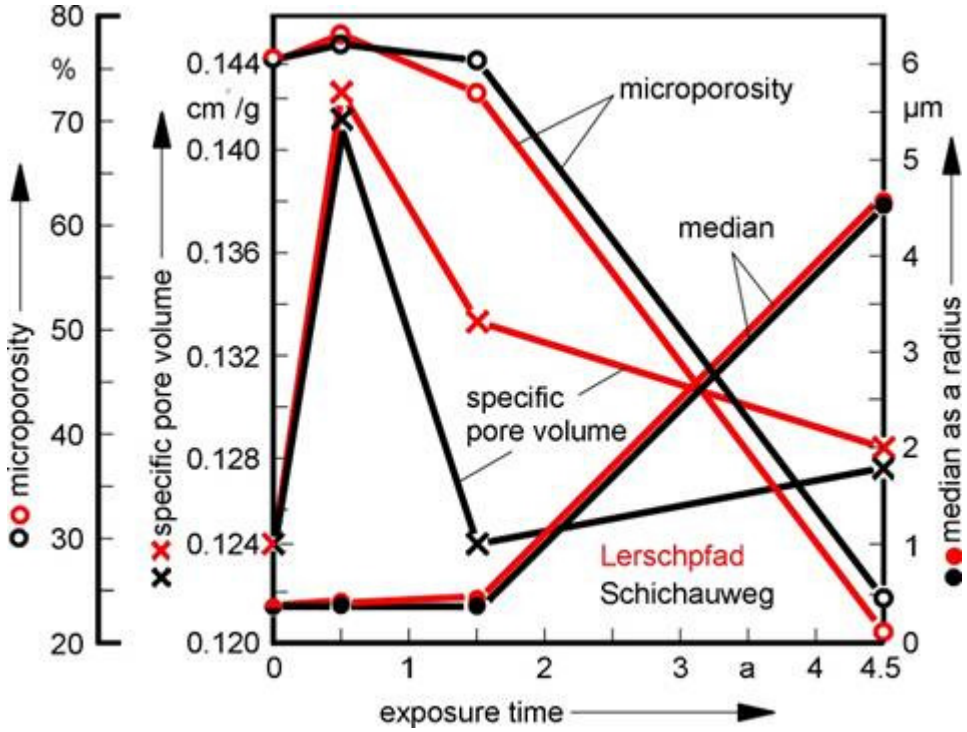

Fig. 58. Variations of pore-related parameters in a lime plaster with Portland cement at two locations after different exposure times

Another type of presentation also permits visualization of those differences, comparing various pore-size intervals by plotting size classes 60 to 5 μm, 5 to 0.1 μm, 100 to 30 nm, 30 to 10 nm, and < 10 nm radius as well as their relative changes compared to the respective starting material (Fig. 59).

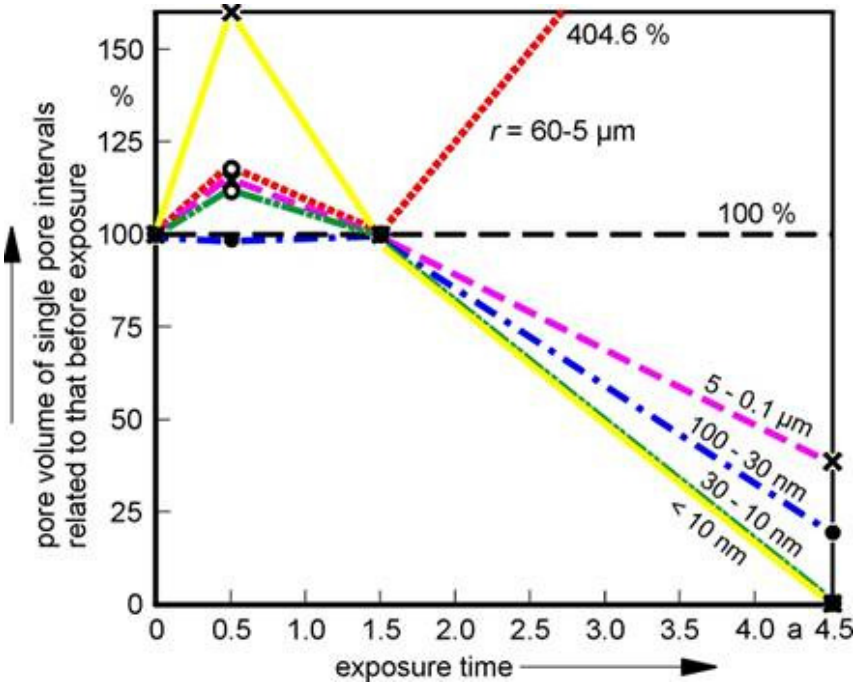

Fig. 59. Relative changes of single intervals each in a lime plaster mixed with Portland cement at Schichauweg location after different exposure times (100% = room stored material)

An increase of the fine pores' range, this especially of < 10 nm, which can occasionally become 60% greater than before exposure is observed within 1.5 years. It may be noticed that this process coincides with an increase of the entire pore volume up to 15% as determined by mercury porosimetry, for which post-hydration of a cement's constituents is obviously responsible. The fine pores' portion, however, decreases with time so that after 4.5 years only pores > 30 nm remain. It is worth mentioning that basically and quite distinctly in the present case, the portion of coarse pores between 5 and 60 µm at a practically equal specific pore volume even quadrupled, so that after this period a rendering exists with considerably coarser pores. Sulphate enrichment only takes place in the first outer millimetres showing at both locations 0.6 or 0.7% related to the mortar's mass. Also vapour diffusion does not show a gradient (Fig. 60).

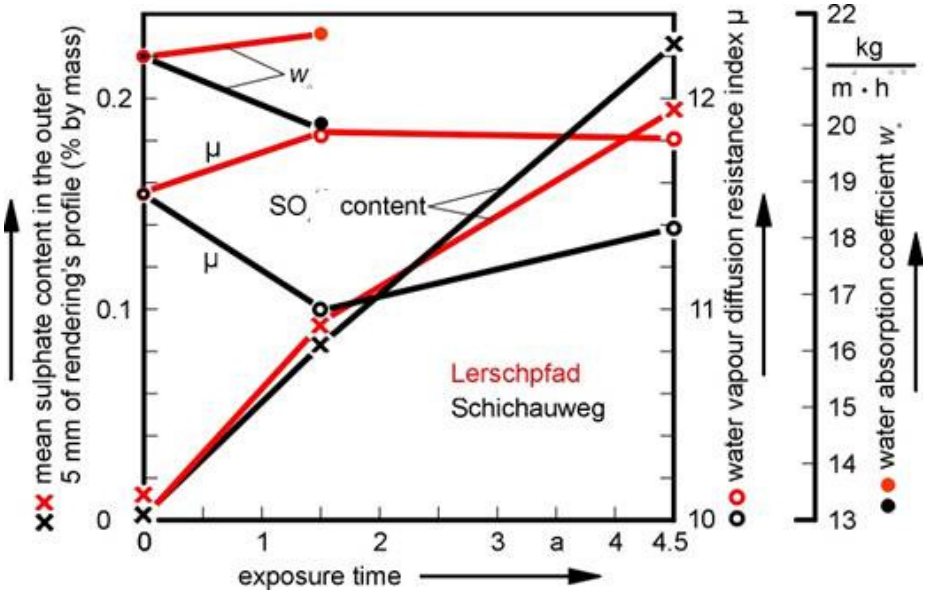

Fig. 60. Variations of physico-technical parameters and the mean sulfate contents in the outer 5 mm of a lime plaster mixed with Portland cement after different exposure times

Due to the slight chemical modifications, renderings made with lime putty or industrially hydrated lime show in contrast to their unexposed equivalents nearly identical abrasion depth profiles after 0.5 as well as 1.5 years. This is valid for exposure locations with high and low gaseous pollution. Lime plaster mixed with Portland cement displays an increased strength only near the highway. There all sample surfaces have become dark-coloured, probably caused by deposition of such pollutants as abraded tire rubber and soot originating from traffic. A process like this however produces a kind of beginning crust formation, so that a continuous abrasive behaviour here presumably almost identical with a later weathering progress over the whole profile depth cannot be expected.
Despite the small SO_2 absorption, it seems amazing that abrasion behaviour also reveals systematic modifications in the direction of increasing or decreasing immission (cf. also Fig. 55 and Fig. 56). But not all materials are concerned: lime renderings are not so much subjected to these influences, though their pore-related parameters did change. Above all, mixes which were placed on racks in a still incompletely hardened state show this phenomenon, i.e. those with cement admixture and those containing a magnesia component. In the direction of decreasing SO_2 and NO_x immissions - namely from Lerschpfad over Gottlieb-Dunkel-Strasse to Roedernallee and Schichauweg - deeper regions of rendering made with dolomitic hydrate are subjected to a consolidation process (cf. Fig. 55), that however is not reflected in CO_2 contents. So samples from Schichauweg down to about 4 mm depth show a mean value of 2.11% and that from Roedernallee 2.97%, whereas at Lerschpfad 2.35% was measured. But more information than indicated by mean values is furnished by a CO_2 distribution given in Table 16 in a tabulation for three locations compared to CO_2 concentration prior to exposure.

Tab. 16. CO_2 concentration profiles in dolomitic rendering at three locations and prior to exposure

Distance from surface (mm)	CO_2 content (% by mass)			
	prior to exposure	after 1.5 years of exposure		
		Schichauweg	Roedernallee	Lerschpfad
1	on average 1.34	2.58	3.85	2.57
2	on average 1.34	2.36	3.27	2.20
3	on average 1.34	2.23	2.30	–
4	on average 1.34	1.28	2.47	2.28

It is to be recognized again that carbonation alone cannot be responsible for a higher strength of a dolomitic rendering, but that at Schichauweg more favourable conditions might have been prevailed for it (compare to section 5.6.1). For an explanation of such differences, probably the so-called "time of wetness" is also offered as a sig- nificant concept being correlated to countercurrent gradients of mean temperature and relative humidity from the city's centre to its outlying areas as it has been discussed by Fitz [23]. Perhaps the reason for this is a low supply of moisture within this location area. For at a small supply, residual MgO internally extracts water from originated $Mg(OH)_2$, in such way contributing to a strength increase [106]. The volume augmentation of binder particles thus caused leads to a diminution of pore volume. Because of subsequent consolidation of plaster by drying and cementing of $Mg(OH)_2$ gel, a high final strength will then be attained. In the course of time this gel becomes crystalline [68], i.e. it "ages" and forms products thermodynamically more resistant with an ordered crystalline structure and elevated grain size [6] thus contributing to a further densification of the rendering.

Dolomitic plasters with cement admixture also show an inverted succession of structural strength, so that the most favourable hardening conditions must have occurred at Lerschpfad and the most unfavourable ones at Schichauweg (cf. Fig. 56). Probable reasons for this have already been indicated. With respect to weathering progress it should additionally be noted that results recently available for a 4.5-year outdoor exposure show in principle comparable trends [44].

5.7 Investigation of plaster components (grain-size distribution, sand and binder portions, and water demand as well) on physico-technical characteristics

In section 5.4, concerning the influence of mix proportion of plasters on their structure and sulphate absorption, it was shown that in the outer surface layer of 1 mm thickness, leaner mixes absorbed more sulphate than did richer ones. This was the starting point for suggestions on how to modify a rendering's structure by varying its components (grain-size distribution, portion of sand and binder, and water demand) and how this procedure would affect physico-technical properties and characteristics. Thus moisture transport and weathering behaviour - naturally according to physical conditions on a building - are directly interrelated, and that way one comes a bit nearer to the objective of explaining properties of a material from its structure.

As a basis serves the idea that here exists a complex mixture of hardened binding agent, aggregate sand as well as pores whose portion, size, and distribution are mainly determined by mix proportion, granulometry of sand, and quantity of mixing water [1]. It is common knowledge that am increase in binder content makes a mortar mechanically more resistant, while its tendency to crack formation increases. With regard to workability of fresh mortar, a fine sand demands an increased quantity of water for mixing. This in turn, however, increases porosity in comparison to another mortar of the same composition and aggregate granulometry and decreases strength at the same time as well. In samples taken from a building, one can determine mix proportion and granulometry without difficulty but not the original content of mixing water which strongly influences structure. Because no additional data were generally obtained by the usual mortar analyses and, nevertheless, transport and storage of moisture occur through open pore space, further criteria for assessing pore structure will be necessary. Therefore, in the case of attempts to reproduce historical renderings (compare [78]), it is necessary to quantify pore volume, distribution of pore radii and physico-technical characteristics, as e.g. capillary water absorption and vapour diffusion, and to identify in this way the influence of these parameters by systematically varying the portions of binder, aggregate and water.

5.7.1 Sand as an aggregate

Given this objective, the following procedure was chosen: for all tests a standardized sand according to EN 196 [16] was used. When the coarse portion is removed by sieving, one obtains fractions with particle sizes ≤ 1.0 mm, ≤ 0.5 mm, ≤ 0.25 mm, and ≤ 0.16 mm. Fig. 61 illustrates the grain-size distributions of the sands used. Now a procedure which is long familiar in soil science - the measuring of matric suction or potential [7] - also allows determination of pore radii in loose granular materials.

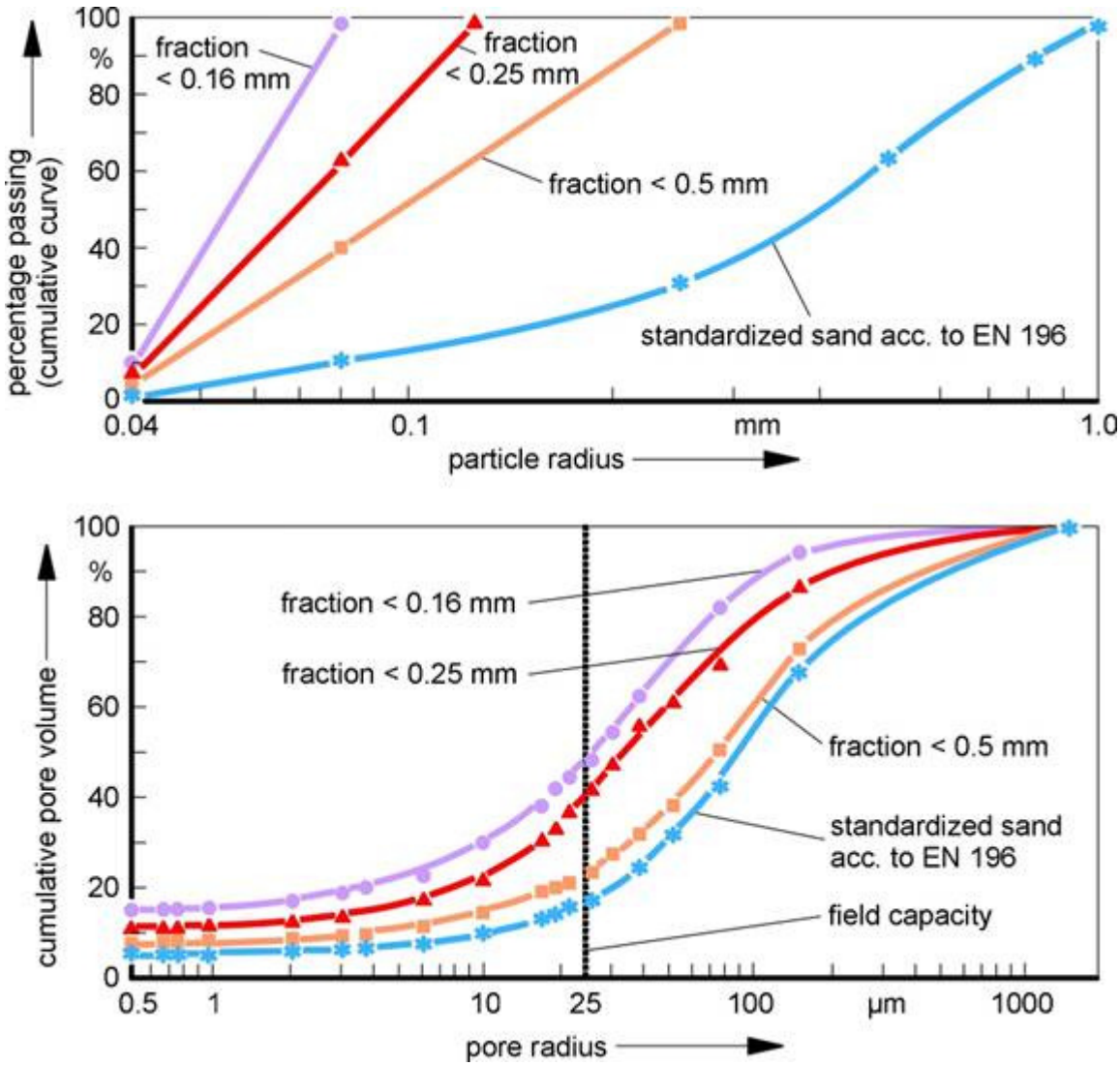

Fig. 61. Grain- and pore-size distributions of the sands used

Since water serves as a test medium, it may be assumed that one can reliably determine processes arising in practice. By exerting a defined pressure, a certain part of water under tension is removed from pores. This way one can predict how much water at what suction or corresponding pressure potential remains in the sample. By gradual pressure variation, a decreasing moisture content in a building material is similarly produced. To each pressure a particular pore radius can be associated. For water the following approximate equation is valid

$$r = \frac{1500}{P} \qquad \text{eq. (9)}$$

where r corresponds to pore radius in nm and P to pressure applied in 10^5 Pa. Among other things, one thereby obtains information on pore volume and distribution of pore sizes [46], [59], [99]. Such curves are shown in the lower part of Fig. 62. There one can find the pore spectrum being shifted to smaller radii with decreasing grain-size of sand. In this Figure, the respective pore volumes of each were set to 100%. In an interval below a diameter of 50 µm, called field capacity in soil science, water can just be retained by capillary forces, whereas with larger pores gravitational draining is predominant. The volume portion of pores of this size could therefore be consulted as a criterion for capillarity.

As reported elsewhere, a regression function for describing capillary liquid rise has been established at the Federal Institute [41]:

$$y_s = a\left(1 - e^{-b \cdot t^s}\right) \qquad \text{eq. (10)}$$

This equation is valid for most bricks, mortars, renderings, some concretes, and numerous natural stones but not for all sands. The curves in Fig. 62 show capillary transport of six sand fractions with different grain size (compare also [76], [77]). Only the absorption curve for the fraction smaller than 0.16 mm in diameter can be fitted to the function with a relatively good measure of precision. From these data the validity range of the above-mentioned relation is determined. In the case of sand only beginning at an amount of pores smaller than 50 µm in diameter of about 20% by volume, can one speak initially about a so-called genuine capillary transport.

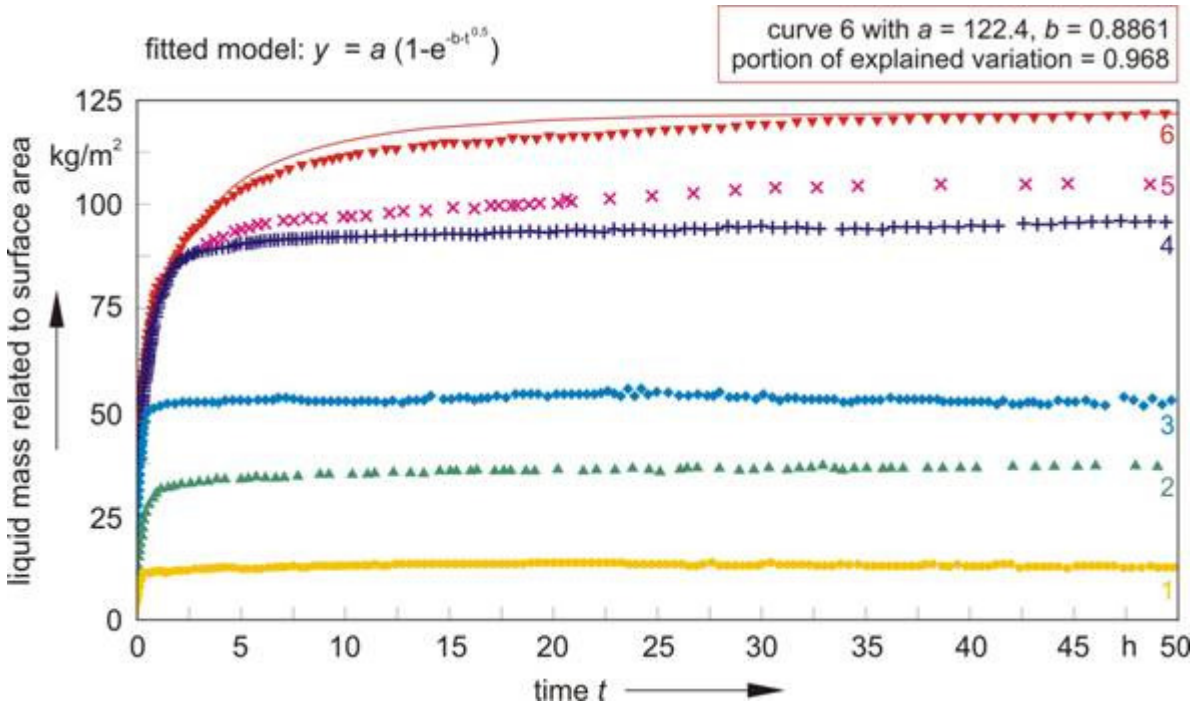

Fig. 62. Liquid rise in sand: 1 - > 0.5 mm fraction of sand standardized according to EN 196; 2 - standard sand; 3 - fraction ≤ 1.0 mm; 4 - ≤ 0.5 mm;0.5 mm; 5 - ≤ 0.25 mm; 6 - ≤ 0.16 mm

One should note that capillarity data obtained, especially on loose granular matter packing could, apart from results on building stone and other solid material, furnish suggestions for local intensifications of moisture rise as would be of interest e.g. in desert regions. There are also other characteristics to be determined as e.g. bulk density, pore volume (porosity), pore size fraction up to the field capacity and filling degree after capillary suction. This was possible because an equal sand volume after defined compaction is always used for these tests. Fig. 63 represents relationships between these parameters and grain size of sand. Bulk density (apparent density of dry material) decreases with increasingly finer sand, whereas pore volume and filling degree correspondingly increase, because more pores occur in the range of capillary activity. This is shown by the increase of pore fraction below the field capacity.

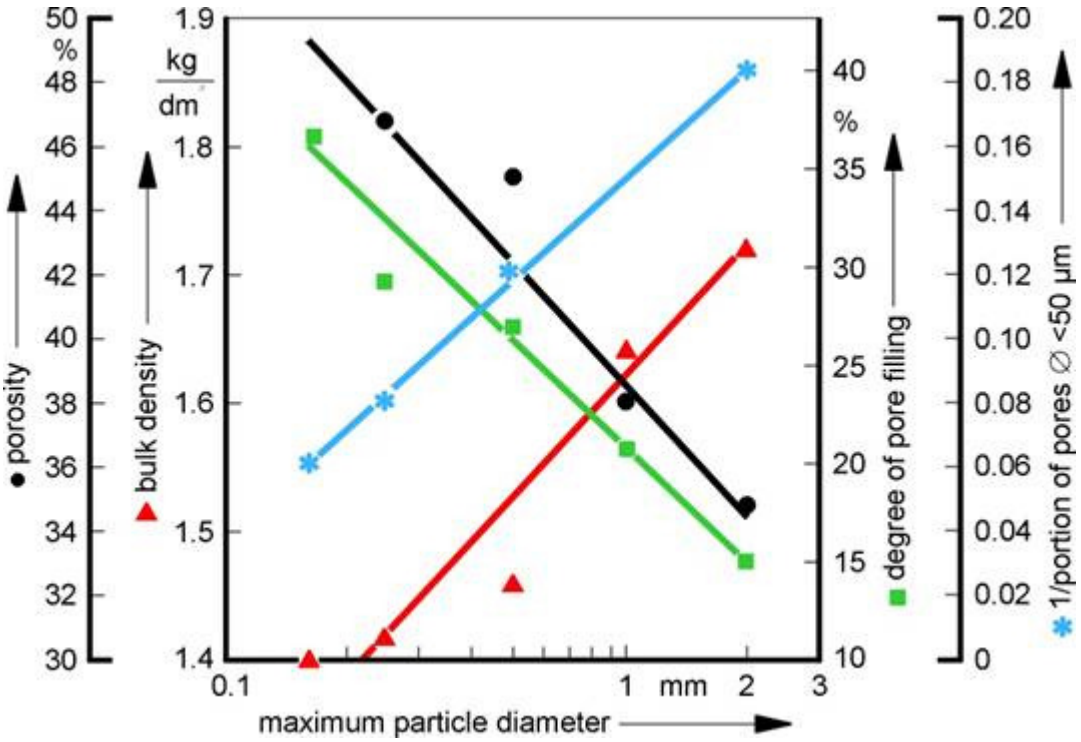

Fig. 63. Changes of structural parameters when using sand with different grain sizes

While it is not our objective to study sand intensely, it is absolutely necessary to define it before mixing it with binding agent and water.

5.7.2 Lime plaster

One can regard a mortar or rendering as cement hardened in an adequate time between or on building blocks where a minimal strength is required at grain boundaries and at the interface to neighbouring materials. Therefore, aggregate grains have to be bound into the whole and the interstitial spaces in such agglomerate must be at least partially filled by a binding agent. In this connection the phenomenon poorly defined up to now and called "leaning" plays a crucial role. The principle is that binder or mortar matrix material more or less surrounds aggregate grains and lines pore walls in such way that stress relief can take place and crack formation can be avoided.

Everyone who has prepared mortar or rendering can report the difficulty in obtaining good reproducibility, even when constant starting conditions such as mix proportion and water demand are maintained and despite performance by the same person with an identical mix having the same characteristics. Fig. 64 shows the scattering of corresponding structural data in which pore-size distribution for lime mortar batches of the same recipe is plotted. These results can only be obtained, as in this case, when strictly maintaining the conditions required as e.g. mixing time.

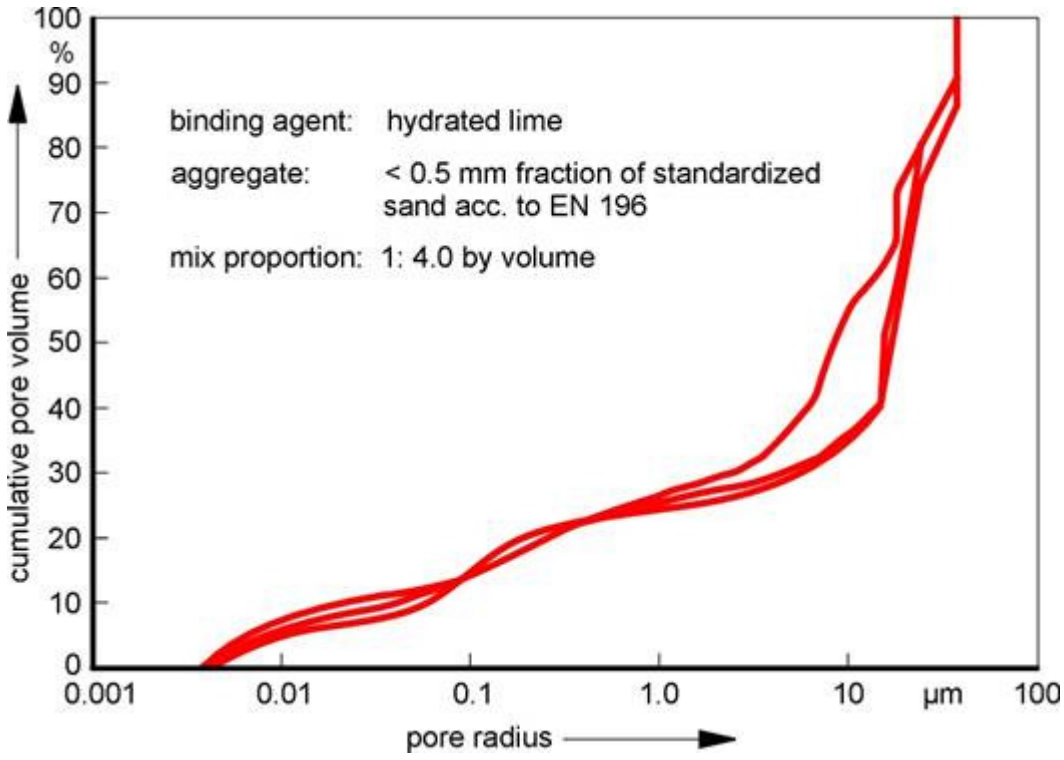

Fig. 64. Comparing pore-size distribution of lime mortar batches while using the same recipe

By increasing the binder portion in a mix, one can generally shift the pore spectrum of the hardened mortar formed from this mix to finer pores (Fig. 65).

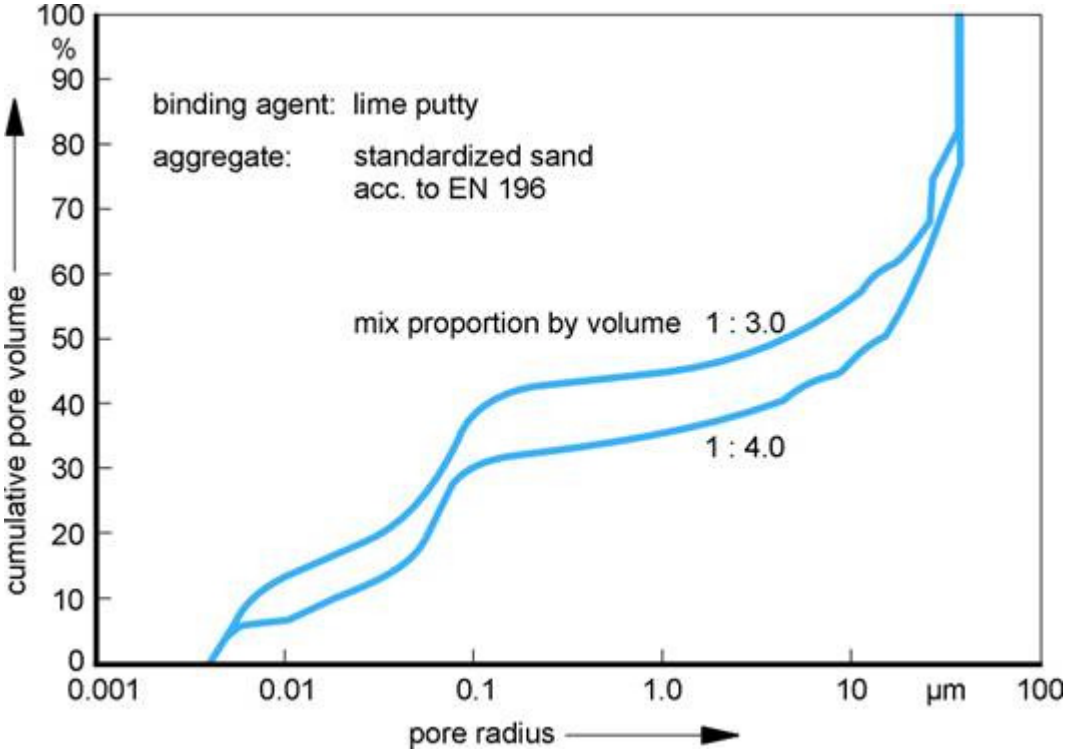

Fig. 65. Shifting pore-size distribution of lime mortar: influence of mix proportion

The portion of fine pores smaller than 5 µm in diameter (the so-called microporosity according to Honeyborne and Harris [53]) here increases by about 5%, whereas the median (the 50% fractile of pore-size distribution) drops from 12 µm to 8 µm. At the same time, one

can observe an elevation of pore volume measurable by mercury intrusion. The mixing water content for both renderings was comparable (21.3 and 21.6% by mass). Since the water absorption coefficient, w_o, could not be determined for the majority of samples due to geometric deficiencies, only limited information was possible. An increasing binder portion obviously causes a rise in this characteristic.
This tendency is still more distinct (Fig. 66) when one compares this mix to a historical mortar which has a mix proportion of lime hydrate to sand of 1 to 0.9 by volume. Caution should be taken, however, with respect to an interpretation, since probably other techniques, as e.g. soaking of quicklime together with sand and also another content of mixing water, were used during the mortar's preparation. One can likewise obtain a pore-size distribution similar to that of the historical material by a slight addition of portland cement (see also this Figure). Since a suitable substitute mortar has to fulfil still other criteria than this, as e.g. similar pore volume and low modulus of elasticity, a reduced quantity of portland cement-containing mortar is out of consideration, at least when lime was used as binding agent for historical material. In order to attain comparable behaviour and structure and also additionally to produce mortar which is free of cracks and will remain so, one cannot evade a revival of older techniques.

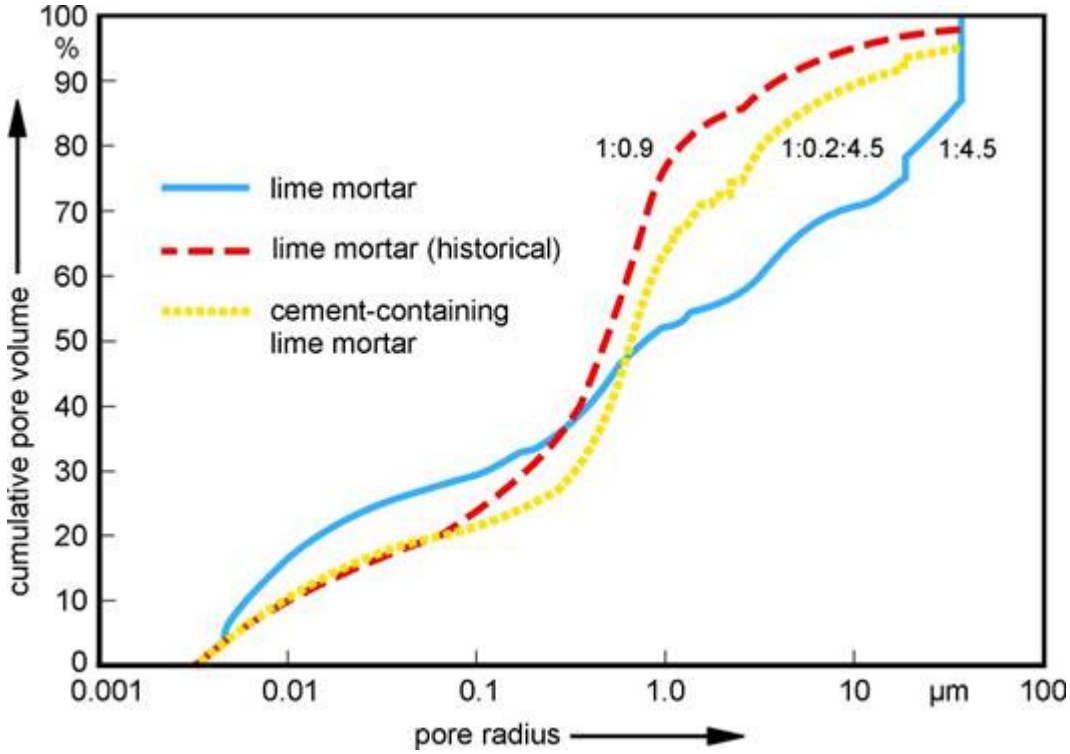

Fig. 66. Shifting pore-size distribution of lime mortar: influence of the mix proportion and a Portland cement admixture

Preliminary results on the influence of an aggregate's grain-size composition on physico technical properties and characteristics are also available. They are based upon mortars with the same mix proportion 1 : 4.0 by volume. This differed considerably in mass depending on the binding-agent aggregate batch, because of the applied standardized sand used and with its fraction smaller than 0.5 mm. Consistency was regulated by means of the spread value (18 cm was selected), so producing an increased water demand of about one third, namely from 18 to 29%, when using mortar manufactured with fine sand. Fig. 67 represents respective pore-size

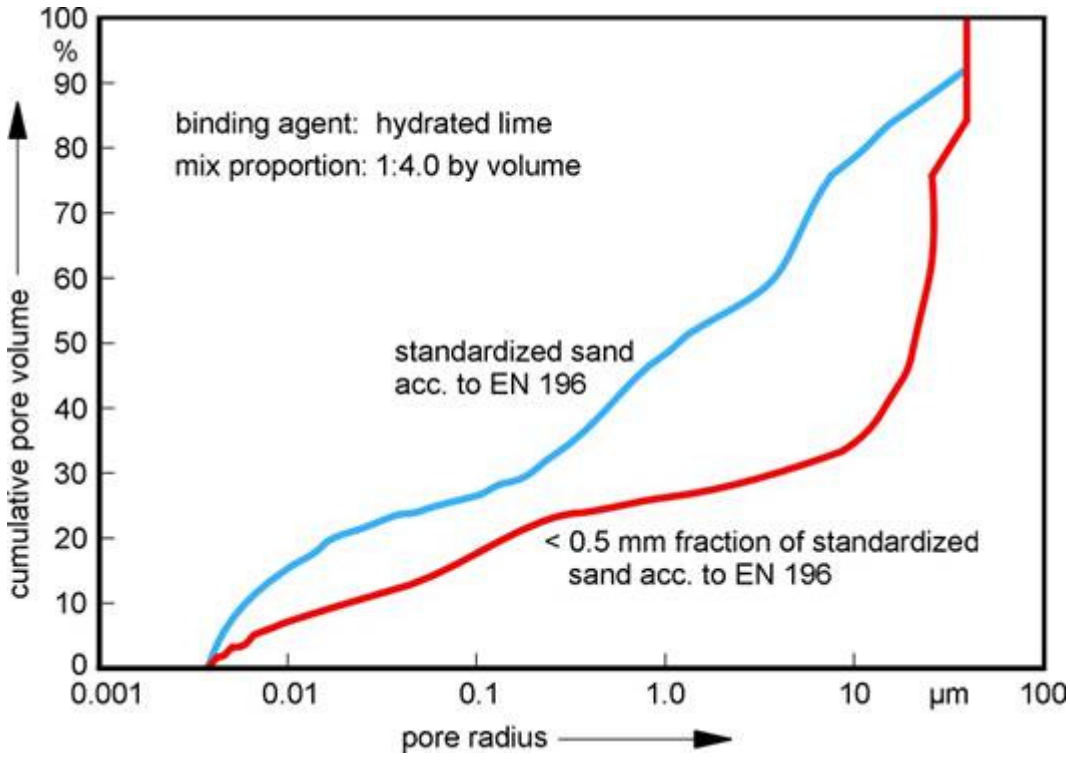

Fig. 67. Shifting pore-size distribution of lime mortar: influence of sand fraction

distributions for corresponding samples. The specific pore volumes were set to 100% again. However, it was not expected that mortar containing a fine fraction would show such a very small amount of fine pores, namely a microporosity of 28% in contrast to one of 55%. It should be emphasized that the pore volume is nearly double, which cannot be recognized by this type of representation. Behaviour occurs here analogous to that observed on sand whereby with increasingly finer fractions, the pore volume expressed as porosity, the pore filling degree, as well as the water absorption coefficient also increase. Does this mean that one can just transfer these conditions to mortars? It does not seem quite so simple, because similar to the grain-size effect, an increase of mixing water content is followed by a higher w_o in hardened mortar. From this one can conclude that both parameters uniquely influence structural changes observed and operate in the same direction. Only systematic tests may help to quantify their contribution to the entire event.

Some additional interesting regularity can be elucidated by a combination of single characteristic values. Due to the lack of sufficient data, only tendencies valid for both kinds of granular matter should be shown. Existing gaps still have to be closed. In such lime mortars, an elevated pore volume always runs parallel to a diminished portion of micropores. But the fewer micropores, or inversely expressed, the more coarse pores such materials possess, the higher are values reached for the water absorption coefficient. This means that microporosity may provide information on frost sensitivity of building materials, but is less involved in capillary transport. According to H. Weber et al., at a diameter smaller than 0.08 µm capillary transport should completely come to a standstill (see [103], p. 17). Of course, the kind of behaviour of such a building material will be furthermore influenced by the base on which the plastering was applied and by the bricks or natural stones situated in between the mortar. Their absorbing behaviour still exerts an additional effect on drying mortar during hardening in its structural development. Therefore from Fig. 68 the matric suctions of sand, the lime mortar produced thereof, and typical bricks of different density demonstrate that it is neither permissible to view a mortar in isolation nor to lose sight of the complexity of the process.

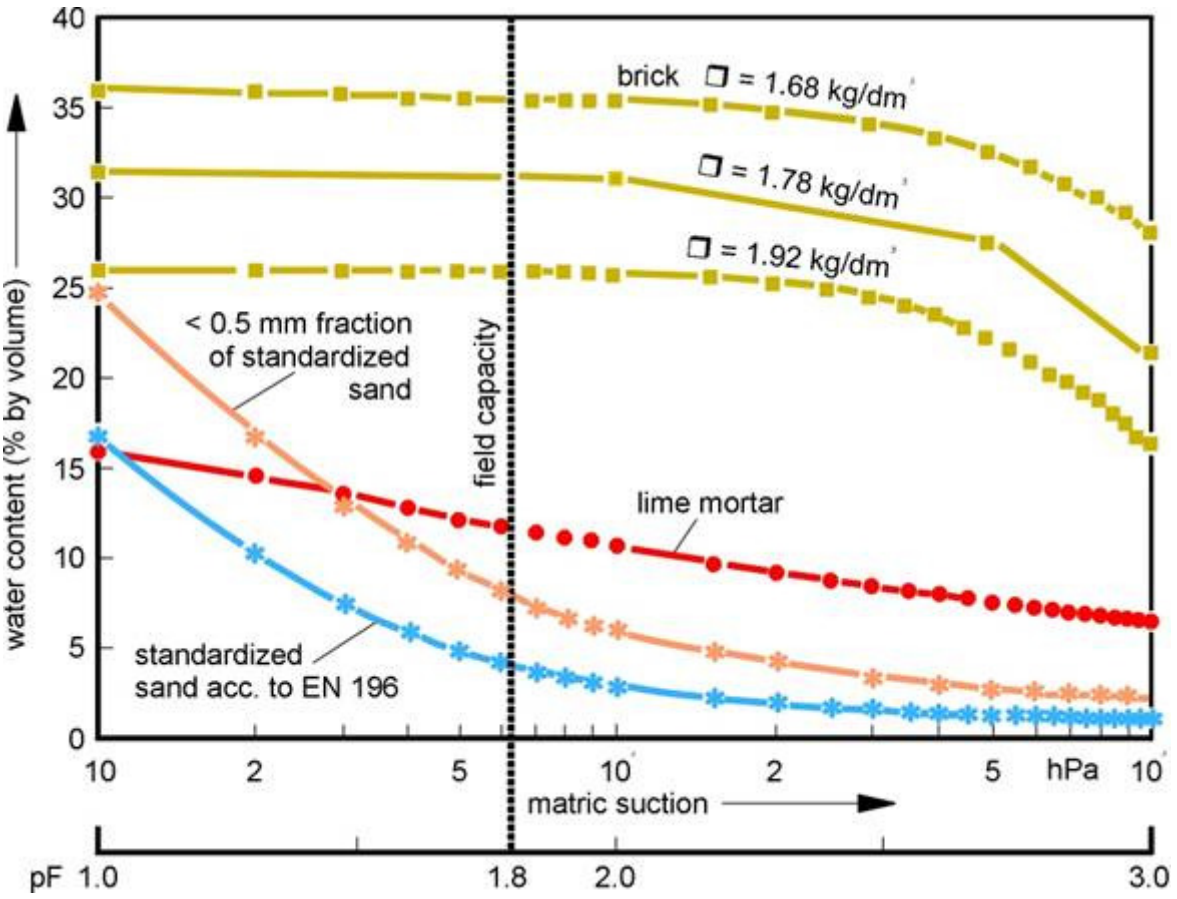

Fig. 68. Water content depending upon matric suction, determined on dry-pressed bricks, lime mortar and aggregate sands

According to the authors' experiences, several correlations can be established between pore-related characteristics for bricks, mortar prisms, rendering fragments and accumulations of aggregate sand. A total survey on capillary and evaporative behaviours will be finally furnished only by the brickwork itself, in which a geometrically complicated scaffold of bed and head joints runs through a regularly stacked brick pile. The current findings would represent the first steps towards this goal. By varying test conditions in a way directed towards an objective, one can appreciably reduce the sample number and test duration, which would otherwise necessarily increase excessively. Therefore one has not only to select measures carefully, but also one has to consider that preparative uncertainties may initially restrict the significance of the results obtained.

5.8 Investigation of capillary absorption in masonry sections

After consideration of the relationships of aggregate sands and mortars, one can obtain information on the transport event in an entire masonry by including bricks (for test procedure see section of 4.2.1). In addition to properties caused by firing conditions such as a decrease of pore volume and an increase of apparent density, such a view of the pore parameters of a satisfactorily characterized ceramic material also shows a reduction in the fraction of fine pores as a result of the sintering process. Correspondingly, w_o diminishes with density (Fig. 69). The curve represents a type of hyperbola for which 473 values were available.

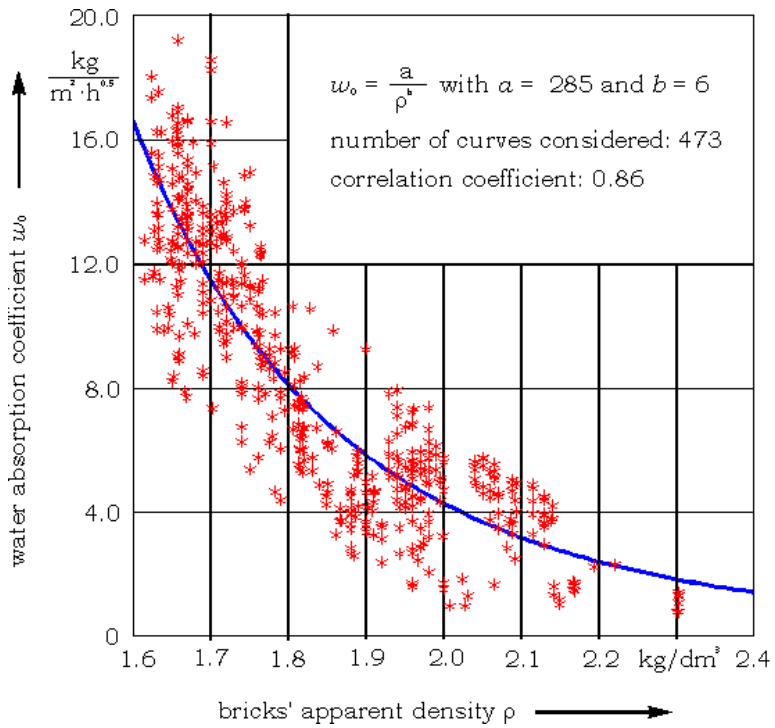

Fig. 69. Water absorption coefficient, w_o, as a function of apparent density, ρ, determined on brick stacks from different production runs. In addition, data for some sedimentary stone specimens are plotted.

At the same time a higher brick density is associated with a smaller pore volume. Further details can be found in the literature on this subject [43], [75], [79], [81].
Regarding the experiments with masonry sections, the relationships are not quite distinct; the schematic presentation shown in the following diagrams should aid in a clarification.

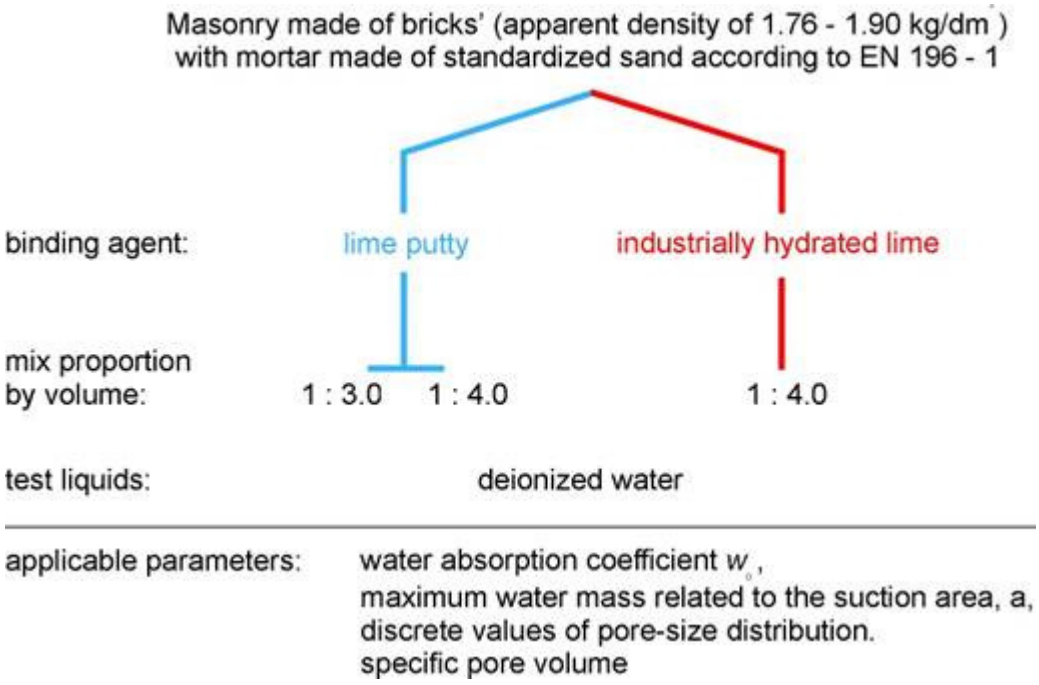

Fig. 70. Schematic presentation of masonry section designs with different binding agents and mix proportions

Dry-pressed facing bricks of similar apparent density were used in their setup, specifically from the same production run. Pure lime mortar with a mix proportion of lime hydrate to sand

of 1 : 4.0 by volume was taken in order to initially avoid a barely testable blocking effect, e.g. caused by cement grout on the bricks' boundary faces. Standardized sand according to DIN EN 196-1 served as the aggregate in addition to a sieve passing ≤ 0.5 mm diameter, with which one can almost fit the absorption behaviour of mortar to that of brick.

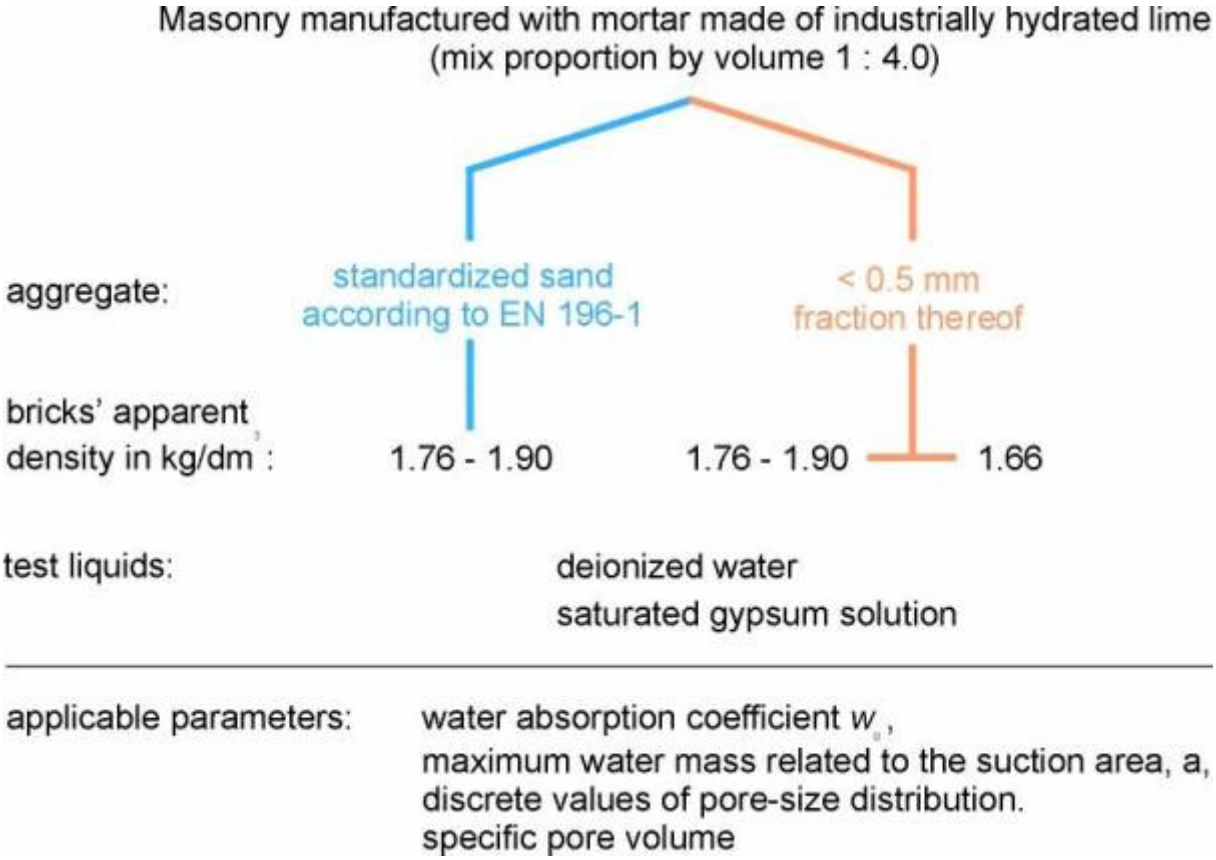

Fig. 71. Schematic presentation of masonry section designs with different aggregates and bricks' apparent densities

For two masonry sections lime putty was also used as a binder. Furthermore, in several cases the mortar mix proportion and brick density were modified as well. Consistency was adjusted by the spread value according to DIN EN 459-2 [18].
The test specimens were situated in water-containing troughs on balances, whereby one could monitor mass change during moisture rise and evaporation events. For determining capillary absorption by weighing the whole specimen, one also has to hold liquid level constant and at the same time to entirely implicate the test setup required for this. So the validity of the above-mentioned regression function can be demonstrated for wall sections of ca. 63 to 36 cm base area (transversal cross section) and 125 cm height brick courses laid in a cross bond with pure lime mortar. After the experiment's end, in general the moisture content of porous bricks freed from mortar is gravimetrically stated. In such way one can remonitor capillary rise in its various stages, and after that a recalibration with the aid of a method based upon measuring a dielectric constant (see Fig. 72).

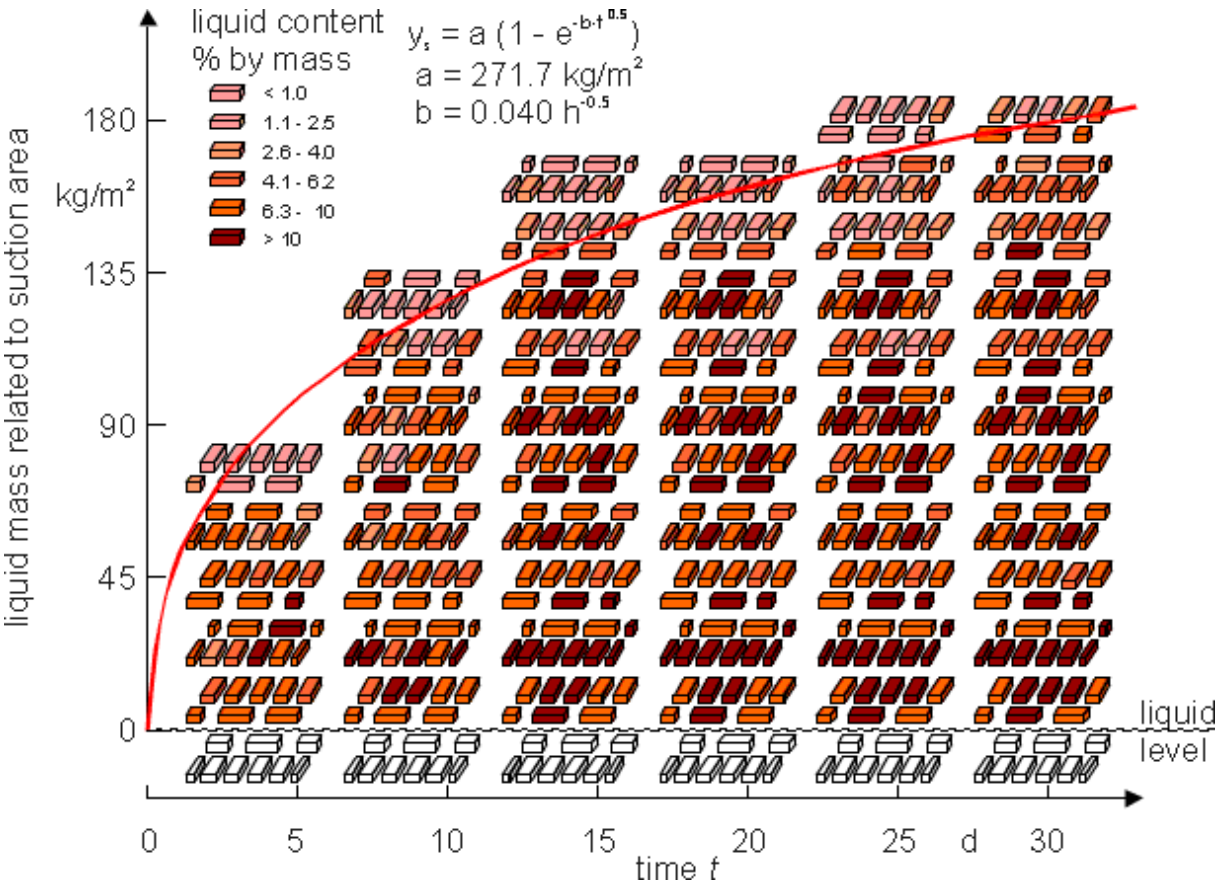

Fig. 72. Exploded view showing moisture distribution within 10 courses of a brick work section participating in capillary water rise

In another exploded view of such a masonry section, the moisture distribution can be seen in Fig. 73. Here the soaking has reached the upper brick layer. But the carbonation of the mortar joints was not as uniform as had been expected. Therefore the tests were started after a one-year curing, corresponding to a periodic moistening with the objective of an utmost uniform carbonation.

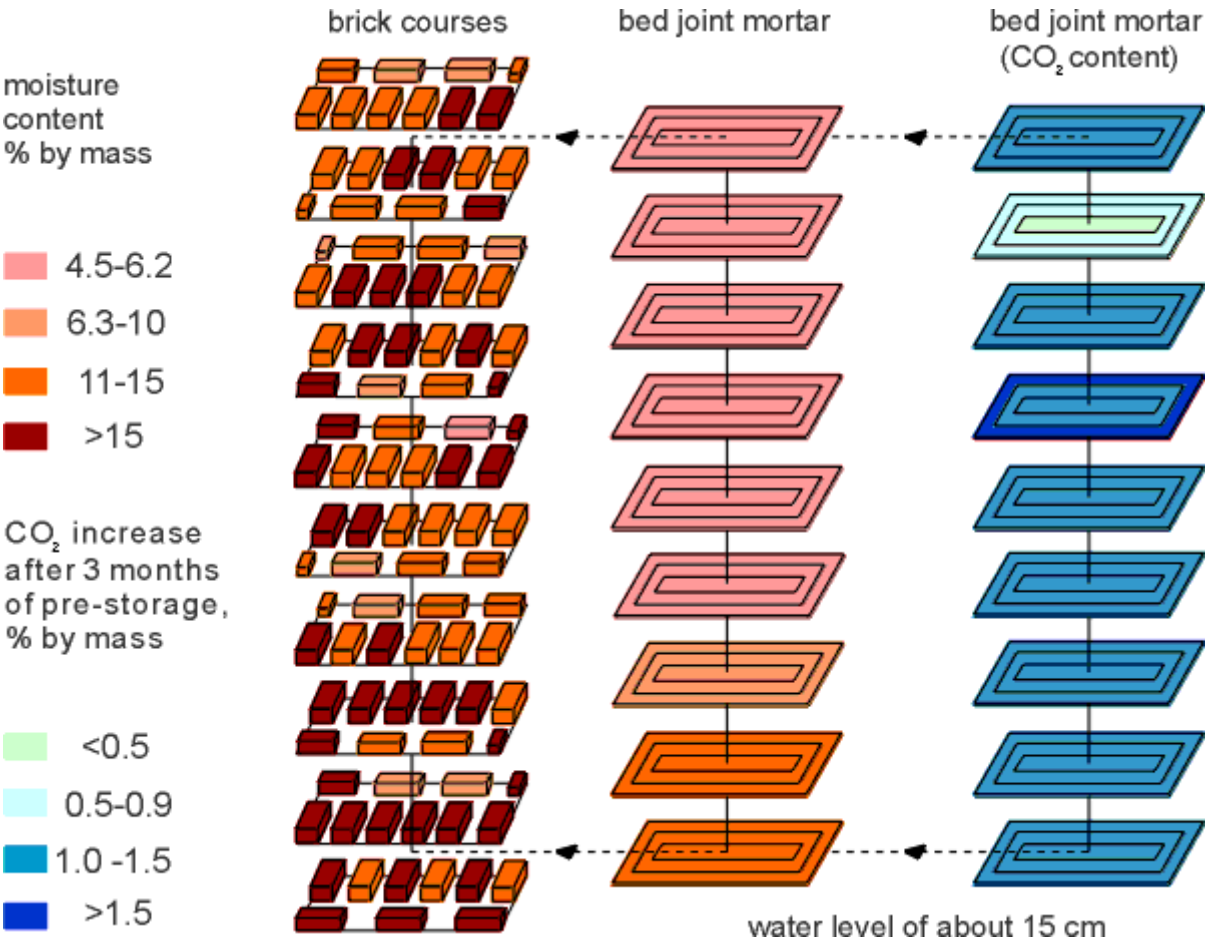

Fig. 73. Exploded view of a 2-year-old masonry section stored in a constant climate without curing: moisture and carbonate distribution

Fig. 74 shows a test setup for determining capillary liquid absorption and evaporative behaviour of masonry sections.

Fig. 74. Masonry section for tests on capillary behaviour and moisture release, placed upon a scale in a tank for the water supply

Within dry brickwork, which is a system of two components with respect to material - and accordingly to matric suction but also to morphology of evaporation surface - a permanent water change takes place between both components during the water supply from below. Of course this depends upon whether brick or mortar is better able to conduct moisture i.e. to transport it quickly or with a higher flow through the cross sectional area. Moreover this event is decisively dependent on each volume portion - here about 20% for mortar.
First, mix proportion and its influence on the capillary behaviour of brickwork is of interest. Mixes with standard sand as aggregate and lime putty as binder were produced in the proportion 1 : 4.0 and 1 : 3.0 by volume. The water demand of fresh mortar was at 21.8% and 20.6%, being comparable with each other. In the curves of the water absorption for corresponding masonry sections, the participation of mortar in the overall event is clearly evident (Fig. 75).

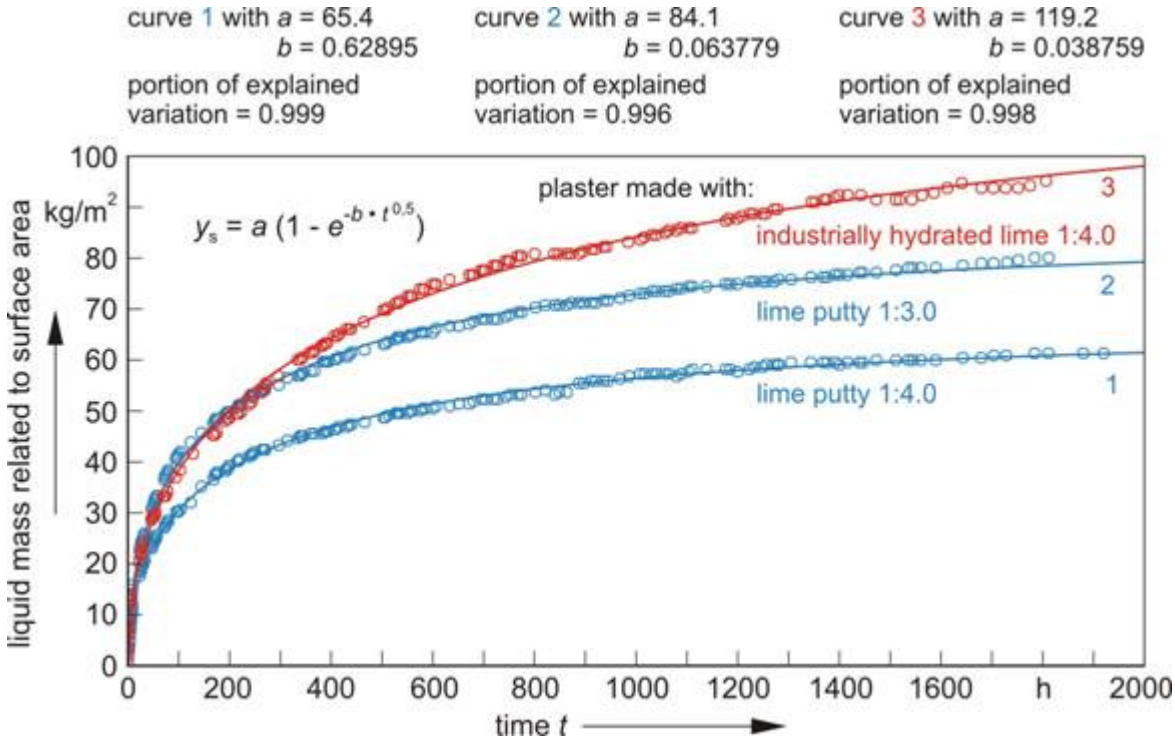

Fig. 75. Capillary liquid rise in masonry (bricks' apparent density 1.76 - 1.90 kg/dm^3, standard sand as a mortar aggregate): influence of mix proportion and binder type

Richer mixes result in an elevated moisture rise. The water absorption coefficient also slightly increases from 4.1 to 5.4 kg/(m^2 h$^{0.5}$), which is caused by the higher content of fine pores as well as a larger pore volume, already found in comparable mortar prisms. If one uses industrially slaked lime hydrate instead of lime putty, with the same mix proportion of 1 : 4.0 and comparable water demand, then masonry using this mortar shows an appreciably higher moisture rise with a similar w_o. Compared with lime putty, mortar with this binder shows a higher pore volume and an increased fraction of fine pores, whereby this behaviour is explained. Every change of mortar composition therefore also exerts a distinct influence on a wall's entire behaviour. When increasing the apparent density of brick from about 1.66 to 1.76 and up to 1.90 kg/dm^3 while holding the same mix proportion and using standard sand's fraction < 0.5 mm, this leads to a decrease of the capillary head and so of its practically equivalent maximal value for water absorption related to the surface of a material column a from ca. 200 to ca. 183 kg/m^2. Also w_o shows only insignificantly lower values (ca. 10 as against 9 kg/(m^2 · h$^{0.5}$)). In such way one can quantify nevertheless the bricks' contribution to water rise.

Since granulometry of aggregate sands exerts an appreciable effect on a mortar's structure, a corresponding behaviour on masonry sections was also inevitably found. Using the fraction < 0.5 mm as an aggregate, moisture rises considerably higher and likewise finds its expression in the a value (i.e. 183 as against 111 or 119 kg/m^2, while employing standard sand). In the same direction, w_o increases from ca. 4 to 9 kg/(m^2 · h$^{0.5}$) (see Fig. 76).

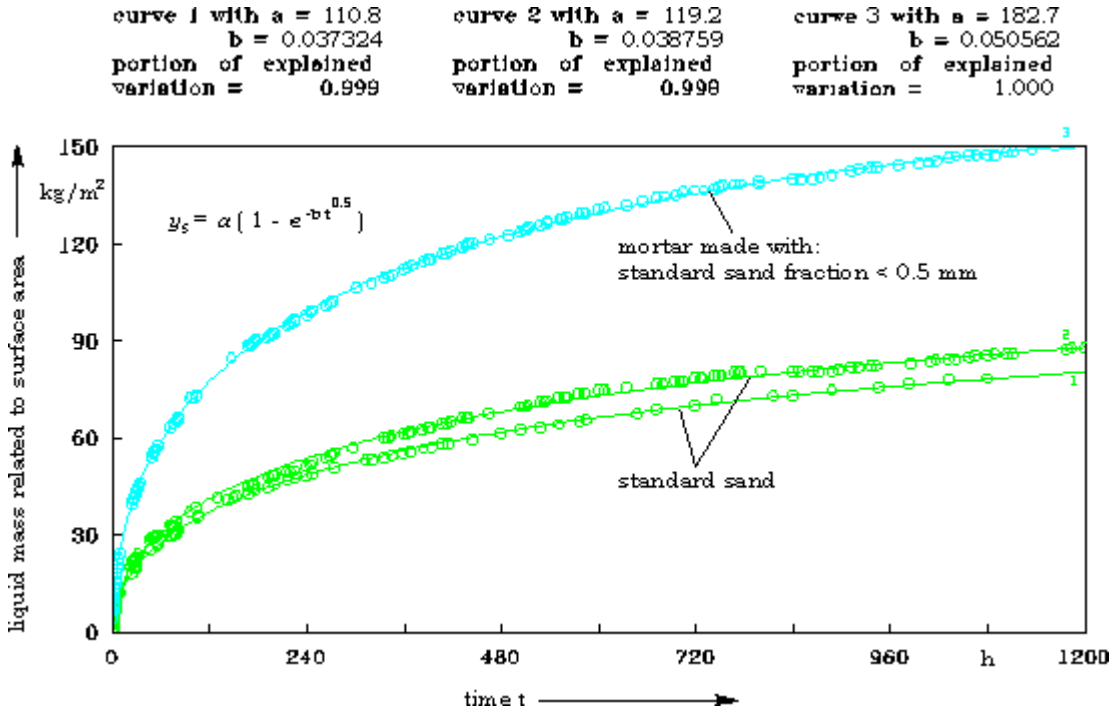

Fig. 76. Intensifying capillary liquid rise in masonry by using sand < 0.5 mm diameter as a mortar aggregate (bricks' apparent density 1.76 - 1.90 kg/dm^3, industrially hydrated lime, mix proportion 1 : 4.0)

On brick it can be shown that a increases, e.g. in the presence of calcium sulphate or sodium sulphate solutions - a phenomenon explainable by their surface tension. Such events are comparable in brickwork when using low-density brick and fine sand < 0.5 mm as a mortar aggregate, where a increases form ca. 200 to 278 kg/m^2 when a saturated gypsum solution serves for a test (Fig. 77).

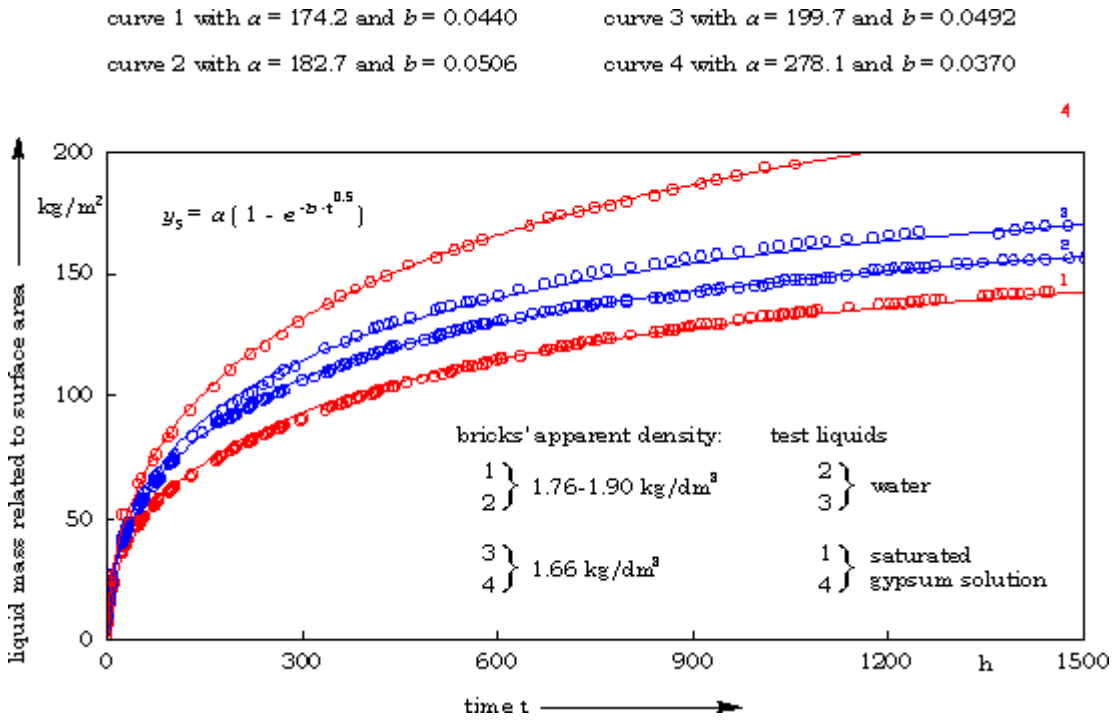

Fig. 77. Elevated capillary liquid absorption of masonry by using a saturated solution of calcium sulphate instead of water (sand < 0.5 mm diameter as a mortar aggregate, industrially hydrated lime, mix proportion 1 : 4.0)

The water absorption coefficient thereby only increases insignificantly from 9.8 to 10.3 kg/(m^2 h$^{0.5}$). When repeating the soaking process with gypsum several times, this increasingly leads to a reduction of a and w_o that is probably caused by further conditions even reverse when using bricks with an apparent density between 1.76 and 1.90 kg/dm^3 (also seen in this Figure). In other words: water rises higher (a = 182.7 kg/m^2) than a gypsum solution does (a = 174.2 kg/m^2). Simultaneously w_o drops from 9.2 to 7.7 kg/(m^2 · h$^{0.5}$). In the first case capillary action of brick apparently dominates, whereas in the second instance the mortar's capillarity pushes itself to the fore. Mortar with standard sand and dense brick behaves similarly. Water absorption diminishes in comparison to the test result with water from 119 to 72 kg/m^2 and w_o has a lowered value, i.e. 3.9 as against 4.7 kg/(m^2 · h$^{0.5}$), which indicates here that a change in the mortar's structure might have occurred. According to mercury porosimetry tests, a gypsum solution obviously induces a distinct reduction of specific pore volume from 0.117 to 0.108 cm^3/g at a nearly uniform pore-size distribution. Similar events presumably happen also in mortars made with fine sand. However, in the case of "favourable" brick (low apparent density, high pore volume, large portion of pores showing capillary activity), this effect appears not to be so distinctly structural changes.

The effect of air circulation on capillary absorption at comparable climatic conditions is shown in Fig. 78. In an ambient air practically without any circulation a liquid

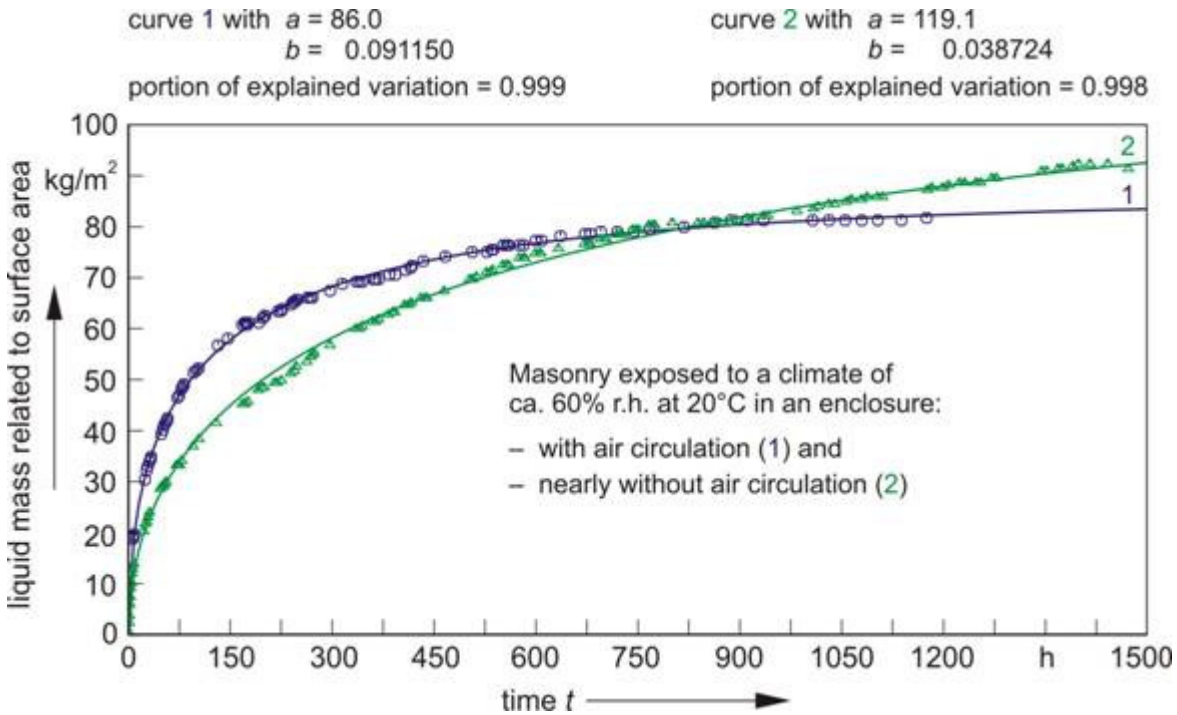

Fig. 78. Air circulation's influence upon capillary rise in masonry (bricks' apparent density 1.76 - 1.90 kg/dm^3, sand <0.5 mm diameter as a mortar aggregate, industrially hydrated lime, mix proportion 1 : 4.0)

mass related to surface area of 182.5 kg/m^2 was absorbed (curve 2), whereas a masonry section exposed to this circulation shows no more than 86 kg/m^2. On behalf of reproducibility and comparability, one therefore has to ascertain a high constancy of all factors which influence climate.

5.9 Investigation of masonry sections' evaporative behaviour

Besides moisture absorption, liquid release during an evaporation process represents an essential specific behaviour. After having reached an equilibrium state at the end of the absorption test, water was drained from the tanks where sections were placed, and the course of evaporation related to visually recognizable surfaces was gravimetrically monitored. Of this about 20% is assignable to the mortar face. The masonry section dries, whereby initially capillary transport and later also diffusion connected with an immobilization of solute salts play a role. The fitting model used for describing the material-specific section of this process reads

$$y_e = a \cdot e^{-b \cdot (t - t_0)} \qquad \text{eq. (11)}$$

as already shown in section 4.2.2

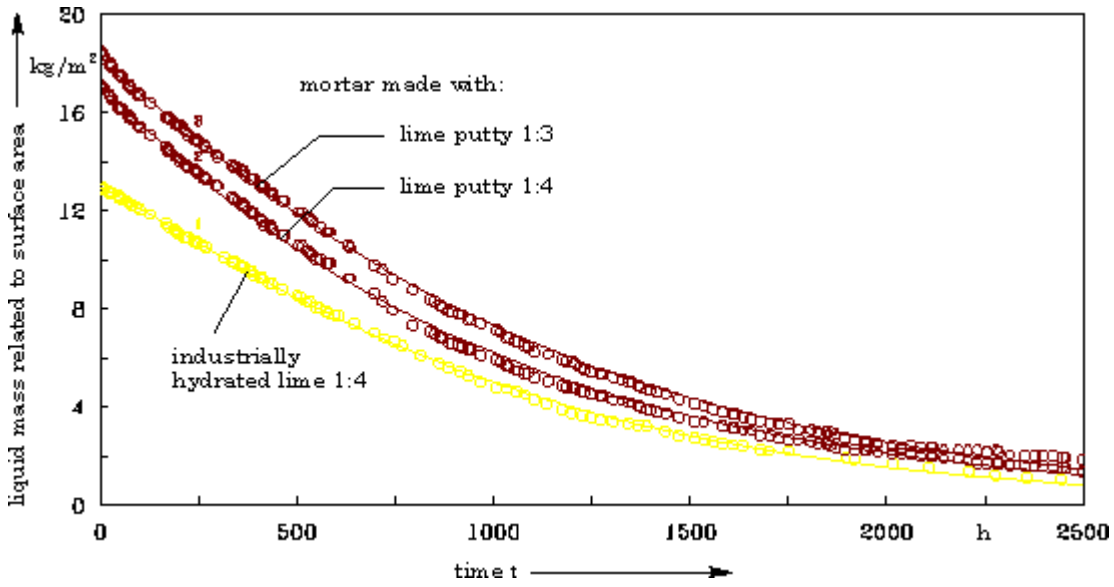

Fig. 79. Evaporation behaviour of masonry sections as shown in Fig. 73 (bricks' apparent density 1.76 -1.90 kg/dm^3, standard sand as a mortar aggregate): influence of mix proportion and binder type

When comparing both of the masonry sections with one another for the mortar of which lime putty was used as a binder (Fig. 79), one can find a nearly parallel course of curves, whereby that with the richer mix (curve 3) is to be found above that containing more aggregate (curve 2). This is also true when looking at the remaining moisture content related to total capillary absorption. Industrially hydrated lime in a comparable mix proportion behaves slightly differently (curve 1). At any time in this brickwork a greater liquid content remains than in its equivalent made with lime putty.

Concerning the influence of bricks' apparent density, one obtains curves with distinct starting points because of different evaporation surfaces being smaller in the case of denser brick, which makes a comparison difficult (Fig. 80). When considering for the time being the course of an evaporative curve one can clearly realize parallelism of their linear sections, each in such way characterizing a constant evaporation velocity.

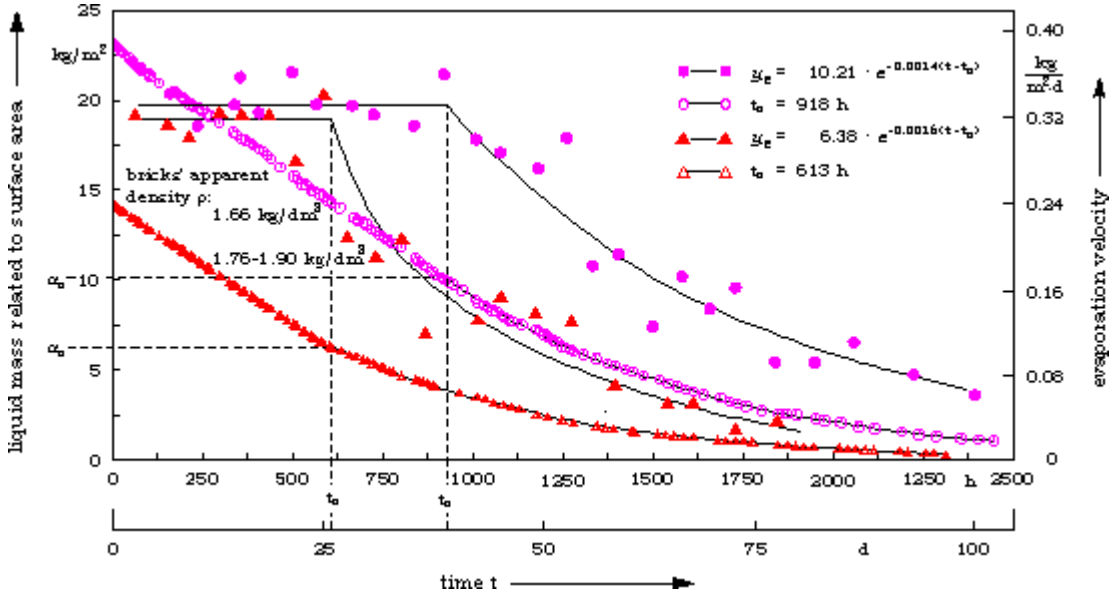

Fig. 80. Modifying evaporation behaviour of masonry by using bricks with different density: determination of corresponding inflection-point moisture, a_o, and evaporation parameter, b

Starting from inflection points of both curves, which run for low density brick at 44% of total capillary absorption and for high density brick at 42% correspondingly, courses according to the evaporation formula result. Observing arbitrarily moisture content after 2000 h, the masonry section having low density brick contains 8.4% and the high density equivalent only 2.4%. This means that the masonry section with low density brick at all times shows an elevated water content, or in other words: a material having highest absorption and so containing most water therefore achieves a final state or its equilibrium moisture content after a longer period. This is a truly remarkable result.

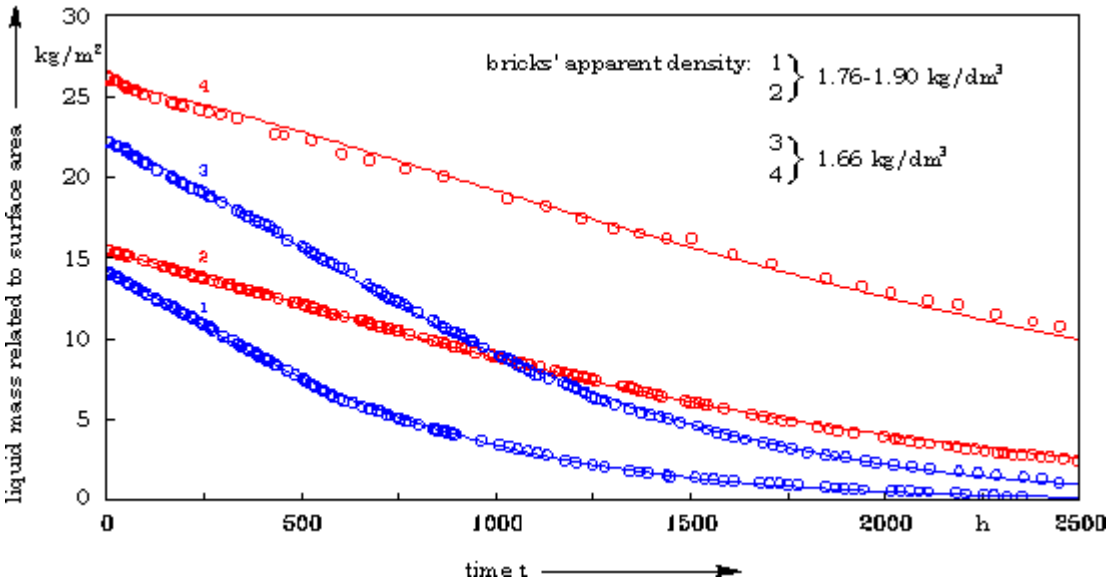

Fig. 81. Modifying evaporation behaviour of same masonry sections as shown in Fig. 75 by using bricks with different apparent density and additionally a saturated solution of calcium sulphate (curves 2 and 4) instead of water (sand < 5 mm dia- meter as a mortar aggregate, industrially hydrated lime, mix proportion 1 : 4.0)

When performing such tests with gypsum solution instead of water (Fig. 81), this has - because of differing rise or evaporation surface respectively - as its consequence also curves with dissimilar starting points. Although during a capillarity test performed on masonry made with sand <0.5 mm diameter, when using calcium sulphate solution, the same water absorption coefficient was found despite a higher capillary head. This corresponds to an unchanged pore structure; evaporation behaviour was so influenced that a clear reduction of evaporation velocity results. Sections having bricks of different density here also show the same velocity down to the end of this linear portion. In both cases, however, remaining moisture content is always above that with water as a test liquid. Low density brickwork shows after 2000 h a considerably higher moisture percentage of about 67% than is the case of dense brick with only 27%. This means that the influence of the kind of solution on this process is effectively increased by low density bricks and so possibly caused by clogging of fine pores with reprecipitated gypsum crystals. Similar findings are also described by F r a n k e and G r a b a u [24].

A shift of grain-size spectrum to smaller diameters leads to a higher water rise, and in this way to a larger evaporation surface and also to an increased liquid mass related to it. The slope of both types of evaporation curves is different (Fig. 82).

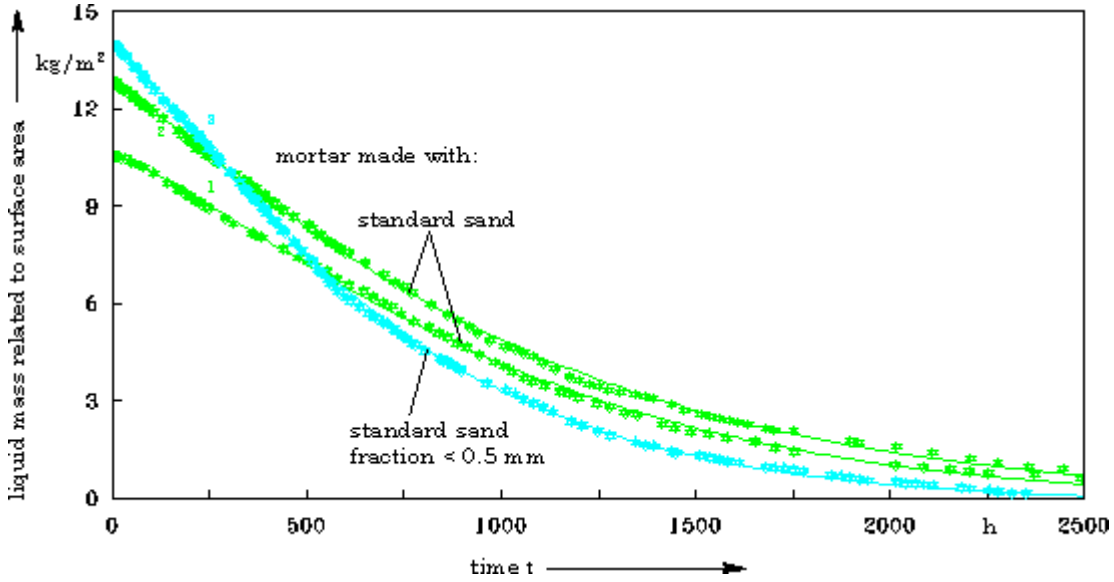

Fig. 82. Evaporation behaviour of masonry (bricks' apparent density 1.76-1.90 kg/dm^3, industrially hydrated lime, mix proportion 1 : 4.0): influence of grain-size distribution of sands used as a mortar aggregate

From 0 to ca. 600 hours on a brickwork section with fine sand as a mortar's aggregate (curve 3), a decrease from 14 to ca. 6 kg/m^2 respectively from 100% to 43% related to total capillary absorption can be observed, whereas in the same time in the case of the last cited mortar, for it still shows 66% as against ca. 52% after 500 hours and still 37% as against 23% of its original moisture content after 1000 hours, whereby the dry state is also reached correspondingly later. Similar results can be found when using curve 2 for interpretation. Expressed in another way, this means that a brickwork with fine sand mortar having otherwise the same brick material releases its moisture more rapidly despite the higher water absorption than that with a mortar containing standardized sand. Hence, one can conclude that a large pore volume and a high number of pores contributing to capillary activity also influences evaporation positively, i.e. accelerates it. Since no important changes in the capillary behaviour of brickwork occurred with standard sand as an aggregate, it is little wonder if it is also not the case during evaporation. Only after the third repetition of a soaking process by a gypsum solution was a deceleration of moisture release compared with the test using water found. That a remarkable influence in the case of fine-sand mortar is caused even after the first soaking process was already indicated in Fig. 81. Pore geometry and surface tension seem to participate in this. During tests the question arose regarding the climatic influence on an evaporative course. Therefore behaviour was determined of one and the same masonry section at the same temperature and relative humidity, but however with different air circulation. In agreement e.g. with K a m e i, who reported about a Kibushi aluminia (cf. [64], p. 314), it results that air movement produces a considerably elevated evaporation velocity (Fig. 83).

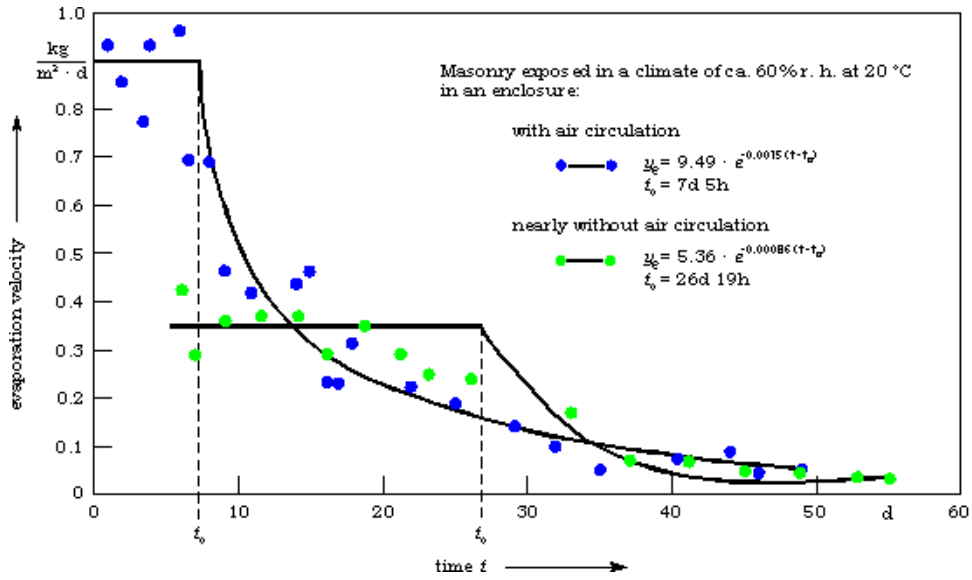

Fig. 83. Modifying evaporation velocity of masonry by air circulation (bricks' apparent density 1.76 - 1.90 kg/dm^3, standard sand, industrially hydrated lime, mix proportion 1 : 4.0)

Having a comparable starting moisture in both cases - capillary absorption taking place under air circulation - there have been presented differing amounts for a_o and b values as well. Through moisture rise and evaporation under the same climatic conditions each, i.e. when equally taking into account water fillings with and without air circulation (compare Fig. 78) and this way also evaporation surfaces, it is surprising because the evaporation parameter b each time shows almost identical values (0.0016 or 0.0015) thus confirming its material-specific character, whereas a_o in turn adopts different amounts. At this time, however, further interpretations are not yet possible.

6 Summary

The main objective of the programme sponsored by the Federal Environmental Agency (UBA) was to gain information on dose-response relations for diverse renderings by means of outdoor exposure tests conducted at six locations in the Berlin region with different SO_2 concentrations over the course of several years. The comparability of results should be ensured by maintaining defined compositions (standardized sand as an aggregate and predominantly aerial non-hydraulic lime as a binder), as well as including measuring stations of Berlin's Air-Quality Monitoring Network. Apart from analysis of water-soluble secondary constituents enriched during exposure and from determination of their phase composition in different depth positions, several physico-technical properties and characteristics relevant during a weathering process were investigated. For their detection also served inter alia improved and newly developed methods which have been partially incorporated in a mortar and rendering manual recently published [30]. The transition to Germany's reunification occurred during the test period so that a material's immission-dependent modifications did appear only to a strongly reduced extent because of stringent legal restrictions and decreasing emissions anyway as a consequence of the shut-down of industries in the former GDR - i.e. just in the prevailing wind direction. In the case of those test plates produced as a scraped finish and mounted on specially constructed racks which exposed them immediately to SO_2 attack but not to direct rainfall, each facing south and arranged perpendicularly as on a building, one therefore could not reckon with a swift reaction process in the time available.
In this connection it has proved to be convenient to necessarily expand time intervals between samplings and to shift the focus of the original program more to building samples which summarized results over a longer stress period, although one can also expect surprises with regard to homogeneity and comparability. So the number of useful plaster fragments partially obtained, requiring a lot of time and energy, was reduced in this way. Tests carried out for this part of the program suggest that with respect to SO_2 - same exposure time provided - the rendered building surface area in one and the same height position represents a uniform reaction face independent of the cardinal point. At this face differing concentration profiles only develop later under conditions of prevailing micro-climate and with the aid of cycles of dissolution, transport and reprecipitation. Compared with this, nitrate and chloride show clear dependence on the façades' orientation to an emission source. Thereby originate systematic modifications of structural data obtained by means of a mercury porosity meter, whereby solar irradiation, temperature changes and dew formation are also responsible. Nevertheless, much greater influence on a pore system of the same age material is its exposure height. On a building whose inferior façade part is decorated with trees and shrubs, one can namely recognize with increasing elevation from ground level a remarkable rise of the water absorption coefficient and specific pore volume determined by Hg intrusion porosimetry, and that as a diminishing of coarse and also of fine pores. This leads to a formation of a preferential diameter between 2 and 100 µm which is practically congruent with the region of capillary activity. Connected with this is a decreasing vapour diffusion resistance. In this way there originates aside from its reference to the cardinal point, height patterns on a building, which are expressed in an increasing weathering intensity at the same exposure duration. So sulphate formation is e.g. determined by quantity and chemistry of binding agent, but extensively influenced by location on a building.
At the end of the programme's duration, exposed 1.5-year-old samples were available for testing which show as expected only a slight sulphate absorption down to about 1 mm depth. Besides this, pores were coarsening in comparison to unweathered reserve samples as by the way a diminishing of the water absorption coefficient which was typical for reaction against sulphur oxidic air pollutants. The same is also true for material of the same age but under

elevated SO_2 concentration at an exposure location. Further insights into the conditions permit measurements of deposition velocity and uptake rate of sulphur dioxide. Cement-containing products show highest values in the dry state. Plaster made with lime putty thereby furnishes a fourfold higher adsorption velocity and a twofold uptake as such made with in- dustrially hydrated lime. After capillary water saturation one can determine a similar sulphate content in all material types having been gassed for the same time period, however with another ranking order regarding velocity. This once more emphasizes the prominent importance of exposure conditions for a weathering progress. Some additional aspects on ageing and pore characteristics are to be found in a more recent paper [45].

Granulometry of sand, mixing water content of lime plaster, as well as mix proportion are parameters which determine structural characteristics and properties such as pore volume, capillary water absorption, and water vapour diffusion resistance. Corresponding information is essential for buildings worthy of being preserved. When augmenting a binder's portion in a mix from 1:4.0 to 1:3.0 by volume at a comparable water content, the portion of fine pores increases, whereby the median shifts to small pore sizes. Additionally an increase of pore volume can be recognized. This tendency is emphasized more distinctly when investigating a historical plaster richer in binding agent. However, not only the contents of binder and sand of a plaster exert such an influence but also the granulometry of the latter which has been given too less attention up to now. For adjusting the consistency of plasters having the same mix proportion (spread value 18 cm), that prepared with fine sand needs about one third more mixing water. Unexpectedly this shows a micropore portion of 28% in comparison to the other with 55%. Especially to be noted is a nearly twofold high pore volume. So a behaviour analogous to sands becomes visible, at which porosity, pore filling degree, and water absorption coefficient, w_o, increase with augmenting fineness. From these results, one can deduce that granulometric composition and elevation of mixing water content together effect a considerable structural modification in hardened plaster, which is also reflected in masonry by capillary and evaporation behaviour. So bricks of a dry-pressed type with decreasing apparent density, cause an increase of maximum liquid absorption reached by capillary action. This is related to surface area $\underline{a}$ being equivalent to maximum absorption height.

Since in the case of a bond applied to this brickwork, mortar covers about 20% of an external surface, one can ascribe to it an essential influence on water rise as well as also on an evaporative process. When using for mortar manufacture, instead of sand standardized according to EN 196-1, its sieve passing plain $\leq$ 0.5 mm, then characteristic values like $\underline{a}$ and w_o shift in the same direction. Similarly effective is an increase of surface tension e.g. when using a saturated solution of calcium sulphate as a test liquid, whereas conditions reverse in case of denser bricks, and that also in the case of the coarser standard sand. Nevertheless, such a solution in comparison to water likewise prevents evaporation on a moisture-saturated masonry section, whereby differences in density because of different absorption heights find their expression in size of evaporation surface, which finally leads to differing starting points of curves. Brickwork made with standard sand shows this phenomenon only after a repeated rise of this solution several times. From these findings it turns out that general behaviour of masonry during moisture transport decisively depends on pore volume and pore-size distribution of brick and mortar, especially in the region of capillary activity; however, above all on grain-size distribution of a mortar's aggregate, whereby the water demand increases with decreasing particle diameter. When monitoring water loss under the same ambient conditions, i.e. also geometrical ones, and not considering the corresponding curve's first, mainly climate-dependent linear portion, however, its material-specific feature can be expressed more stringently by means of the evaporation parameter of a resulting newly developed regression function. Although its physical meaning is not yet clarified, this could serve as a promising tool in the hand of an expert during the attempt to interpret a porous material's properties from its structure.

7 Acknowledgement

Thanks are expressed to the Federal Environmental Agency (Umweltbundesamt) for allocating funds, without which it would not have been possible to carry through the project in its present form. Also gratitude to colleagues in the laboratories Chemical and Electro-Chemical Methods, Physical and Chemical Characteristics, and Technology of Building Materials.
Special mention is made of the contributions of Mrs. Gabriele Müller, Mrs. Elgin Rother, Mrs. Edith Tessmann and Mr. Jürgen Götze, which exceeded their normal workloads. The preparation of drawings was accomplished by Mrs. Gudrun Blamberg, Mrs. Karin Glöckner and the stressful spade-work of processing text and figures for web pages done by Mr. Carsten Prinz , Mrs. Karin Braetz, Mr. Mathias Lindemann, Mr. Norbert Neumann and André Gardei. Mr. Christian Kowalec devoted his close attention to the mathematical aspects of the project, expecially in computer graphics and the application of his own software development. Dr. Detlef Hanus also participated in the realization of this project.
Appreciation is expressed to Dr. Stephan Fitz of the Federal Environmental Agency for generous support and the international cooperation he made possible within the framework of the NATO-CCMS Pilot Study "Conservation of Historic Brick Structures".

8 Bibliography

[1] ASTM C 91-87a:
Standard specification for masonry cement, Edition March 1987, 5 pp.

[2] ASTM C 448-88:
Standard methods for abrasion resistance of porcelain enamels, Edition May 1988, 8 pp.

[3] Barcellona, S.; Barcellona Vero, L.; Guidobaldi, F.:
The front of S. Giacomo degli Incurabili Church in Rome: Biological and chemical surface analyses.
Istituto di Fisica Tecnica - Consiglio Nazionale delle Ricerche, Roma: Centro di Studio Cause de Deperimento e Metodi di Conservazione delle Opere d'Arte 1972, No. 15.

[4] Brunauer, S.; Emmett, P.; Teller, E.:
Adsorption of gases in multimolecular layer.
J. Amer. Chem. Soc. 60 (1938) 309 - 319.

[5] Building Research Board:
Report for the year 1928; edit. by Department of Scientific and Industrial Research, London: H.M. Stationery Office 1929, 9 - 13.

[6] Calyj, V. P.:
The ageing mechanisms of single metal hydroxides and their systems (orig. Russ.).
Z. neorg. Chim. 8 (1963), Vgp. 2, 269 - 273.

[7] Croney, D.; Coleman, J. D.; Bridge, P.M.:
The suction of moisture held in soil and other porous materials.
Road Res. Techn. No. 24 (Dept. Sci. Ind. Res., Road Res. Lab.); London: H.M.S.O. 1952, 42 pp.

[8] D'Havé, R.; Motteu, H.:
Étude de la résistance au gel des matériaux de construction.
build, bâtiment international 1 (1968) No. 2, 18 - 23.

[9] DIN 1060 Part 1:
Baukalk; Teil 1: Definitionen, Anforderungen, Überwachung.
Edition March 1995, 7 pp.

[10] DIN 4188 Part 1:
Siebböden; Drahtsiebböden für Analysensiebe; Maße.
Edition October 1977, 4 pp.

[11] DIN 18 555 Part 1:
Prüfung von Mörteln mit mineralischen Bindemitteln, Frischmörtel; Bestimmung des Wasserrückhaltevermögens nach dem Filterplattenverfahren.
Edition September 1982, 2 pp.

[12] DIN 52 108:
Prüfung anorganischer nichtmetallischer Werkstoffe; Verschleißprüfung mit der Schleifscheibe nach Böhme; Schleifscheiben-Verfahren.
Edition August 1988, 3 pp.

[13] DIN 52 615:
Wärmeschutztechnische Prüfungen; Bestimmung der Wasserdampfdurchlässigkeit von Bau- und Dämmstoffen. Edition November 1987, 10 pp.

[14] DIN 66 131:
Bestimmung der spezifischen Oberfläche von Feststoffen durch Gasadsorption nach Brunauer, Emmett und Teller (BET); Grundlagen.
Edition October 1973, 7 pp.

[15] DIN 66 132:
Bestimmung der spezifischen Oberfläche von Feststoffen durch Stickstoffadsorption; Einpunkt-Differenzverfahren nach Haul und Dümbgen.
Edition July 1975, 5 pp.

[16] DIN EN 196-1:
Prüfverfahren für Zement; Bestimmung der Festigkeit.
Edition March 1990, 16 pp.

[17] DIN EN 196-2:
Prüfverfahren für Zement; Chemische Analyse von Zement.
Edition March 1990, 18 pp.

[18] DIN EN 459-2:
Baukalk; Teil 2: Prüfverfahren. Edition March 1995, 19 pp.

[19] Efes, Y.; Luckat, S.:
Relations between corrosion of sandstones and uptake rates of air pollutants at the Cologne cathedral.
in: 2nd Internat. Symp. on the Deterioration of Building Stones, Athens 27/09/ - 01/10/1976. Athens: The Chair of Physical Chemistry of the National Technical University of Athens 1977, 193 - 200.

[20] EN 1925:1999
Natural stone test methods: Determination of water absorption coefficient by capillarity,
Edition May 1999, 10 pp.

[21] Fagerlund, G.:
Determination of specific surface by the BET method.
Matér. Constr. 6 (1973) No. 33, 239 - 245.

[22] Félix, C.:
Répartitions du soufre dans les grès calcareux (“molasses”) altérés de bâtiments anciens de la région lausannoise.
Chantiers/Switzerland 18 (1987) No. 2, 119 - 123.

[23] Fitz, S.:
Conservation of historic brick structures. How many open questions were left after seven years of joint efforts within the NATO CCMS Pilot Study?
Proc. EC Workshop “Research on conservation of brick masonry monuments”, Heverlee/Leuven 24/10/ - 26/10/1994.

[24] Franke, L.; Grabau, J.:
The influence of salt content on the drying behaviour of bricks.
in: Proc. 7th Expert Meeting Nato-CCMS Pilot Study “Conservation of Historic Brick Structures”, Venezia, Italy 22/11/ - 24/11/1993, edit. by S. Fitz, Berlin: Umweltbundesamt 1990, 132 - 141 (=Conservation of Historic Brick Structures. Case Studies and Reports of Research. Edit. by N.S. Baer, S. Fitz and R.A. Livingston; Donhead St. Mary, Shaftesbury, Dorset/U.K.:Donhead Publishing Ltd. 1998, 59-68; a more detailed version: Bauphysikalische Folgen von Gipshautbildungen an Mauerwerksoberflächen. Bautenschutz u. Bausanierung 18 (1995) No. 7,83-84; No. 8, 27 - 30).

[25] Gall, L.:
Über ein neues Gerät zur schnellen Bestimmung spezifischer Oberflächen. Angew. Mess.
Regeltechn. 4 (1964) 107.

[26] Graf, O.:
Über die Prüfung der Baukalke.
Der Bautenschutz 5 (1934) No. 11, 121 - 135; No. 12, 137 - 143.

[27] Gregg, S.J.:
The surface chemistry of solids. 2nd ed.; London: Chapman and Hall Ltd. 1965, 393 pp.

[28] Grimm, W. D.; Schwarz, U.:
Naturwerksteine und ihre Verwitterung an Münchner Bauten und Denkmälern. Überblick über eine Stadtkartierung.
in: Natursteinkonservierung. Internat. Kolloquium, München, 21/05/ - 22/05/1984, München: Bayer. Landesamt für Denkmalpflege 1986, Arbeitsheft 31, 28 - 118.

[29] Grün, R.:
Die Verwitterung der Bausteine vom chemischen Standpunkt.
Chemiker-Ztg. 57 (1933) No. 41, 401 - 404.

[30] Handbuch Mörtel und Steinergänzungsstoffe in der Denkmalpflege.
Sonderheft aus der Publikationsreihe der BMFT-Verbundforschung zur Denkmalpflege, edit. by D. Knöfel und P. Schubert; Berlin: Verlag Ernst & Sohn 1993, 225 pp.

[31] Hanus, D.; Hoffmann, D.:
Richtungsabhängige Veränderungen von Putzmörteln als Folge unterschiedlicher Expositionsbedingungen.
in: Werkstoffwissenschaften und Bausanierung, Tagungsber. 3. Internat. Kolloquium zum Thema Werkstoffwissenschaften und Bausanierung, Techn. Akademie Esslingen, Ostfildern, 15/12/ - 17/12/1992 (Kontakt & Studium TAE Nr. 420), edit. by F. H. Wittmann; Ehningen bei Böblingen: expert-Verlag 1993, part 2, 1012 - 1024.

[32] Hanus, D.; Niesel, K.:
Influence of air pollutants on rendering.
in: Proc. 3rd Expert Meeting Nato-CCMS Pilot Study "Conservation of Historic Brick Structures", Hamburg 02/11/ - 04/11/1989, edit. by S. Fitz, Berlin (West): Umweltbundesamt 1990, 104 - 131.

[33] Haul, R., Dümbgen, G.:
Vereinfachte Methode zur Messung von Oberflächen durch Gasadsorption.
Chem.-Ing.-Techn. 35 (1963) 586 - 589.

[34] Herrmann, A. G.; Knake, D.:
Coulometrisches Verfahren zur Bestimmung von Gesamt-, Carbonat- und Nichtcarbonat-Kohlenstoff in magmatischen, metamorphen und sedimentären Gesteinen.
Z. Anal. Chem. 266 (1973) No. 3, 196 - 201.

[35] Hirschwald, J.:
Die Prüfung der natürlichen Bausteine auf ihre Wetterbeständigkeit.
Berlin: Verlag von Wilhelm Ernst & Sohn 1908, 675 pp.

[36] Hoffmann, D.:
The Federal Institute for Materials Research and Testing: Study on lime mortar and rendering.
in: Contrib. EUROLIME Colloquium Karlsruhe, 26/05/ - 28/05/1991, edit. by German EUROCARE Secretariat, Karlsruhe 1992, Newsletter No. 1, 32 - 35.

[37] Hoffmann, D.; Hanus, D.:
Effects of air pollutants on rendering.
in: Proc. 5th Expert Meeting Nato-CCMS Pilot Study "Conservation of Historic Brick Structures", Berlin 17/10/ - 19/10/1991, edit. by S. Fitz; Berlin: Umweltbundesamt 1992, 32 - 56.

[38] Hoffmann, D.; Niedack-Nad, M.; Niesel, K.:
Evaporation as a feature of characterizing stone.
in: Proc. 8th Internat. Congress on Deterioration and Conservation of Stone, Berlin, 30/09/ - 04/10/1996, edit. by J. Riederer; Berlin 1996; vol. 1, 453 - 460.

[39] Hoffmann, D.; Niesel, K.:
Ein neues Verfahren zur Beurteilung des Verschleißverhaltens von mineralischen Baustoffen.
Tonind.-Ztg. 99 (1975) No. 9, 221 - 223.

[40] Hoffmann, D.; Niesel, K.:
Moisture movement in brick.
in: Proceedings 5th Internat. Congress on Deterioration and Conservation of Stone, Lausanne/Schweiz 25/09/ - 27/09/1985, edit. by G. Félix; Lausanne: Presses Polytechniques Romandes 1985, vol. 1, 103 - 111.

[41] Hoffmann, D.; Niesel, K.:
Quantifying capillary rise in columns of porous material.
Amer. Ceram. Soc. Bull. 67 (1988) No. 8, 1418.

[42] Hoffmann, D.; Niesel, K.:
Vorgänge des kapillaren Feuchtigkeitsaufstiegs und der Verdunstung in porösen Baustoffen.
AID Schriftenreihe der Sektion Architektur, TU Dresden, 1990, No. 30, 110 - 115.

[43] Hoffmann, D.; Niesel, K.:
Relationship between mechanical characteristics and the pore structure of building materials. Silicates Industriels 61 (1996) No. 11/12, 253-261.

[44] Hoffmann, D.; Niesel, K.:
Parameters of lime rendering modified by atmospheric influence.
in :Proc.UN ECE Convention on Long-Range Transboundary Air Pollution: workshop on quantification of effects of air pollutants on materials, Berlin 24/05/-27/05/1998; Federal Environmental Agency, TEXTE series, edit.by S.Fitz and N. Baer,No. 24, Berlin 1999, 97-107..

[45] Hoffmann,D., Niesel, K.:
Relationship between some physico-technical characteristics of stone.
In: Proc. 2nd Internat.Congress on Studies in Ancient Structures, Istanbul 09/07/ - 13/07/2001; edit. byG. Arun andN. Seçkin, Istanbul: YILDIZ Techn. Univ. 2001, vol. II, 589 – 598.

[46] Hoffmann, D.; Niesel, K.; Plagge, R.:
Water retention characteristics and conductivity of porous media.
Amer. Ceram. Soc. Bull. 74 (1995) No. 11, 48 - 50.

[47] Hoffmann, D.; Niesel K.; Rooß H.:
Zur rechnerischen Erfassung des Kapillaraufstiegs in Säulen poröser Baustoffe.
Bautenschutz u. Bausanierung 10 (1987) No. 5, 69-70; 11 (1988) No. 1, 11.

[48] Hoffmann, D.; Niesel, K.; Wagner, A.:
Capillary rise and the subsequent evaporation process measured on columns of porous material.
Amer. Ceram. Soc. Bull. 69 (1990) No. 3, 392, 394, 396.

[49] Hoffmann, D.; Rooß, H.:
Wechselwirkung zwischen Schwefeldioxid und Kalkmörteln.
Materialprüfung 19 (1977) No. 8, 300 - 304.

[50] Hoffmann, D.; Rooß, H.:
Zur Erhärtung von Purpasten aus Kalk.
Bautenschutz u. Bausanierung 17 (1994) No. 3, 48 - 51, No. 4, 57 - 63.

[51] Hoffmann, D.; Schimmelwitz, P.; Rooß, H.:
Interactions of sulfur dioxide with lime plasters.
in: 2nd Internat. Symp. on the Deterioration of Building Stones, Athens 27/09/ - 01/1976; Athens: The Chair of Physical Chemistry of the National Technical University of Athens 1977, 37-42. - German version: Wechselwirkung zwischen Schwefeldioxid und Kalkmörteln. Materialprüf. 19 (1977) No. 8, 300 - 304.

[52] Holmes, F. E.:
Apparatus for maintaining constant levels in a water bath and a distilling flask.
Ind. Eng. Chem.12 (1940) No. 8, 483 - 484.

[53] Honeyborne, D. B.; Harris, P. B.:
The structure of porous building stone and its relation to weathering behaviour. The structure and properties of porous materials.
in: Proc. Tenth Symp. of the Colston Research Society, London: Butterworths Scientific Publications 1958, 343 - 365.

[54] Jedrzejewska, H.:
New methods in the investigation of ancient mortars.
Archeological chemistry, a symposium, edit. by M. Levey; Philadelphia: Univ. Pennsylvania Press 1967, 147 - 166.

[55] Informationstransfer der LaborPraxis, IonenChromatographie, Literaturdokumentation zur chemischen Analytik; edit. by G. Schwedt, No. 4, 2nd edition 1987.

[56] Johne, R.; Severin, D.:
Die Oberflächenmessung mit dem Areameter.
Chem.-Ing.-Techn. 37 (1965) 57 - 61.

[57] Kieslinger, A.:
Zerstörungen an Steinbauten, ihre Ursachen und ihre Abwehr.
Leipzig, Wien: Franz Deuticke 1932, 346 pp.

[58] Krischer, O.; Kast, W.:
Die wissenschaftlichen Grundlagen der Trocknungstechnik, 3rd edition; Berlin, Heidelberg, New York: Springer-Verlag 1978, 489 pp.

[59] Krus, M.; Kiessl, K.:
Vergleichende Untersuchungen zur Bestimmung der Porenradienverteilung von Natursandsteinen mittels Saugspannungsmessung und Quecksilber-Druckporosimetrie.
IBP (Fraunhofer-Inst. f. Bauphysik)-Bericht FtB - 11/1991, 14 pp., 6 pp. Appendix

[60] Künzel, H.:
Sind wirklich Schadstoffe aus der Luft an der fortschreitenden Zerstörung unserer Denkmäler schuld?
Bautenschutz u. Bausanierung 10 (1987) No. 4, 139 -142.

[61] Künzel, H.:
Mechanismus der Steinschädigung bei Krustenbildung.
Bautenschutz u. Bausanierung 11 (1988) No. 2, 61 - 68.

[62] Luckat, S.:
Ein Verfahren zur Bestimmung der Immissionsrate gasförmiger Komponenten.
Staub-Reinhalt. Luft 32 (1972) No. 12, 484 - 486.

[63] Luckat, S.:
Die Einwirkung von Luftverunreinigungen auf die Bausubstanz des Kölner Domes. II.
Kölner Domblatt 38/39 (1974) 95 - 106.

[64] Lutz, P., Jenisch, R.; Klopfer, H.; Freymuth, H.; Krampf, L.:
Lehrbuch der Bauphysik, Schall, Wärme, Feuchte, Licht, Brand; Teil 1 einer Baukonstruktionslehre, Stuttgart: B.G.H. Teubner 1985, 650 pp.

[65] Mayer, N.:
Eine Vielfach-Meßdüse zur Bestimmung von Dickenänderungen an sehr rauhen Materialproben.
Techn. Messen 46 (1979) No. 12, 459 - 461.

[66] Mayer, N.; Niesel, K.:
Verschleißprüfung mineralischer Baustoffe mit rauher Oberfläche unter Anwendung eines pneumatischen Dickenmeßgeräts.
Materialprüf. 21 (1979) No. 4, 112 - 116.

[67] Meucci, C.; Rossi-Doria, P.:
Analyse et caractérisation de quelque type d'anciens mortiers orientals.
in: Mortars, cements and grouts used in the conservation of historic buildings, Proc. ICCROM Symposium, Rome; Italy 03/11/ - 06/11/1981, Rome: ICCROM 1981, 351 - 358.

[68] Nacken, R.:
Über den Abbinde- und Erhärtungsvorgang der Zemente.
Zement 16 (1927), No. 43, 1017 - 1023; No. 44, 1047 - 1051.

[69] Ney, P.:
Die Erhärtung von Luftkalkmörteln als Kristallisationsvorgang.
Zement-Kalk-Gips 20 (1967) 429 - 434.

[70] Niesel, K.:
Zur Verwitterung von Baustoffen in schwefelhaltiger Atmosphäre - Literaturdiskussion.
Fortschr. Miner. 57 (1979) No. 1, 68 -124.

[71] Niesel, K.:
Aspekte der Natursteinverwitterung aus der Sicht eines Materialprüfers.
Bautenschutz u. Bausanierung 9 (1986) No. 1, 16 - 23; No. 2, 60 - 66.

[72] Niesel, K.:
Quelques aspects expérimentaux de l'étude du transfert d'humidité en maçonnerie.
Silicates Industriels 54 (1989) No. 3 - 4, 47 - 54.

[73] Niesel, K.:
Migration d'humidité en maçonnerie de briques.
Revue des Archéologues et Historiens d'Art de Louvain 1989, No. 22, 99 - 106.

[74] Niesel, K.:
Einfache Wege zum Erhalt von Kenndaten des kapillaren Flüssigkeitsaufstiegs.
GIT Fachz. f. d. Laboratorium 36 (1992) 347 - 349.

[75] Niesel, K.:
Porositätsdaten zur Kennzeichnung des Feuchtigkeitstransports in Ziegelmauerwerk.
in: „Werkstoffwissenschaften und Bausanierung", Tagungsber. 3. Internat. Kolloquium zum Thema Werkstoffwissenschaften und Bausanierung, Techn. Akad. Esslingen, Ostfildern, 15/12/1992 (Kontakt & Studium TAE No. 420), edit. by F. H. Wittmann; Ehningen bei Böblingen: expert-Verlag 1993, part 1, 67 - 80.

[76] Niesel, K.:
Feuchtigkeitsaufstieg in porösen Baustoffen.
Materialprüfung 36 (1994) No. 10, 432 - 437.

[77] Niesel, K.:
Détermination de l'ascension capillaire de liquide dans des matériaux poreux de construction.
in: Actes de la journée ICOMOS/Direction du Patrimoine "Les remontées d'eau du sol dans les maçonneries", Paris: Musée des Monuments Français 25/01/1994, Paris: 1994, 21 pp.

[78] Niesel, K.:
Zum Problem des Nachstellens von Kalkmörteln.
Bautenschutz u. Bausanierung 17 (1994) No. 2, 65 - 68.

[79] Niesel, K.; Hoffmann, D.:
Pore characteristics and moisture in brick masonry.
in: Proc. 7th Internat. Congress on Deterioration and Conservation of Stone, Lisboa, 15/06/ - 18/06/1992, edit. by J. Delgado Rodrigues, F. Henriques and F. Telmo Jeremias; Lisboa: Laboratório Nacional de Engenharia Civil 1992, vol. 2, 735 - 743.

[80] Niesel, K.; Nehring, G.:
Ein Verfahren zur Erfassung der Volumenänderungen von Purpasten und Mörteln im Frühstadium ihrer Erhärtung.
Tonind. - Ztg. 100 (1976) No. 10, 362 - 364.

[81] Niesel, K.; Rooß, H.:
Aspekte der Untersuchung von Porenraumveränderungen in feuchtem Mauerwerk - Aspects of the testing of pore volume changes in damp masonry.
Ziegelindustrie International 36 (1983) No. 7, 339 - 349.

[82] Niesel, K.; Schimmelwitz, P.:
Zur Kenntnis der Vorgänge bei der Erhärtung und Verwitterung von Dolomitkalkmörteln.
Tonind.-Ztg. 95 (1971) No. 6, 153 - 161.

[83] Niesel, K.; Schimmelwitz, P.:
Zur quantitativen Kennzeichnung des Verwitterungsverhaltens von Naturwerksteinen anhand ihrer Gefügemerkmale.
BAM Research Report No. 86, Berlin (West): Bundesanst. Materialprüf. 1982, 100 pp. (fairly abridged English version: Niesel, K.: The weathering behaviour of natural building stone. Stone Industries 1983, No. 10, 30 - 31).

[84] Ohnemüller, W.; Solf, A.:
Bestimmung von Kohlendioxyd in Kalksteinen und gebrannten Kalkprodukten durch „Coulometrische Titration".
Zement-Kalk-Gips 23 (1970) No. 5, 200 - 202.

[85] Orr, C., Dallavalle, J.M.:
Fine particle measurement. New York: MacMillan 1959, 353 pp.

[86] Purcell, W. R.:
Capillary pressures: Their measurement using mercury and calculation of permeability therefrom.
Trans. Amer. Inst. Miner. Met. Engrs. 186 (1949) 1 - 30.

[87] Ravaglioli, A.; Vecchi, G.:
Assessment of frost resistance of ceramic bodies by means of porosity meter tests.
in: Proc. RILEM/IUPAC Internat. Symp. on Pore Structure and Properties of Materials, Prague 18/09/-21/09/1973, edit. by S. Modrý and M. Svatá, Prague: Academia 1974, final report, part IV, vol. VI, F-117 - F-127.

[88] Ravaglioli, A.:
Il problema della gelività nei cotti ceramici: parametri chimico-fisici connessi col fenomeno e metodi di misura.
Ceramica Informazione 12 (1977) No. 10, 543 - 557.

[89] RILEM 25 P.E.M.: Essai No. IV. 2:
Résistance à l'abrasion - Abrasion resistance. Essais recommandés pour mesurer l'altération des pierres et évaluer l'efficacité des méthodes de traitement. Essais caractérisant les propriétes mécaniques de la surface.
in: UNESCO/RILEM Internat. Symp. on the Deterioration and Protection of Stone Monuments, Paris 05/06/ - 09/06/1978, suppl. vol. V, 1979, 4 pp. (Matér. Constr. 13 (1980) No. 75, 230 - 233).

[90] RILEM Recommendations MR 1 - 21; 1982 (E):
Testing methods of mortars and renderings. 1st Edition December 1982, 24 pp.

[91] Ritter, H. L.; Drake, L. C.:
Pore-size distribution in porous materials.
Ind. Engng. Chem., Anal. Ed. 17 (1945) 782-786.

[92] Rodt, V.:
Zum Erhärtungsproblem der hydraulischen Bindemittel.
Tonind.-Ztg. 62 (1938) No. 17, 188-190.

[93] Rooß, H.; Rother, E.:
Changes in concentration of chemical constituents and of physical characteristics perpendicular to the surface of external rendering.
in: Proc. 4th Expert Meeting Nato-CCMS Pilot Study "Conservation of Historic Brick Structures", Amersfoort, The Netherlands 25/10/1990, edit. by S. Fitz, Berlin: Umweltbundesamt 1991, 93 - 119.

[94] Rooß, H.; Niesel, K.; Hoffmann, D.:
Über Phänomene des Feuchtigkeitstransports in Ziegeln und Mauerwerk.
GIT Fachz. f. d. Lab. 32 (1988), Suppl. 5: Materialprüfung, 16 - 21.

[95] Samson-Gombert, C.:
Relations entre les altérations d'un calcaire en oeuvre et les paramètres de l'environnement, principaux résultats et applications.
in: Actes du Colloque International ASESMO/LCCM sur la Détérioration des Matériaux de Construction, La Rochelle 12/06/ - 14/06/1991, edit. by F. Auger; La Rochelle: Univ. de Poitiers, Institut Universitaire Technique (IUT) 1991, 185 - 194.

[96] Schimmelwitz, P., Hoffmann, D.:
Untersuchung über die Erhärtung von Außenputzen aus Luftkalkmörtel und ihre Verwitterung unter besonderer Berücksichtigung der Einwirkung von Luftverunreinigungen.
ERP-Forschungsbericht 1977, Az. 2222, 170 pp.

[97] Small, H.; Stevens, T.S.; Bauman, W.C.:
Novel ion-exchange chromatographic method using conductimetric detection.
Anal. Chem. 47 (1975) No. 11, 1801 - 1809.

[98] Spohn, E.:
Das Wasserhaltevermögen von Putz- und Mauermörteln.
Zement-Kalk-Gips 8 (1955) No. 9, 299 - 301.

[99] Tombers, J.:
Untersuchungen zur Salzverteilung in verbautem Naturstein.
Diss. Univ. Saarland., Saarbrücken 1991, 188 pp.

[100] Venzmer, H; Zacharias, B.:
Zum zeitlichen Verlauf von Abdunstungsprozessen an Ziegelproben bei ausgeschlossener Wassernachförderung.
Acta Polytechnica - Práce CVUT v Praze 18, 1985 Ser. 1, No. 1/3, 71 - 89.

[101] Wagner, A.; Niesel, K.:
Kapillarkenngrößen von Mauerziegeln. Ihre Bestimmung durch Saugversuche an Probekörpern.
Materialprüfung 31 (1989) No. 4, 109 - 113.

[102] Wagner, A.; Niesel, K.; Kowalec, C.:
Bestimmung einiger Parameter des kapillaren Feuchtigkeitstransports in porösen Baustoffen, part 1 to 3.
Z. Pflanzenernähr. Bodenk. 158 (1995) 375 - 377; 379 - 387; 389 - 392.

[103] Weber, H.; Iversen, K.; Klock, H.; Schoer, H.: Winkler, H.:
in: Mauerfeuchtigkeit, Ursache und Gegenmaßnahmen. (Kontakt & Studium Techn. Akad. Esslingen No. 137: Bauwesen); Grafenau/Württ.: expert Verlag, 1984, 143 pp.

[104] Weiß, J.; Göbl, M.:
Analyse anorganischer Schwefelverbindungen mit Hilfe der Ionen-Chromatographie.
Z. Anal.Chem. 320 (1985) 439 - 444.

[105] Wittenburg, C.:
Trockene Schadgas- und Partikeldeposition auf verschiedene Sandsteinvarietäten unter besonderer Berücksichtigung atmosphärischer Einflußgrößen.
Diss. Fachber. Chemie, Univ. Hamburg, 14/03/1994 (publication series Angewandte Analytik, Univ. Hamburg, No. 22), 137 pp.

[106] Würzner, K.:
Die physikalischen Grundlagen des Abbindens und Erhärtens.
Zement 8 (1919) No. 46, 559 - 562; No. 47, 571 - 574.

[107] Zacharias, B; Preuß, W.; Venzmer, H.:
Zum zeitlichen Verlauf von Abdunstungsprozessen in Baustoffen bei ausgeschlossener Wassernachförderung.
AID Architekturinformation Techn. Univ. Dresden, 1984, No. 20, 407 - 413.

[108] Zehnder, K.; Arnold, A.:
Crystal growth in salt efflorescence.
J. Crystal Growth 97 (1989) 513 - 521.